CENTRIFUGAL COMPRESSOR DESIGN CRITERIA - A COMPARISON OF THEORY AND EXPERIMENT

Samy Baghdadi, et al

General Motors Corporation

Prepared for:

Army Air Mobility Research and Development Laboratory

December 1974

Unclassified

SECURITY CLASSIFICATION OF THIS PAGE (When Data Entered)

REPORT DOCUMENTATION PAGE	READ INSTRUCTIONS BEFORE COMPLETING FORM
1. REPORT NUMBER: USAAMRDL-TR-74-69	2. GOVT ACCESSION NO.
	3. RECIPIENT'S CATALOG NUMBER: AD-004 011
4. TITLE (and Subtitle): CENTRIFUGAL COMPRESSOR DESIGN CRITERIA A Comparison of Theory and Experiment	5. TYPE OF REPORT & PERIOD COVERED: Final Report June 73 - Sep 74
	6. PERFORMING ORG. REPORT NUMBER: EDR 8216
7. AUTHOR(s): Samy Baghdadi Brink A. Hopkins William F. Osborn	8. CONTRACT OR GRANT NUMBER(s): DAAJ02-73-C-0089
9. PERFORMING ORGANIZATION NAME AND ADDRESS: Detroit Diesel Allison Division of General Motors Corporation Indianapolis, Ind. 46206	10. PROGRAM ELEMENT, PROJECT, TASK AREA & WORK UNIT NUMBERS: 1G262207AH89
11. CONTROLLING OFFICE NAME AND ADDRESS: Eustis Directorate U. S. Army Air Mobility R&D Laboratory Fort Eustis, Va. 23604	12. REPORT DATE: December 1974 13. NUMBER OF PAGES: 123
14. MONITORING AGENCY NAME & ADDRESS (if different from Controlling Office)	15. SECURITY CLASS. (of this report): Unclassified 15a. DECLASSIFICATION/DOWNGRADING SCHEDULE

16. DISTRIBUTION STATEMENT (of this Report)

Approved for public release; distribution unlimited.

17. DISTRIBUTION STATEMENT (of the abstract entered in Block 20, if different from Report)

18. SUPPLEMENTARY NOTES

19. KEY WORDS (Continue on reverse side if necessary and identify by block number)

Centrifugal compressors
High pressure ratio
Test data
Instrumentation

20. ABSTRACT (Continue on reverse side if necessary and identify by block number)

The objective of this program was to define the utility of the Detroit Diesel Allison Centrifugal Compressor Performance (CCP) analysis.

This objective was accomplished by comparing the preexisting analysis of the performance of a new high-pressure-ratio centrifugal compressor (RC-2) with the test data obtained in the course of this program. After the first

DD FORM 1 JAN 73 1473 EDITION OF 1 NOV 65 IS OBSOLETE

Unclassified

SECURITY CLASSIFICATION OF THIS PAGE (When Data Entered)

20. Continued.

or baseline compressor tests, the test results were analyzed on the basis of the CCP program, and initial compressor modifications were recommended and carried out. An additional modification was also completed. Prior to each test of the modified compressor, an estimate of the unit's performance was obtained by using the CCP program, and the test results were subsequently compared with this estimate.

In general, the CCP calculation was in agreement with the test data as far as the compressor's overall pressure ratio was concerned. However, the program's efficiency calculation appeared to be high by amounts progressively decreasing from 4.5% in the initial test to 0.7% in the final test. The test data also indicate that the hardware is sensitive to certain profile parameters at the inlet of both the diffuser and the inducer in a manner which the calculation does not predict. This sensitivity to flow profile was deduced from the intrastage performance measurements and is not accounted for in the CCP program. The CCP calculated mass flow rate through the compressor was found to differ from the measured value by amounts varying from 1 to 6% as a function of the accuracy with which the program distributed the compressor's internal losses.

The final modification to the compressor consisted of cutting back the rotor to a radius 8% smaller than the original radius. In spite of the consequent mismatch between the impeller and the diffuser, the overall compressor efficiency was increased by this modification. The overall compressor efficiency probably would be further increased if a properly matched diffuser were substituted for the current one.

EUSTIS DIRECTORATE POSITION STATEMENT

The conclusions derived from work performed during this centrifugal compressor design criteria program underscore a primary, long-standing problem: neither the compressor design nor the prediction of a "paper" compressor's performance can be accurately completed without benefit of detailed definition of the internal aerodynamics of the machine either by rigorous analytical treatment of the geometry or by acquisition of test data. While it may be possible to complete designs or performance predictions using advanced internal-aerodynamics computer analyses, the most successful attempts at the effort rely on test data either from the hardware under investigation or from another compressor closely related to it.

This report has been reviewed by technical personnel from this Directorate, and the conclusions and recommendations contained herein are concurred in by this Directorate. The project engineer for this contract was Mr. Robert A. Langworthy, Technology Applications Division.

PREFACE

The program reported herein was conducted by the Detroit Diesel Allison Division (DDA) of General Motors Corporation for the U.S. Army Air Mobility Research and Development Laboratory, Eustis Directorate, under the terms of Contract DAAJ02-73-C-0089, DA Project 1G262207AH89.

The program was directed at DDA by Dr. S. Baghdadi; Dr. W. F. Osborn, the principal analyst, developed the centrifugal compressor performance calculation; and Mr. B. A. Hopkins was responsible for the design of the RC-2 Compressor. The compressor tests were performed under the direction of Mr. W. C. Gitzlaff of the DDA Test Department. Mr. R. M. Kaufman was responsible for the test stand computer programming.

The authors gratefully acknowledge the program guidance provided by Mr. R. A. Langworthy of the Eustis Directorate, USAAMRDL.

TABLE OF CONTENTS

LIST OF ILLUSTRATIONS

LIST OF ILLUSTRATIONS (cont)

LIST OF TABLES

I. PROGRAM THEORY

THERMODYNAMIC FRAMEWORK

The Detroit Diesel Allison (DDA) CCP calculation computes compressor pressure ratio and efficiency for each speed line as a function of the mass flow rate.

The relationship between rotor pressure ratio and rotor internal efficiency is

$$R_{c_{rotor}} = \left[1 + \frac{\eta_{ri}\, U_2^2}{gJC_pT_{0_1}}\ \Delta q_{th}\right]^{\gamma/(\gamma-1)}$$

where η_{ri} is the rotor internal efficiency defined by

$$\eta_{ri} = \frac{\Delta q_{th} - \Delta q_{ri}}{\Delta q_{th}}$$

where Δq_{ri} represents rotor internal losses which degrade the rotor pressure, such as aerodynamic friction losses along the flow surface, losses caused by the growth of the boundary layers in the rotor, blade wake mixing, shock wave losses, and secondary flow losses; Δq_{th} is the theoretical head

$$q_{th} = \frac{C_{\theta_2}}{U_2} - \frac{C_{\theta_1} U_1}{U_2^2}$$

= (SF - PF) for a radial exducer. (Note that all the q values are nondimensionalized by dividing by U_2^2/Jg.)

The adiabatic (overall) rotor efficiency must account for aerodynamic losses external to the rotor, such as frictional losses* on the rotor back plate, losses caused by the recirculation of low energy fluid in and out of the rotor, and losses associated with the clearance between the rotor and the stationary shroud.

Thus, the compressor's adiabatic efficiency is defined as

$$\eta_{ad} = \frac{\Delta q_{th} - (\Delta q_{ri} + \Delta q_{diffuser} + \Delta q_{IGV})}{\Delta q_{th} + \Delta q_{external}}$$

The sum in parentheses in the numerator may be termed the total internal flow losses. This equation expresses the fact that the internal flow losses decrease the useful output of the compressor, while external losses increase the work input required to run the compressor. Figure 1 shows the various losses according to their origins.

---

*Mechanical losses (such as those caused by bearing and seal friction) cannot be accounted for in an aerodynamic calculation.

Clearly, the rotor external losses increase the temperature of the fluid at the diffuser exit. However, it is difficult to determine what fraction of this heat addition is fed into the working fluid while it is in the rotor, and what fraction is fed into the fluid outside the rotor. The CCP program somewhat arbitrarily splits or assigns half the rotor external losses to the fluid inside the rotor, and the other half to the fluid as it leaves the rotor (at the rotor "dump" station). Checks of the effect on the program of varying this fraction show the overall performance parameters to be relatively insensitive to the split. O. E. Balje*[1] recommends adding the entire rotor external loss at the rotor exit; however, this was found to be extreme.

The compressor overall pressure ratio may be written

$$R_{cOA} = \left[1 + \eta_{ad} U_2^2 \frac{(\Delta q_{th} + \Delta q_{ex})}{Jg\, C_p\, T_0} \right]^{\gamma/(\gamma-1)}$$

The thermodynamic framework described here may be represented conveniently in an H-S diagram, Figure 2.

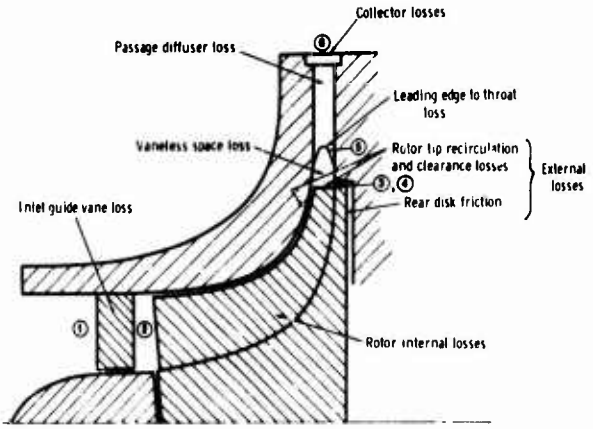

Figure 1. Centrifugal compressor loss mechanisms.

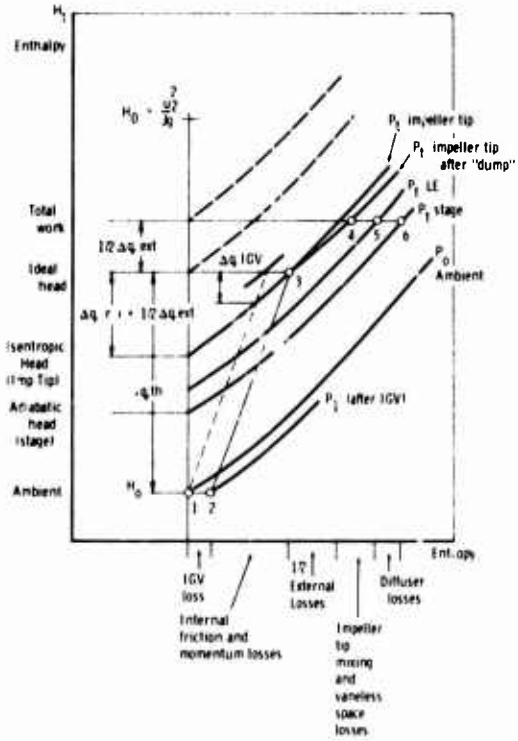

Figure 2. Mollier diagram for centrifugal compressor.

*Superscript numbers correspond to the references listed in Section VII.

[1] Balje, O.E. A Study on Design Criteria and Matching of Turbo Machines. Part B—Compressor and Pump Performance and Matching of Turbo Components. ASME Paper 60-WA-231.

LOSS CALCULATIONS

The CCP program calculates both internal and external losses by means of equations derived theoretically from data correlations and from the literature.

Inlet Guide Vane Losses

The inlet guide van losses are computed as a function of the blade turning and the ex Mach number. Typically, this loss amounts to 1.5% of the inlet total pressure at the design point for RC-2.

Rotor Internal Losses

The calculation of the rotor internal losses is the heart of the CCP program. The calculation was developed for radial rotors and subsequently modified to take into account back-curved rotors. The radial rotor theory is based on a unique relationship between the rotor pressure coefficient and the tip speed and inlet swirl. The following description applies to radial rotors.

The rotor pressure coefficient, ψ, is defined as

$$\psi = (SF - PF) - \Delta q_{ri}\,(SF,\ PF,\ U,\ a) \qquad (1)$$
$$= \Delta q_{th} - \Delta q_{ri}$$

where Δq_{ri} is the rotor internal loss. The relationship $\psi = \psi\,(U, a)$ has been derived from correlation studies for rotors close to the state of the art, which will be referred to as "model rotors" in this report. This key relationship may be derived from the assumption that, for a given rotor ideal (isentropic) head, the rotor internal losses are directly related to the rotor tip speed. Thus, the model rotor internal loss may be obtained from equation (1),

$$\left(\Delta q_{ri}\right)_{model} = \psi\,(U, a)_{model} - SF + PF$$

This rotor internal loss is modified by a factor F_m, which accounts for various effects which cause deviation from $(\Delta q_{ri})_{model}$ as computed here, so that, for real rotors,
$\Delta q_{ri} = F_m\,(\Delta q_{ri})_{model}$, where

$$F_m = f_1 \times f_2 \times f_3 \times \text{-----} f_n = \prod_{i=1}^{n} f_i$$

Each of the factors f_i is a modifier by which the rotor internal loss is multiplied to account for a particular effect. Some of the factors f_i follow:

(a) The inlet axial Mach number

$$f_1 = 1 + C_1 (M - M_{cr_1})$$
$$C_1 > 0, \; M > M_{cr_1}$$
$$C_1 = 0, \; M < M_{cr_1}$$

where the subscript cr_1 indicates a critical value,

(b) The inducer tip relative Mach number

$$f_2 = 1 + C_2 (M_{rel} - M_{cr_2})$$
$$C_2 > 0, \; M_{rel} > M_{cr_2}$$
$$C_2 = 0, \; M < M_{cr_2}$$

(c) Rotor negative incidence at high Mach number

$$f_3 = 1 + C_3 i$$
$$C_3 > 0, \; i < 0, \text{ if } M_{rel} > M_{cr_2}$$
$$C_3 = 0, \; i > 0, \text{ or if } M_{rel} < M_{cr_2}$$

(d) Rotor blade surface roughness

$$f_4 = 1 + C_4 (\epsilon - \epsilon_{cr})$$
$$C_4 > 0, \; \epsilon > \epsilon_{cr}$$
$$C_4 = 0, \; \epsilon < \epsilon_{cr}$$

where ϵ is the blade surface roughness.

For rotors close to choking in the inducer, a choke flow coefficient factor is also included. Except for the latter, all the functions are linear.

The rotor outlet axial (or "wall") blockage at design point is input. Typically, the values range from 0.85 to 0.95. The rotor outlet wake (or tangential blockage) is calculated at design point as a function of the rotor pressure ratio, the number of blades, the inlet hub/tip ratio, and one of three flow quality factors. (Refer to the CCP Calculation Flow Chart, Figure 3.) These flow quality factors may only be used a posteriori in analyzing test data; obviously, in doing an a priori analysis (i.e., before the machine has been tested) of a machine, the quality of the flow (which is a function of the impeller blading design and the diffuser entry conditions) cannot at present be determined.

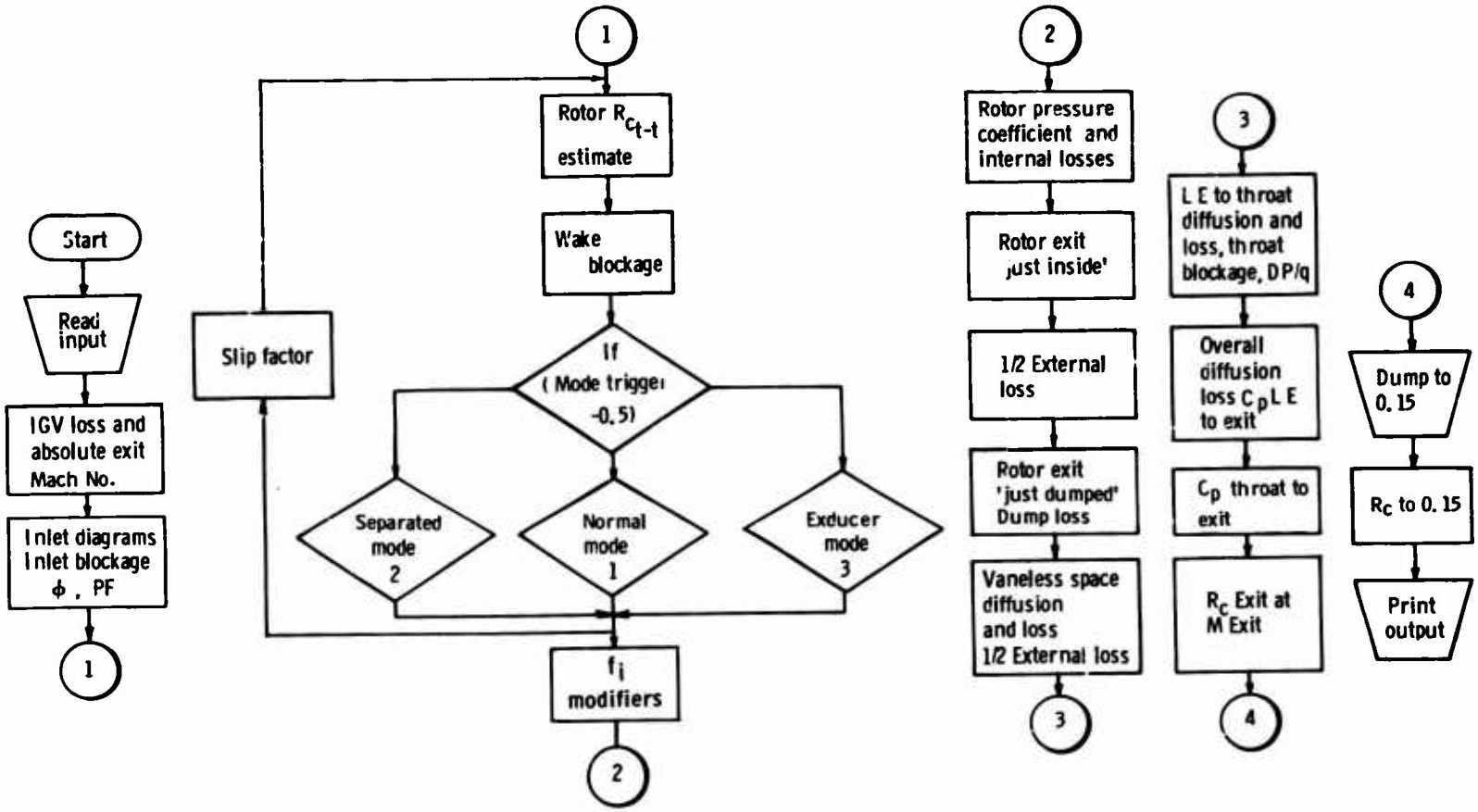

Figure 3. CCP Calculation flow chart.

Clearly, the designer intends his blading to produce the highest quality flow (i.e., the lowest wake amplitude). The designer typically uses an inviscid or quasi-inviscid flow calculation to schedule the impeller blading, and his quality criteria are usually based on the blade surface diffusion factors indicated by this program. However, such programs do not accurately take into account boundary layer migration and other secondary flow effects that are known to affect the blading velocity gradients. The proximity of the diffuser leading edges to the impeller and the number of diffuser passages are also known to affect the impeller flow quality, although these effects are not yet included in the CCP correlations. This aspect of the compressor performance calculation is still an art. In general, when the CCP program is run a priori, the blading is assumed to produce high-quality flow and thus a low-amplitude tangential blade wake.

Both the "wall" and "wake" values of the impeller exit blockage are calculated at off-design operating points by means of modifiers applied to the design point value (or "amplitude"). These modifiers are functions of dimensionless quantities ϕ/ϕ_{DP}, where

$$\phi = \text{inlet flow coefficient} = V_a/U_2$$

U_2 is the rotor tip speed, and the subscript DP indicates a design point value.

The aerodynamic slip factor is calculated at design point by a formula which is based on data correlations. The slip factor relationship depends strongly on the value of the wake blockage as well as on the number of blades. The off-design value of the slip factor depends on the flow factor and tip speed in a manner similar to the impeller exit blockages.

Once the slip factor amplitude has been calculated at the design point, the program returns to the calculation of the rotor pressure coefficient and blockages as indicated in the flow chart, Figure 3. Finally, a new rotor pressure coefficient is computed, and then Δq_{ri} is calculated from equation (1).

The correlations and calculations used in CCP were derived originally for impellers with radial exducer blading. The calculation was subsequently modified to take into consideration rotors with back-curved exducer blading. This was done primarily by using the pressure coefficient-tip speed correlation to transform a given back-curved rotor into an equivalent radial machine at each calculation point. In addition, the rotor slip factor and blockage relations contain terms accounting for back-curvature.

Rotor External Losses

The rotor external losses consist of the rear disk frictional loss, the impeller tip recirculation loss, and the losses associated with the clearance between the rotor and the shroud.

The external loss is calculated in two parts in CCP:

$$\Delta q_{ext} = f_1 + f_2$$

f_1 is the contribution resulting from clearance effects in the inducer section of the rotor. This parameter is a function of the inlet hub/tip ratio and the inlet hub diameter as well as the clearance between the rotor and the shroud.

f_2 is the contribution resulting from the radial section of the impeller and, thus, includes the rear disk friction, the clearance effects, and the recirculating flow losses at the impeller exit. f_2 is a function of the rotor tip Reynolds number, the static pressure rise across the impeller, the rotor tip speed, and the clearance.

Diffuser Losses

The diffuser losses include the rotor wake mixing loss, the frictional losses in the vaneless space, the passage entry loss, and the diffusing passage losses.

The mixing of the rotor wakes is assumed to occur instantaneously and at constant static pressure. This loss includes the loss caused by the addition of half the rotor external losses at this station.

The diffuser throat blockage is computed using boundary layer considerations. Once the throat blockage is known, the total pressure at the throat of the diffuser is deduced from an empirical curve correlating the product of throat blockage and pressure at the throat with the diffuser leading-edge Mach number. This curve is similar to—but not identical to—that of Kenny.[2] The losses and pressure recovery in the diffuser downstream of the throat are obtained from a correlation of the total pressure loss in such a diffuser with throat blockage and Mach number. Consideration is being given to replacing this section of the calculation with a calculation based on the published results of two-dimensional and conical diffuser testing by Creare, Inc.[3,4]

[2] Kenny, D. P. A Novel, Low-Cost Diffuser for High Performance Centrifugal Compressors. ASME 68/GT-38.

[3] Dean, R. C., Jr., and Runstadler, P. W., Jr. Straight Channel Diffuser Performance at High Inlet Mach Numbers. Creare, Inc., Hanover, New Hampshire.

[4] Dolan, F. X., and Runstadler, P. W., Jr. Pressure Recovery Performance of Conical Diffusers at High Subsonic Mach Numbers. Creare Report TN-165, Hanover, New Hampshire, July 1973.

II. COMPRESSOR DESIGN

The RC-2 compressor is the second in a series of high-pressure-ratio research compressors designed and built at DDA. The first compressor of this series, RC-1, had a design point pressure ratio of 8:1 and a mass flow of 4.2 lbm/sec at a specific speed of 70.* The RC-1 design, which used an impeller with a straight radial exducer of high solidity, proved to have an unusually wide range of operation with the peak efficiencies well removed from the surge line.

DESIGN PHILOSOPHY

The purpose of the second design (RC-2) is to provide a unit with a higher efficiency potential than the original design (RC-1). The RC-2 was to use as much of the existing RC-1 hardware as was compatible with a reasonable performance improvement increment. Thus, only features believed to be quantitatively important would be included if these features materially influenced costs. On the other hand, any features which could be added at little or no cost could be considered for inclusion.

In the new design the flow and pressure ratio could be specified to values other than those used for the RC-1. From a research standpoint alone, there is merit in maintaining the same design goals for a series of units to minimize the difficulties of rigorous comparison. Therefore, it was the intent of DDA to carry over the original flow and pressure ratio goals unless detailed study dictated otherwise.

The major changes to which study was directed were related to:

- Increased specific speed
- Decreased friction-producing surface (wetted area)
- Scheduled impeller diffusion
- Back-curved impeller blading

A basic change in the design of the RC-2 as compared with the RC-1 was in the area of specific speed (N_S). While specific speed as a performance parameter is not independent of other factors (e.g., Mach number), there are considerable data in the literature which show that an optimum exists at a higher value than that of the RC-1. Figure 4 shows examples. Data for Figure 4 are from O. E. Balje[1] and C. Rodgers.[5] While these curves do not agree on the optimum specific speed, they do show that a value of 70 as used for the RC-1 is lower than desirable. The original value of 70 was chosen low in order to achieve a reasonably low inducer Mach number (0.87).

---

[5] Rodgers, C. A Cycle Analysis Technique for Small Gas Turbines; Technical Advances in Gas Turbine Design. Paper No. 5, Institution of Mechanical Engineers. April 1969.

*See N_S under List of Symbols for definition and units.

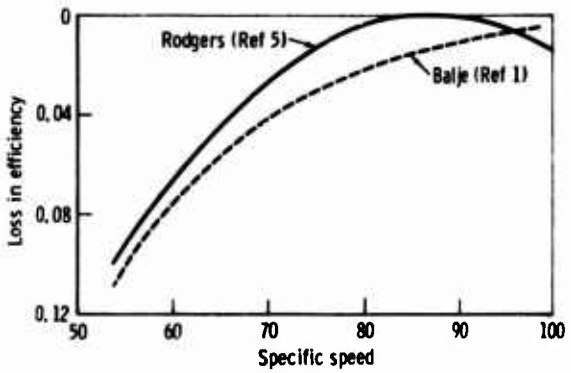

Figure 4. Effect of specific speed on efficiency.

A specific speed of 90 was believed to be a suitable increment above the 70 value, and, therefore, was used as the design goal. Specific speed can be increased by an increase in airflow per unit area, an increase in rotative speed, or a reduction in pressure ratio. A change in airflow consistent with retention of inlet ducting would produce only a fraction of the desired specific speed change. In any case, both flow and pressure ratio should be the same as for the RC-1 for good parametric comparisons of test data. On the other hand, shaft speed could be readily changed. The change in specific speed from 70 to 90 produces a comparable change (+28%) in shaft speed. The existing shaft support system and bearings were considered to be capable of accommodating this speed change. Thus, the specific speed was increased by a shaft speed change only.

Included in the design philosophy was the intent to decrease the friction-producing wetted area. In principle, this results in increasing the rate of diffusion, which is also generally referred to as increasing "loading."

Several interrelated factors are involved in pursuing a loading change. Foremost among these factors is the problem of computing the impeller velocities with sufficient reality so that a particular diffusion rate can be identified. Then, of course, there is the problem of establishing the criteria for the appropriate diffusion gradients throughout the impeller on both suction and pressure surfaces. Also pertinent to a change in loading is a review, in general terms, of the relationship of the impeller design procedures to the real flow field therein. A thorough discussion of these generalities has been presented in an ASME publication.[6]

[6] Advanced Centrifugal Compressors. ASME Turbomachinery Committee, Gas Turbine Division, New York. 1971.

The ideal inviscid flow field in an impeller is generally computed by a quasi-two-dimensional potential flow solution, such as DDA BC46 computer program. The real flow develops secondary flows; this means that there is a transverse migration of low-energy fluid toward the low-pressure corner of the flow passage. The boundary-layer loss is generated to different degrees on hub, pressure, and suction walls. In addition, the stationary-shroud-rotating-impeller relationship produces "extra" tangential shear forces. The result is that the total energy head becomes distributed in a different manner from that postulated by the inviscid analytical solution. In a short flow-path length, such as a typical axial stage, there is insufficient time for this cross flow to produce any significant discrepancy between the computed and real flow field. However, the centrifugal compressor is inherently one of considerably longer passages. This can produce the situation wherein the exit transverse velocity distribution at the impeller exit is "reversed" when measured in test, as compared with the computed distribution. This is produced by a displacement of energy heads by the cross-flow effects.

Despite its limitations, potential flow impeller flow field calculation has considerable merit. Through use of an allowance for bulk loss and blockage, the average velocity level is reasonably correct through the impeller. In the "early" part of the impeller the computation of surface velocities should be reasonably valid. Further, major deviations from rational design velocities can be avoided even though exact velocities may be in doubt.

A major advantage of the potential flow calculation is the obvious capability of comparing one design with another. Here the differences in comparable analytical results are important and useful, keeping in mind the computational limitations.

As stated, the intent was to decrease the RC-2 impeller friction surface compared with the RC-1. The increase in specific speed contributes directly to this by the reduction in required diameter and indirectly through requiring less tangential loading (force), allowing return to original loading by using fewer vanes. A further decrease in the number of vanes, other factors remaining fixed, has the effect of increasing, in proportion, the velocity differential vane to vane. This trend is shown schematically in Figure 5 and illustrates that the magnitude of local diffusion is increased on each surface. In addition, the impeller channel cross-flow driving forces will be greater when the velocity (pressure) differentials, vane-to-vane, are greater.

The amount of diffusion which can be tolerated is not quantitatively known. It would seem that optimum loading should be qualitatively of the same nature as an optimum diffuser (i.e., a carefully adjusted "ratio" of diffusion to the friction-producing wetted surfaces producing the diffusion). It is generally agreed that boundary layer calculations in the impeller are not sufficiently accurate to warrant detailed application. Cross flows, pressure gradients normal to the vane, and rotation of the flow path all conflict with the conventional assumptions. F. Dallenbach[7] proposes a diffusion velocity ratio limit. He derived this limit from simple

[7]Dallenbach, F. The Aerodynamic Design and Performance of Centrifugal and Mixed-Flow Compressors; Symposium on Centrifugal Compressors. ASME. 1962.

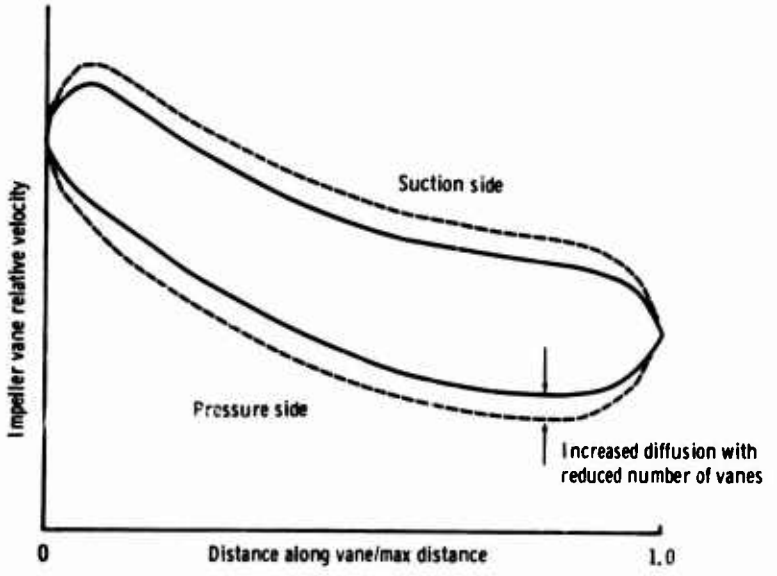

Figure 5. Effect of vane number change on impeller loading.

boundary layer propositions, but it gained credibility by use in a series of designs wherein better performance was obtained than in a series where the proposed limit was exceeded. A value of impeller final relative velocity divided by an initial relative velocity of 0.6 is suggested as a minimum value. The application of this criterion was considered in the RC-2 design.

Qualitative scheduling of the impeller internal diffusion in a manner consistent with simple boundary layer characteristics was considered desirable for the RC-2. Such calculations show that the accumulated energy loss is less when a given diffusion is obtained by a more rapid velocity reduction in the early portion than in the latter portion of a diffuser.

Use of an impeller that incorporated back-curvature at the outlet was also considered desirable for the RC-2. Such a design reduces the diffuser inlet Mach number for a given vaneless space while adding somewhat to the impeller diameter. Curves showing such trends are shown in Figures 6 and 7. One obstacle to the use of a back-curved impeller is the stress produced at the tip as a result of centrifugal force acting on the nonradial section. However, improvements in the last few years in the stress calculation capability indicate that the stresses in this zone are not as high as previously assessed and, further, that the use of the titanium material provides superior strength.

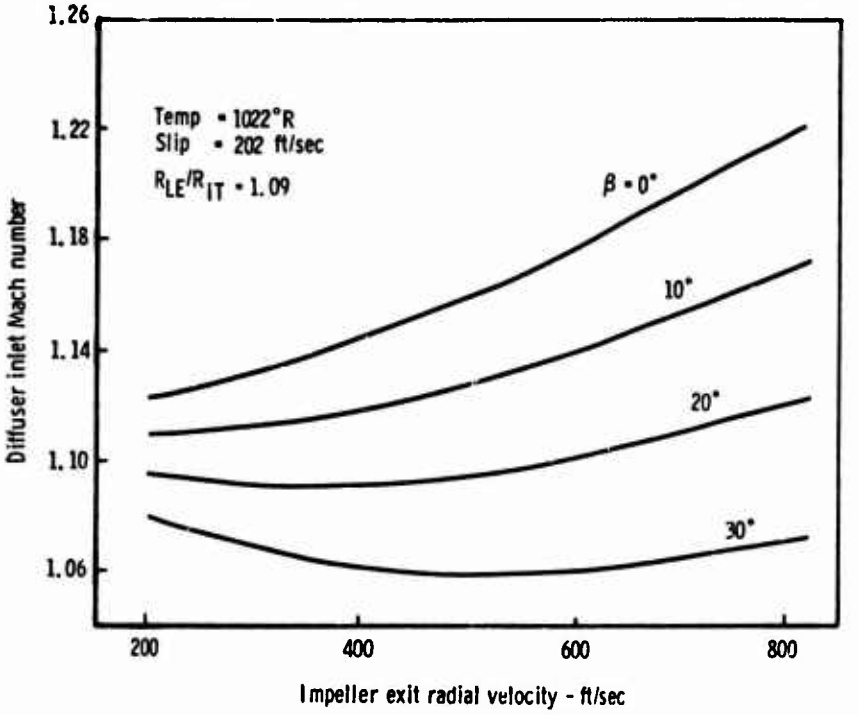

Figure 6. Effect of impeller back-turn angle on diffuser inlet Mach No. potential flow calculation.

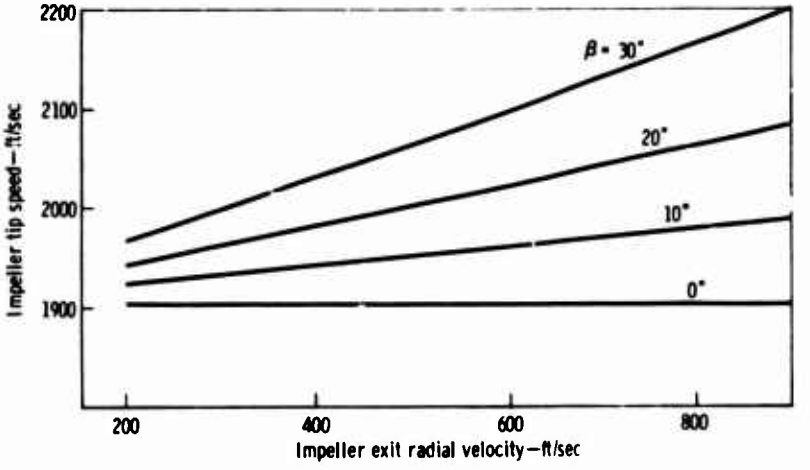

Figure 7. Effect of back-turn angle on tip speed.

IMPELLER AERODYNAMIC DESIGN

The impeller velocity patterns were computed using the DDA BC46 computer program described by D. M. Davis.[8] The calculation is basically straightforward, inviscid solution à la J. D. Stanitz[9] wherein various clerical features (e.g., data input, solution stations) were most recently influenced by the methods of T. Katsantis.[10]

The impeller inlet vector diagram quantities are displayed in Table 1. The inlet guide vanes, for which the design is reported by B. A. Hopkins,[11] and the inlet ducting were retained from the RC-1 design. Shaft speed was chosen through use of a specific speed of 90 and the RC-1 values of flow and pressure ratio of 4.2 lb/sec and 8:1. The resulting shaft speed is 56,000 rpm as compared with 43,800 rpm for the RC-1.

The impeller exit radial velocity choice was a matter of considerable deliberation. A high value of exit velocity decreases impeller diffusion but increases the absolute Mach number at the impeller exit. Logically, the proper value of exit velocity would seem to be that which produces maximum diffusion consistent with off-design requirements. However, the issue is clouded by the possibility that the impeller exit flow quality may deteriorate, even at modest diffusion levels, to the point where subsequent diffusion recovery is reduced.

The impeller internal flow field is considered to be too complex for boundary layer analysis. Simple flat plate calculations were nonetheless used as a guide by F. Dallenbach,[7] who suggested that a relative velocity ratio, outlet to inlet, be 0.6 or above. This value is supported with several sets of test results showing improvements in performance by the elimination of excess diffusion.

The bulk performance correlation indicates that overall efficiency of the RC-2 compressor should vary with exit velocity as shown in Figure 8. In this range of interest, efficiency continues to rise as exit velocity reduces. If a meridional velocity of 400 ft/sec exists at the impeller exit, the shroud stream surface relative velocity ratio, outlet to inlet, will be 0.52. If computed using maximum suction surface velocity, a value of more nearly 0.46 might result. These values are appreciably less than 0.6 minimum as suggested by F. Dallenbach.[7] On the other hand, to achieve a 0.6 value, a meridional exit velocity of 600 ft/sec or higher might be required. At this value the CCP calculation would indicate a considerable loss in efficiency.

---

[8] Davis, D. M. Radial Flow Compressor and Turbine Design Program. Mathematics Sciences Report. Detroit Diesel Allison Division, General Motors. August 1971.

[9] Stanitz, J. D. Some Theoretical Aerodynamic Investigations of Impellers in Radial and Mixed-Flow Centrifugal Compressors. Trans. ASME, Vol 74, pp 473-497. 1952.

[10] Katsantis, T. Computer Program for Calculating Velocities and Streamlines on a Blade-to-Blade Stream Surface of a Turbomachine. NASA TN D-4525. April 1968.

[11] Hopkins, B. A. Inlet Guide Vane Design for Centrifugal Compressor. Research Note RN 69-79, Detroit Diesel Allison Division, General Motors. December 1969.

TABLE 1. ROTOR INLET VECTOR QUANTITIES.

	Hub	Mean	Tip
Radius, ft	0.100	0.171	0.216
Relative velocity, ft/sec	586	944	1203
Absolute velocity, ft/sec	538	619	699
Axial velocity, ft/sec	478	567	651
Absolute tangential velocity, ft/sec	247	248	255
Blade velocity, ft/sec	587	1003	1268
Relative Mach number	0.54	0.87	1.12
Absolute angle, deg	27.3	23.6	21.4
Relative angle, deg	35.4	53.1	57.2
Inlet guide vane exit angle, deg	22.3	24.2	25.0

The final choice in velocity at the exit was taken more nearly after the indications of the performance calculations than the recommendations of F. Dallenbach.[7] Impeller exit blockage, slip factor, and impeller loss numbers were acquired from the CCP calculations. Impeller internal exit design values are shown in Table 2.

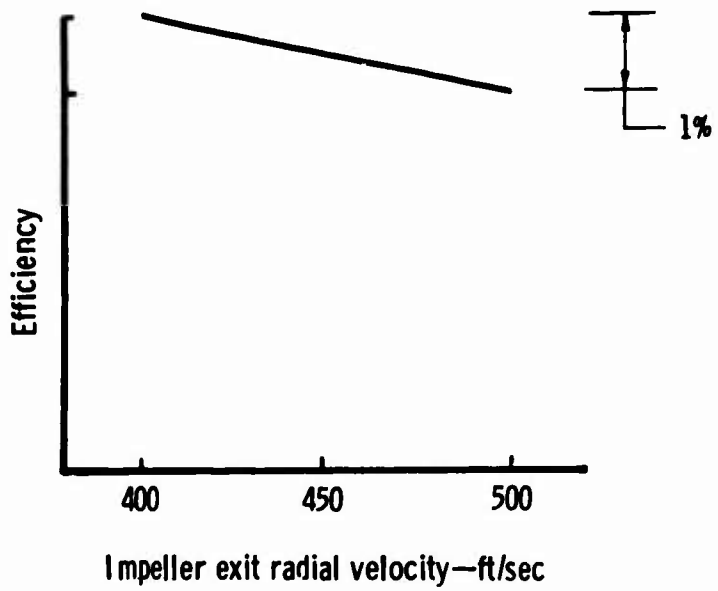

Figure 8. Computed efficiency—velocity trade-off.

TABLE 2. IMPELLER INTERNAL EXIT VALUES.

Radius, in.	4.224
Wheel speed, ft/sec	2064
Average velocities, ft/sec	
Radial	480
Relative	672
Tangential	1593
Absolute	1664
Average angles, deg	
Blade (from radial)	32.5
Relative (from radial)	44.5
Absolute (from tangential)	16.8
Average absolute Mach number	1.205
Slip factor	0.920
Aerodynamic blockage, %	24.5
Exit flow-path width, in.	0.336
Exit vane metal blockage (circumferential), %	5.9

The impeller vane surface velocities, as computed, are shown in Figures 9 and 10. Shown are shroud and hub streamline velocities for pressure and suction sides of the vane. The velocities on the shroud stream surfaces (Figure 9) show a rapid diffusion in the very early portion of the impeller. This is primarily caused by inducer throat sizing. With a desire to maintain inlet dimensions, suitable maximum flow capacity must be obtained by incidence or blade angle change from inlet to throat. The blade tip incidence was adjusted according to experience on transonic axial stages. In so doing, consideration was given to the fact that the flow field at the inducer inlet was not computed in the same manner as normally used for transonic stages. In axial stages, the flow field within the blade row has not been computed. In consequence, the effect of blade blockage and local blade turning has not been reflected in the vector diagrams normally computed as stage inlet. In the centrifugal impeller calculation, considerable effect of blade presence is seen. For this reason, a computation station about 0.6 in. upstream was used as a reference station for considering incidence.

Figure 11 shows the air angles as computed both at the incidence reference station and at the inducer leading edge. Also shown is the blade leading-edge angle. Incidence is defined as air angle minus blade angle. The restrictions imposed on the physical blade shape include the requirement for a straight-line mean blade element at a constant percentage of meridional distance running between specified blade angle schedules, hub and shroud. The result is that only incidence at hub and shroud can be specified. A slightly negative hub incidence was chosen to minimize the magnitude of positive incidence at the mean radius.

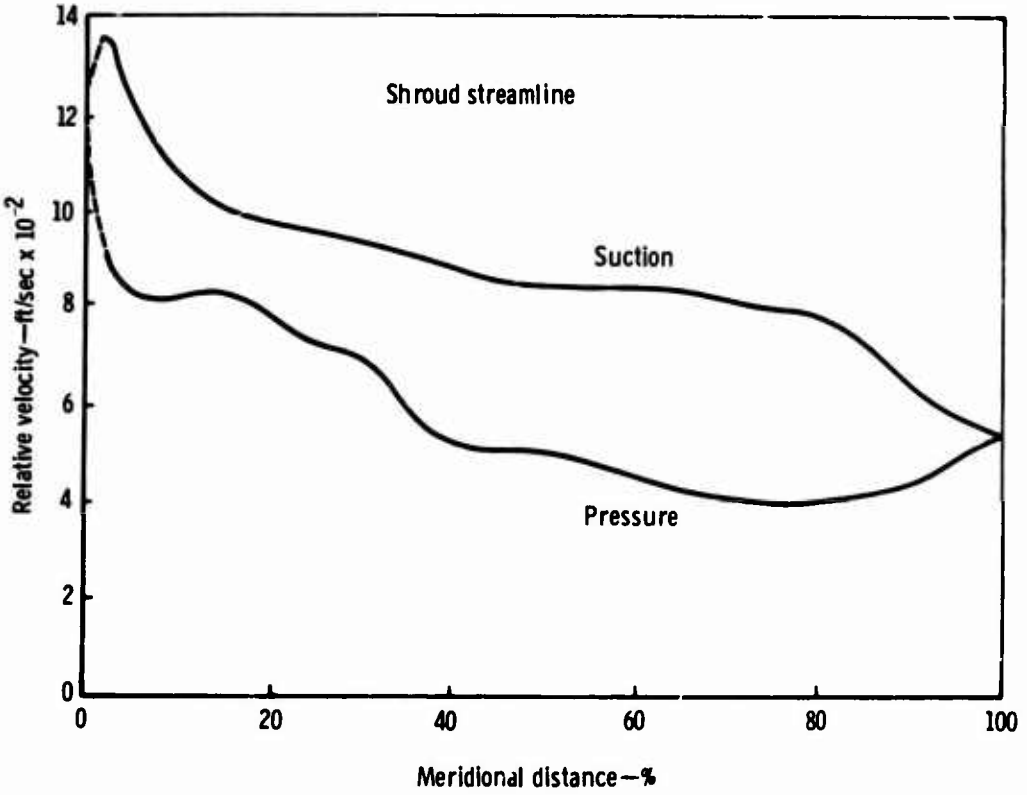

Figure 9. Impeller vane surface velocities at design point—RC-2 shroud.

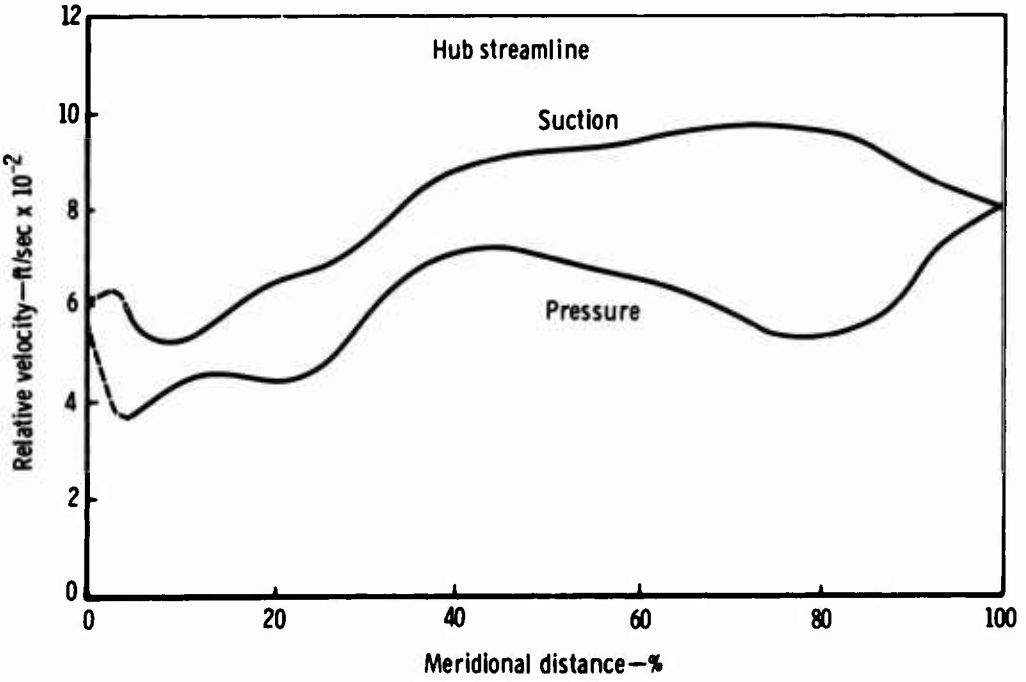

Figure 10. Impeller vane surface velocities at design point—RC-2 hub.

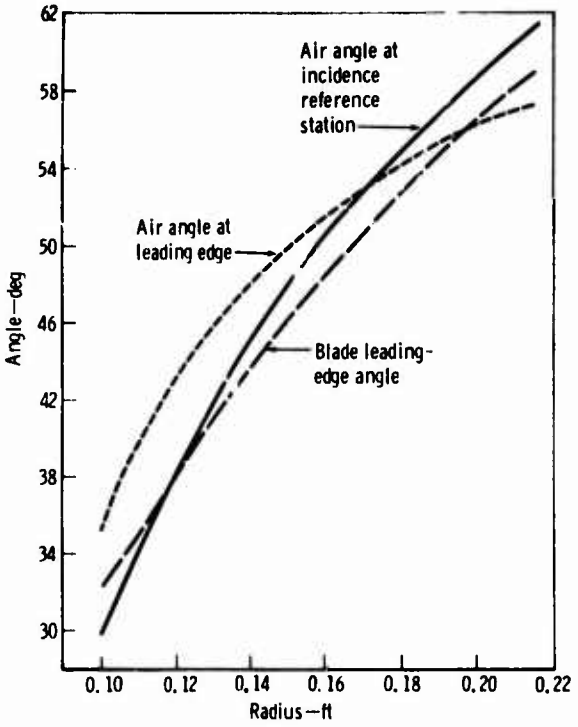

Figure 11. Angle distribution at impeller inlet.

Choke margin has been assessed at 7% by using the average velocity at the throat location as computed by the potential flow solution. This simple method of computed flow capacity was 1% low when compared with test data on a similar design.

The vane surface velocities—and particularly the vane-to-vane differential—are largely a function of the turning angle distribution and the number of vanes. The RC-1 impeller contained 16 primary vanes, 16 splitters, and 32 secondary splitters. In reducing the wetted area, all of the vanes could be reduced in proportion. A different choice was made in the RC-2, according to the following reasoning. The introduction of splitters abruptly reduces the loading by a factor of 2 and introduces local blockage at the same point. Uniformity of loading distribution is thus compromised. However, maintenance of a reasonable maximum level of loading does require splitters. The secondary splitter location, necessarily well aft in the flow path, produces the possibility of poor incidence matching because of the questionable flow field calculation.

For the RC-2 design, the secondary splitters were abandoned, while the number of vanes was maintained at 16. The loading distribution was adjusted by scheduling the tangential turning. In the zone where the secondary splitters would normally be required, loading was reduced by back turning. This load was, in turn, picked up in the knee of the impeller, where solidity is still high, by overturning. The tangential turning angle schedule is shown in Figure 12. The values were basically chosen for the shroud, while hub values result from the need for the vane itself to be essentially radially oriented for stress reasons, except for the latter portion of the flow path. In the 80-to-90% position of the flow path, the hub angles were held to zero. The result is that the back-curved impeller can be machined to a lesser diameter to make a radial bladed impeller of approximately the same pressure ratio output. (That is, there is very little blade loading in the last 8% of the blading.)

DIFFUSER DESIGN

A pipe-type diffuser was chosen for the design. The basic changes featured, as compared with the RC-1, are in the choice of diffuser inlet-to-impeller tip radius ratio and in departure from a constant-width vaneless space.

The effect of radius ratio on vaneless space loss, diffuser inlet Mach number, and efficiency to the diffuser exit (Mach No. = 0.35) is shown in Figure 13. Diffuser pressure recovery is held at a constant value of 0.70, and vaneless space loss is from the CCP analysis. Although the vaneless space loss increases with radius ratio, the reduced diffuser inlet velocity allows somewhat greater pressure to be developed at the diffuser exit and, therefore, better compressor efficiency. However, insufficient data have been available at the higher values of radius ratio to establish complete confidence in that design regime. In reality, diffuser pressure recovery may vary with radius ratio. The radius ratio for the RC-2 was chosen to be 1.13, comparable with a reworked RC-1 configuration.

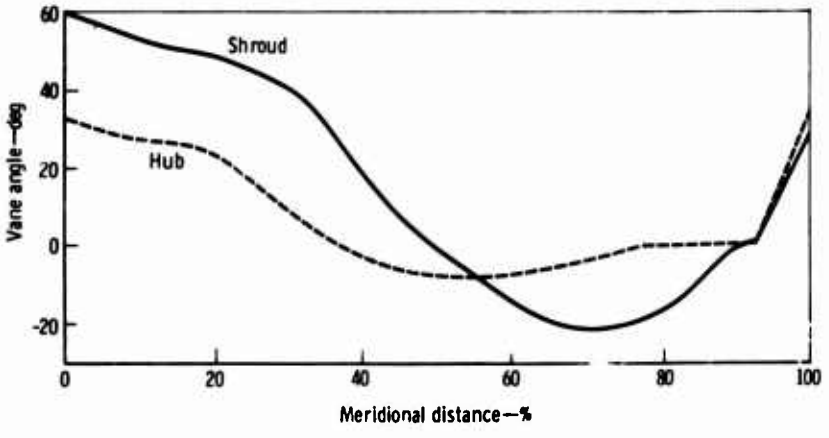

Figure 12. Impeller vane angle schedule.

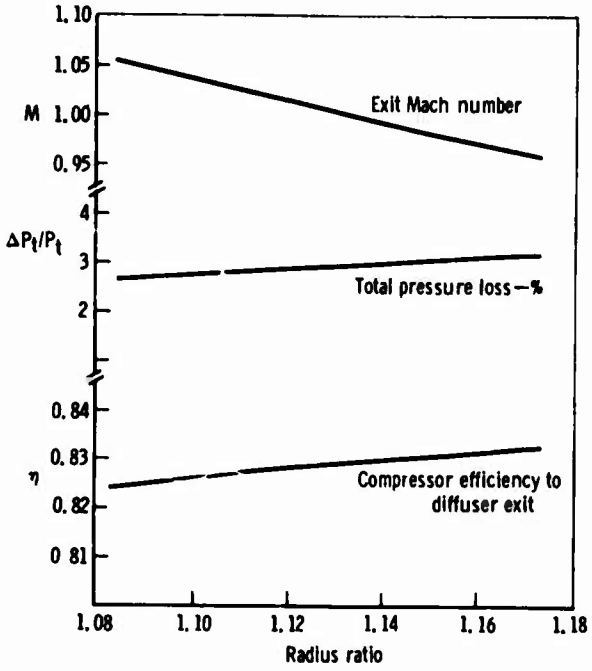

Figure 13. Vaneless diffuser.

To reduce the boundary layer buildup on the vaneless space walls, the width was reduced in proportion to radius change. Thus, the physical area was maintained constant with radius up to the radius where the pipe ridges are encountered.

Geometrical relationships among the many variables involved dictate the exact dimensions used. A constant width was used from the constant area section to the diffuser throat. Thus, the throat diameter is identical to the final width in the constant area section The throat width is set by choke requirements. Figure 14 shows the trend of the dimensional requirements. A choice of 27 pipes in the diffuser was made. The variable width section terminates at the pipe centerline tangency radius, and thus does not enter the pipe ridge zone.

The throat area was chosen to provide a 2% margin to choke. The area is further adjusted to allow for losses and blockage totaling 8%, according to Figure 15, which was taken from Morris and Kenny.[12]

[12] Morris, R. E., and Kenny, D. P. High-Pressure Ratio Centrifugal Compressors for Small Gas Turbine Engines. Report No. 6, 31st Meeting of the Propulsion and Energetics Panel of AGARD, Ottawa, Canada. June 1968.

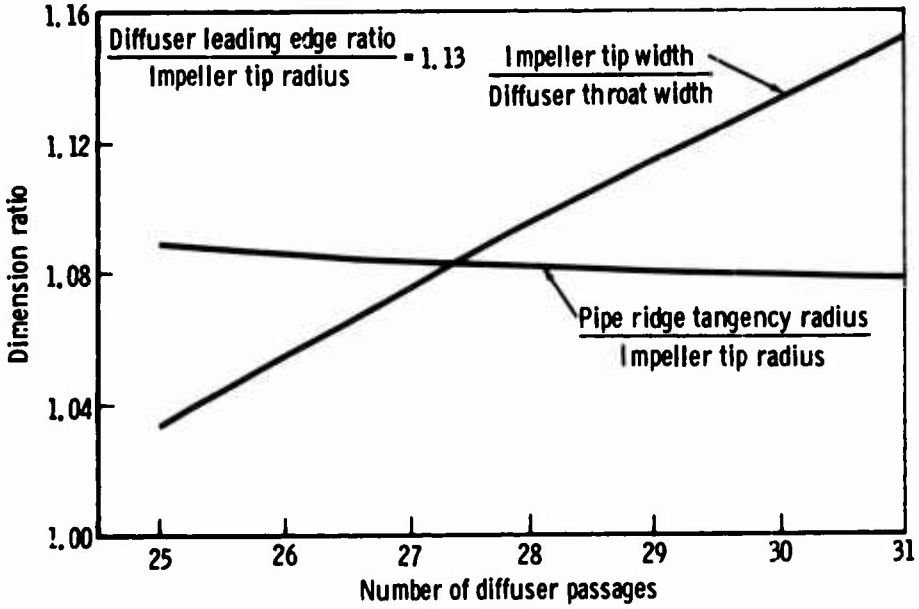

Figure 14. Vaneless diffuser geometry for fixed throat.

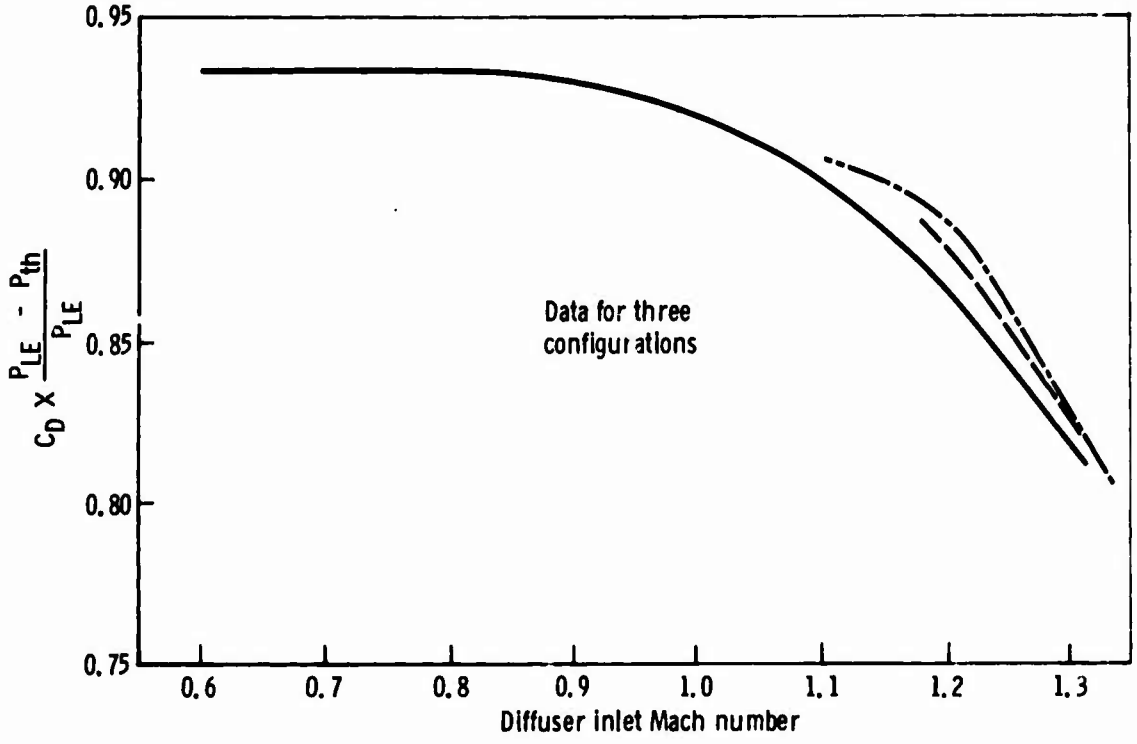

Figure 15. Pipe diffuser throat blockage factor.

The diffuser exit Mach number is designed to be 0.35. Diffuser geometry was chosen primarily by reference to high Mach number data from two-dimensional diffusers as discussed by Runstadler and Dean.[3] A cross plot of data taken from that report[3] is shown in Figure 16. Performance and geometry for two area ratios are shown plotted against blockage. The blockage at choke of the RC-1 has been computed to be 3.5%, assuming a one-dimensional throat flow. However, this blockage definition is not compatible with the Figure 16 blockage definition. One to two percent apparently must be added to the 3.5% in order to use these data from Runstadler and Dean.[3]

The area ratio was chosen as 2.15. The diffuser length was based on a length-to-inlet radius ratio of 11.5.

As on the original design, there was no attempt made to convert the diffuser exit velocity to a higher pressure. It was recognized that there is, in general, a requirement in engine use for a lower compressor exit Mach number. The performance of a secondary diffuser is conservatively estimated when data are presented to a lower level of Mach number. A value of static pressure recovery of 0.30 to a Mach number of 0.15 was assumed for performance calculation.

The diffuser design parameters are presented in Table 3.

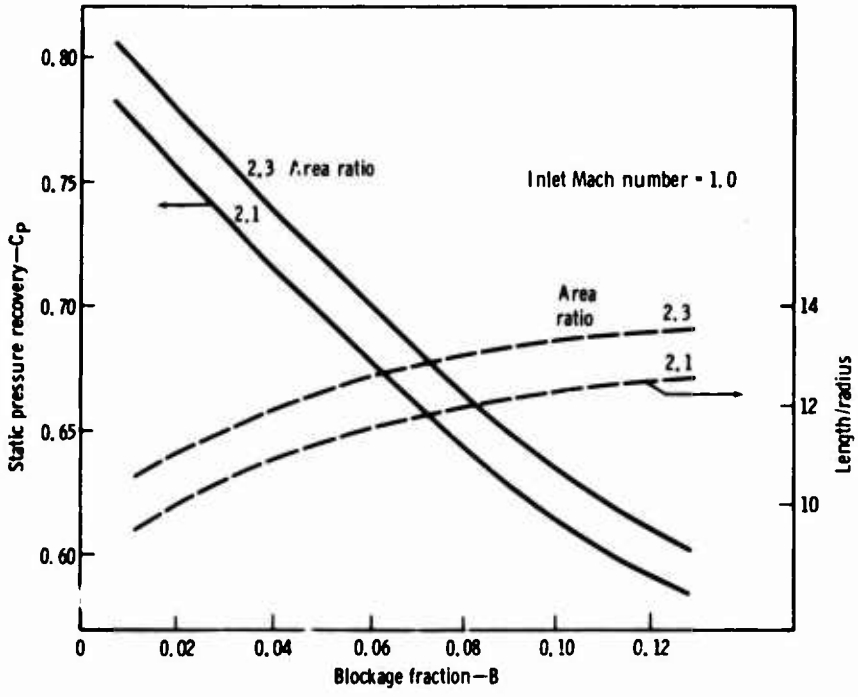

Figure 16. Plane wall diffuser performance.

TABLE 3. DIFFUSER DESIGN PARAMETERS.

Vaneless space	
Exit radius (leading edge), in.	4.773
Width at inlet, in.	0.336
Final width, in.	0.3125
Radius at final width (tangency), in.	4.5484
Total pressure loss, %	2.9
Diffuser	
Number of pipes	27
Throat diameter, in.	0.3125
Total throat area, $in.^2$	2.07089
Leading-edge wedge angle, deg	8.7
Leading-edge mean angle from tangential, deg	16.4
Diffuser exit/throat area ratio	2.15
Diffuser exit radius, in.	6.018
Length to inlet radius ratio	11.5
Included cone angle, deg	4.6
Inlet Mach number	1.00
Exit Mach number	0.35
Static pressure recovery coefficient	0.70
Total pressure drop, %	6.6

PERFORMANCE

The compressor performance was computed by means of the performance prediction calculation CCP.

In actual compressor rig operation, overall performance was measured at the diffuser exit. Design Mach number was 0.35. A conservative static pressure recovery of 0.30 was used as an assessment of probable collector and diffusion loss to a Mach number of 0.15. Performance numbers were quoted both at diffuser exit and after allowing for the previously mentioned loss for further diffusion.

The performance details are given in Table 4; the pressure ratio shown is the originally computed value of 8.3 at an efficiency of 0.807 (total-to-total at a Mach number of 0.15) and a flow rate of 4.2 lbm/sec. Later computations with a different slip factor formulation slightly modified these original design numbers to a pressure ratio of 8.5 and an efficiency of 0.805 at a Mach number of 0.15. These modified design numbers are those quoted in the proposal which led to the contract work reported herein.

TABLE 4. DESIGN PERFORMANCE.

	Original design value		Value quoted in contract (Table 9)	
Flow rate, lbm/sec	4.2		4.2	
Shaft speed, rpm	56,000		56,000	
Specific speed	85		85	
Pressure ratio and efficiency developed	R_c	η	R_c	η
Impeller exit	9.67	0.884	9.777	0.8895
Diffuser leading edge	9.30	0.864	9.54	0.869
Diffuser exit	8.68	0.829	8.857	0.825
Adjusted to Mach number = 0.15	8.32	0.807	8.5	0.805

MECHANICAL DESIGN

The mechanical design effort consisted of that required to validate the integrity of the new parts and to adapt the new design to the existing rig. Thus, certain parts were new as necessary for dimensional adaptation. The major design effort, however, was the stress and vibration analysis and accommodation of results into the rotating parts.

The rig layout may be seen in Figure 17. Air is taken from a 30-in.-diameter inlet plenum by an inlet bell. Between the inlet bell and the impeller, inlet guide vanes are cantilever mounted from the outer wall. The inlet guide vanes are adjustable in angle. The inlet bell structure contains four struts supporting an inner body and results in an annular flow path forward of the impeller. This construction was used to provide a location for installing a shaft-driven strain gage signal transfer device. This provides the structural capability for acquiring stress and vibration data from the impeller, should it appear necessary.

The inlet ducting as previously discussed is unmodified from the RC-1 for the new design, except for an adaptor that fills in a gap in the hub flow path.

The impeller is, of course, a new design. The covering shroud also is new. The existing RC-1 shroud could have been reworked to accommodate the new impeller, but it was retained to continue testing the RC-1 design. The diffuser also is a new design. The diffuser and shroud are mounted on the main support, which is unchanged except for minor rework.

As on the RC-1, the shaft is integral with the impeller. Detailed rotor dynamic analysis of the system showed that use of the existing bearings and bearing support system would produce excessive radial excursions of the coupling end of the shaft at the new design speed. To avoid this, that end of the shaft required a larger diameter, which, in turn, forced the use of a larger diameter bearing. Thus, a new bearing housing was required.

The rotor dynamic analysis is reported by R. Trent.[13] The report states that, while vibratory response is expected to be within acceptable limits, a soft mount for the front bearing should be considered. Therefore, sufficient design effort was accomplished to ensure that the initial hardware could be reworked to provide controlled mount flexibility in the event it should be required.

The impeller design was subjected to a vibration analysis as reported by L. Burns.[14] Natural frequencies of the primary vane, splitter vane, and wheel were computed. Certain potential vibratory modes were identified. However, it is believed that excitation forces for these points do not exist to sufficient degree to warrant concern.

A stress analysis was made on the titanium impeller, and reported by M. Clute.[15] Stresses were computed and are quoted at 7% overspeed. Maximum steady-state stress in the vanes of 54,000 psi occurs in the inducer section of the primary vane. A value of 52,000 psi occurs at an intermediate meridional position on the primary vane. Splitter vane stresses do not exceed these values. No significant level of stress was computed in the region of the back-curved tip section.

With an assumed 15,000-psi vibratory stress for 10^7 cycles, this titanium material can sustain a steady-state load of 76,000 psi.

The maximum wheel stress, 74,000 psi, occurs at the rear face near the hub. The wheel has no bore. The ultimate tensile strength of the material at 200°F is 119,000 psi.

---

[13]Trent, R. Dynamic Analysis RC-2 Compressor Rotor Case System. Engineering Department Report TDR AX.0220-016, Detroit Diesel Allison Division, General Motors. June 1972.

[14]Burns, L. Vibration Analysis of the RC-2 Impeller. Engineering Department Report TDR AX.0201-037, Detroit Diesel Allison Division, General Motors. July 1972.

[15]Clute, M. Stress Analysis of the RC-2 Impeller. Engineering Department Report TDR AX.0201-036, Detroit Diesel Allison Division, General Motors. July 1972.

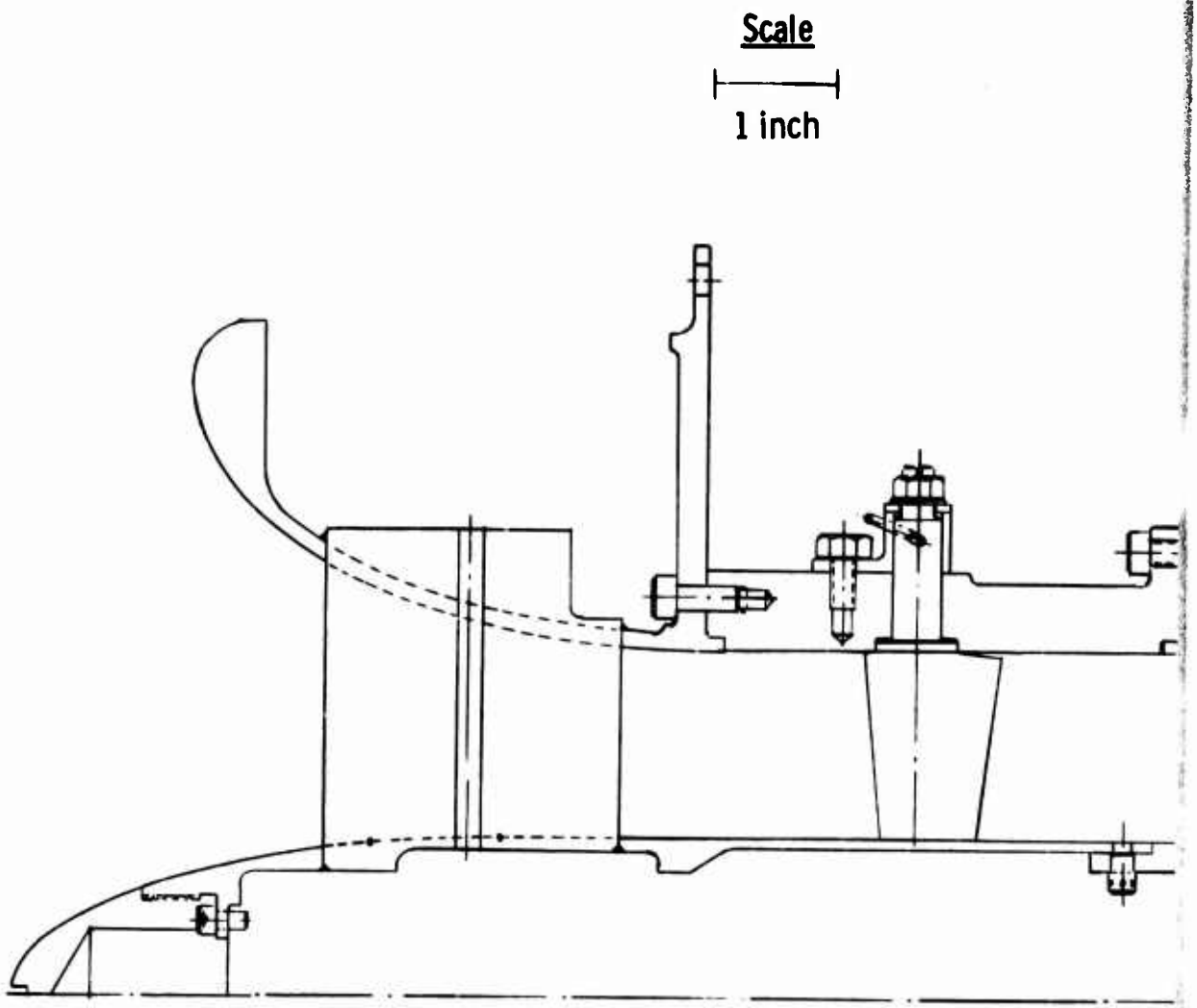

Figure 17. Compressor rig layout.

A

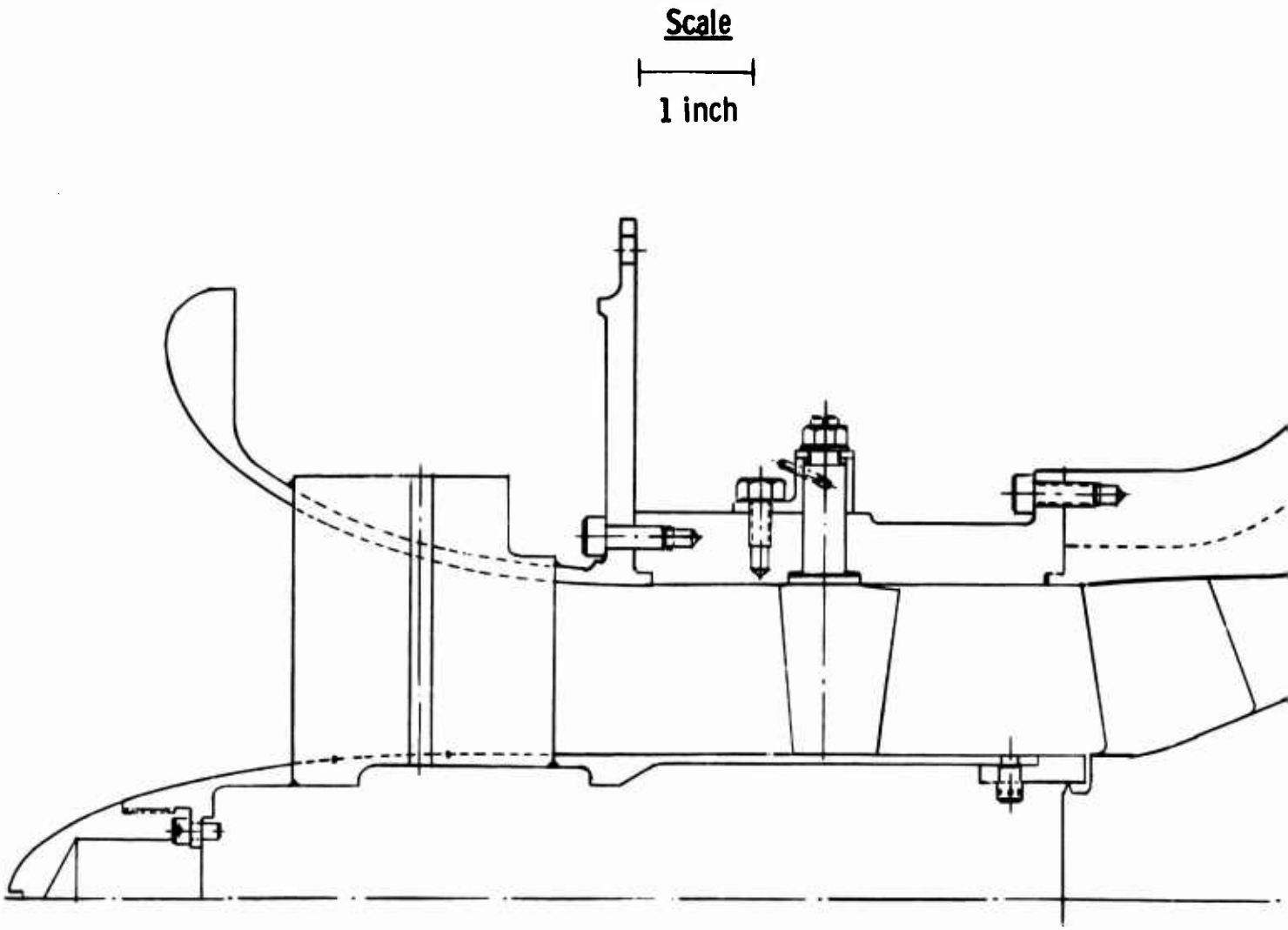

Figure 17. Compressor rig layout.

B

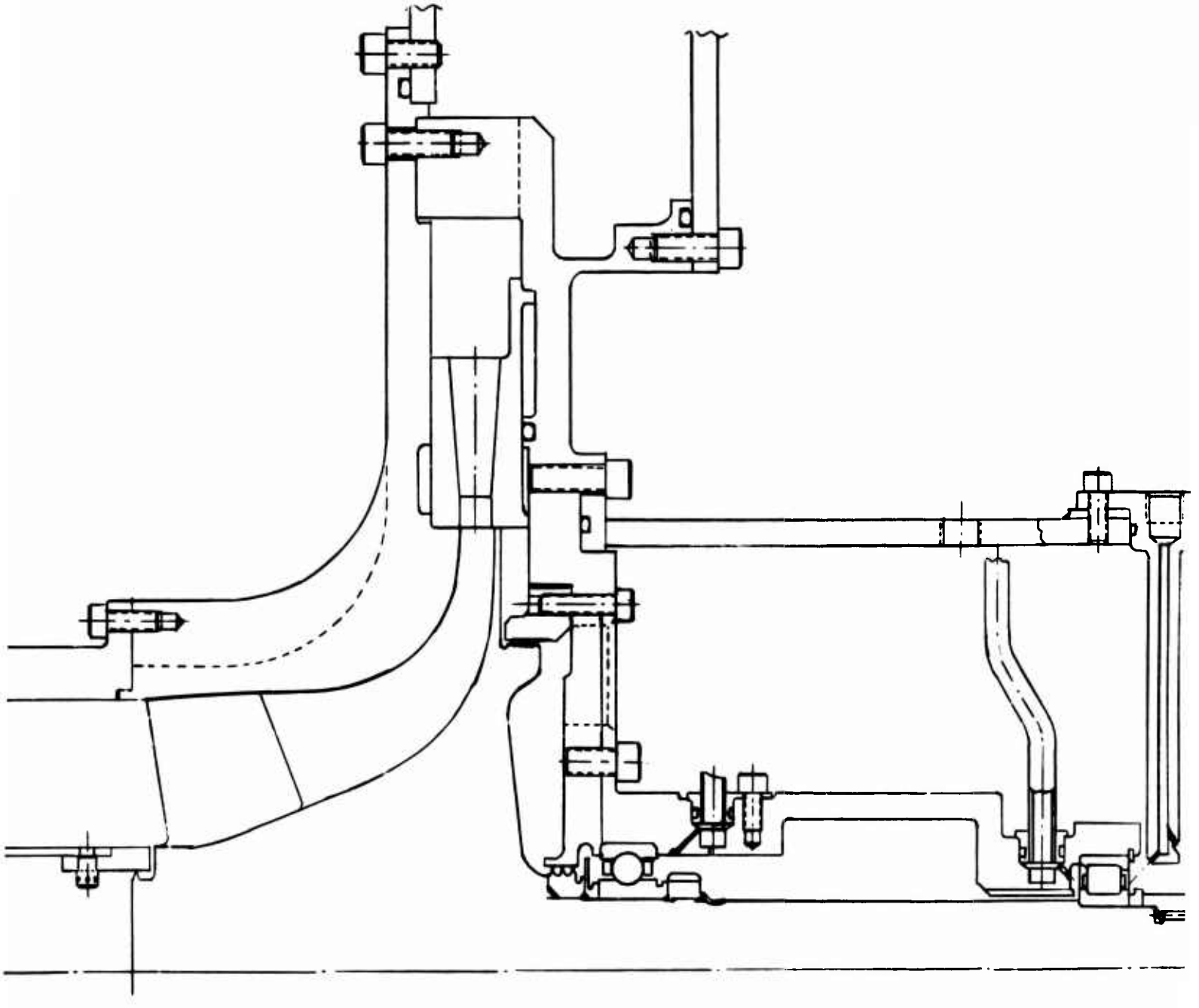

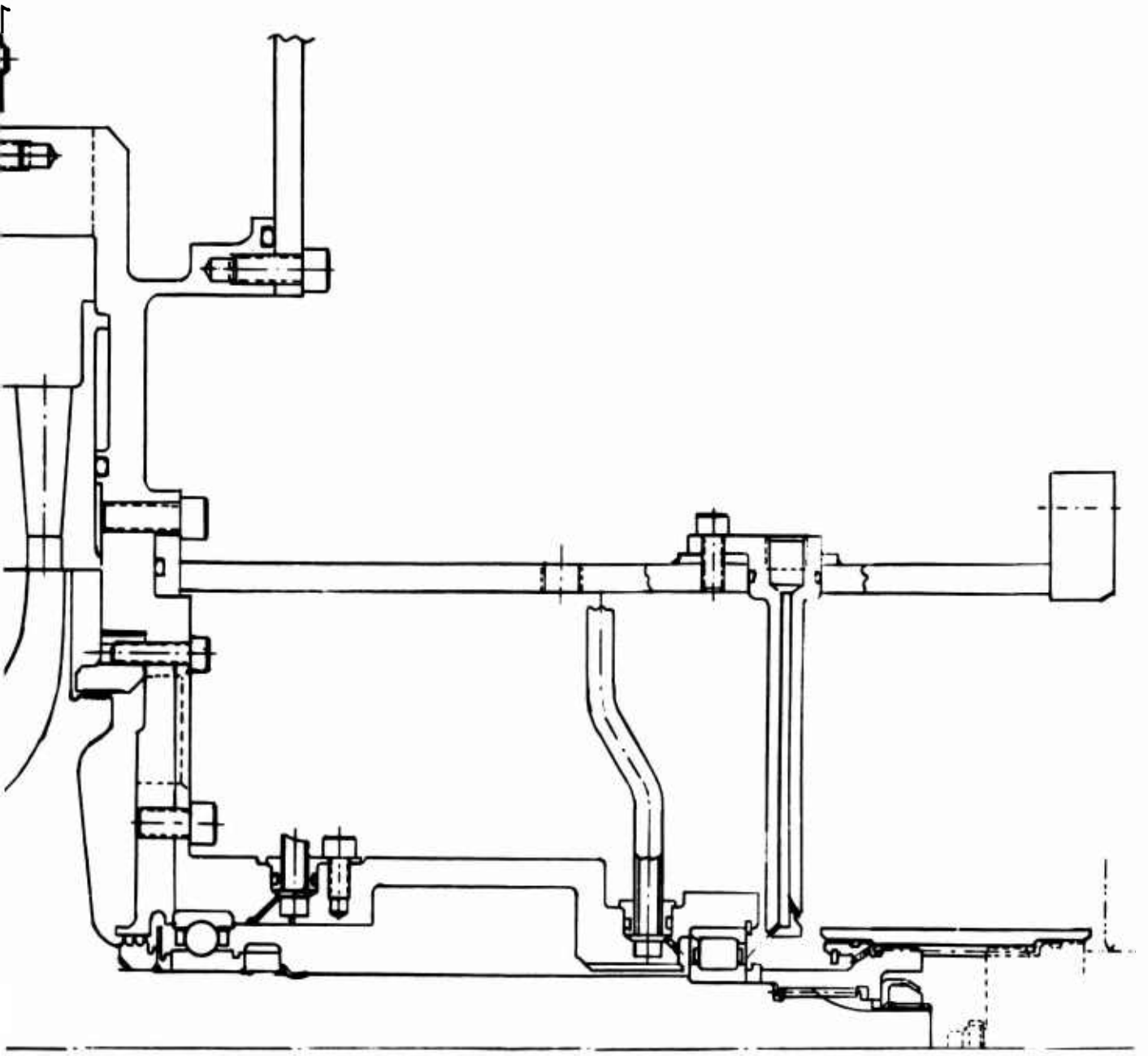

These wheel and blade stresses were arrived at with an anticipated thermal pattern imposed as reported by Colborn.[16] Final wheel stress values are given in Figures 18 and 19.

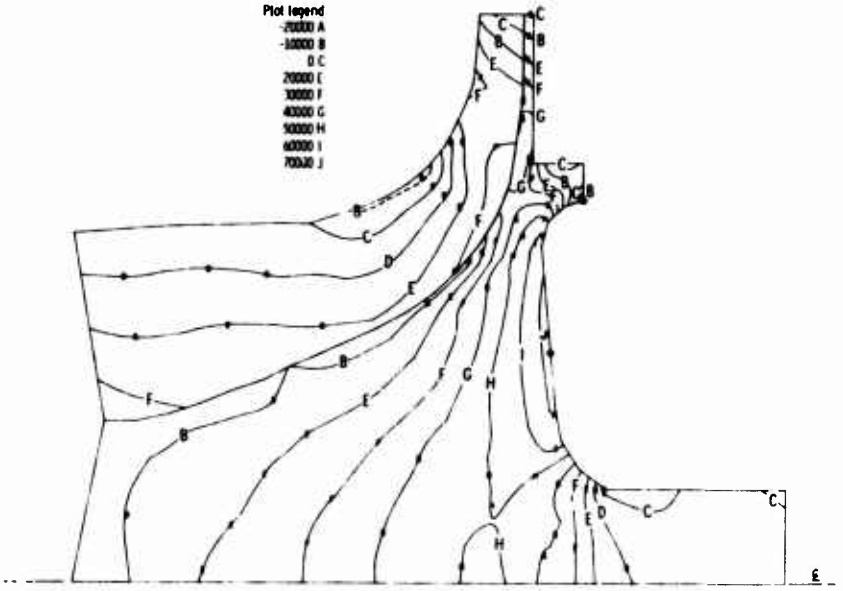

Figure 18. RC-2 impeller radial stress.

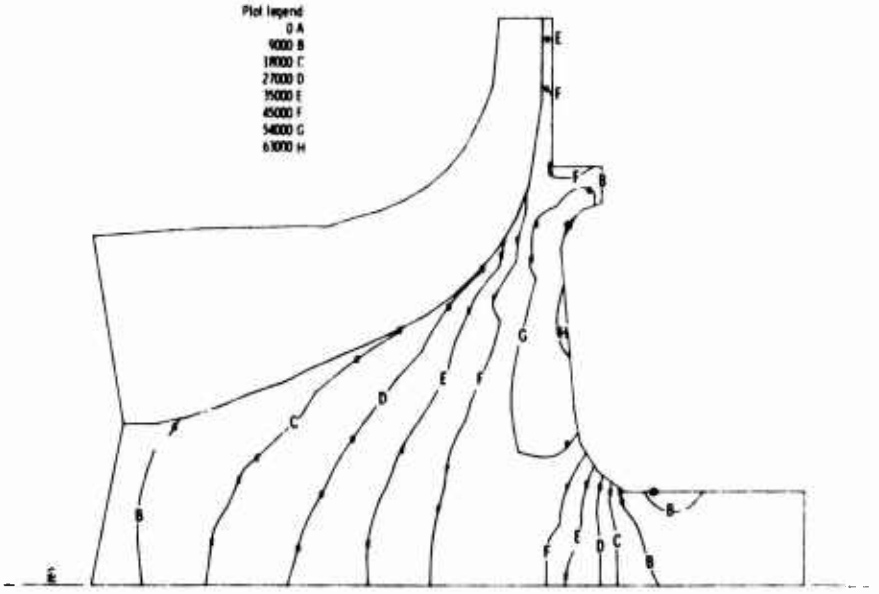

Figure 19. RC-2 impeller tangential stress.

[16]Colborn, J. H. Temperature Distributions in the RC-2 Impeller. Engineering Department Report TDR AX.0201-035, Detroit Diesel Allison Division, General Motors. May 1972.

III. COMPRESSOR TESTS

The RC-2 compressor was tested and modified to determine the degree of validity of the performance analysis previously described. The first, or baseline, test was run with the compressor "as designed," and at two inlet guide vane settings other than the design setting. This build of the compressor is designated RC-2.5. RC-2.1 through RC-2.4 were short rig mechanical check runs necessitated by initial rotor whip and vibration difficulties. Instrumentation checks were also obtained during these tests. The tests resulted in the addition of six rear bearing stiffening struts.

The second test, RC-2.6, was run with the inlet guide vanes twisted +8 deg at the hub and -8 deg at the tip, and with the diffuser plated so as to decrease the throat area by 4%. These compressor modifications were made as a result of the analysis of the RC-2.5 data, which indicated:

- Impeller exit hub-to-shroud total pressure and angle profiles were weak on the shroud side.
- Inducer was starting to choke earlier than the diffuser at design speed.

The third test, RC-2.7, was run with the RC-2.6 hardware, except that the impeller tip diameter was reduced by 7.5%, so the exducer was essentially radial rather than bent back. The radial space between the impeller tip and the original diffuser was reworked to result in a constant-width vaneless space up to the original vaneless space inlet (see Figure 20). This impeller modification was suggested by the very rapid blade curvature in the original exducer design, which apparently resulted in a deviation of the airflow from the blade pressure surface, as evidenced in RC-2.5 and RC-2.6 by the higher than predicted work output of the rotor.

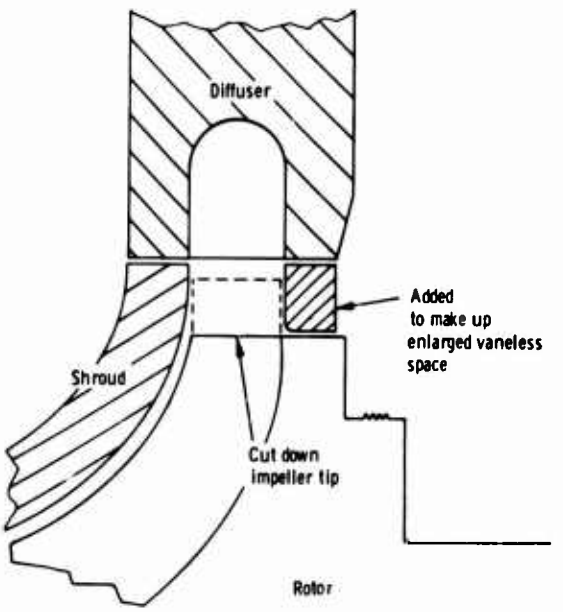

Figure 20. RC-2.7 configuration.

INSTRUMENTATION

The compressor was instrumented in such a manner that the intrastage losses could be deduced as accurately as possible. Additional instrumentation was added as the test program progressed and certain areas of concern emerged.

RC-2.5 Instrumentation

Inlet Station

The compressor's inlet total temperature and pressure were measured upstream of the inlet in a large (36-in.-diameter) plenum. The instrumentation consisted of four static pressure taps and four total temperature probes.

Inducer Inlet

Three static pressure taps were distributed circumferentially at each of the following locations:

- On the shroud, before the inlet guide vanes
- On the hub, before the inlet guide vanes
- On the shroud, after the inlet guide vanes
- On the hub, after the inlet guide vanes

In addition, a six-element boundary layer rake was located on the hub behind the inlet guide vanes.

Impeller Shroud

Two rows of eleven static pressure taps each were distributed along the impeller cover. The two rows were separated circumferentially by 125 deg. Three additional taps were distributed circumferentially at the radius of the last pressure tap of the two rows.

Vaneless Space

The vaneless space instrumentation included:

- Eleven static pressure taps were distributed along the presumed flow path from the impeller tip to the diffuser throat, on each of the hub and shroud sides of the diffuser.
- Four static pressure taps were distributed circumferentially to span one diffuser passage at a radius 3% outboard of the original impeller tip radius, on each of the hub and shroud sides of the diffuser.
- Four static pressure taps were distributed circumferentially to span one diffuser passage at a radius 7.7% outboard of the original impeller tip radius (the "tangency" radius of the pipe diffuser), on each of the hub and shroud sides of the diffuser.

- Three total pressure probes were imbedded in the leading edge of the diffuser, one at the apex of the leading edge, and one on either side of the apex. The apex total pressure probe consistently read a value lower than the maximum diffuser outlet total pressure, thus indicating that this probe was operating at some significant incidence to the flow, so this pressure was discounted.

Diffuser Inlet Throat

Seven static pressure taps were located in the throat of the diffuser. The taps were located 45 deg apart around the circular throat, as shown in Figure 21.

In addition, a static pressure tap was located 0.10 in. ahead of and 0.10 in. behind the throat on the shroud side of the diffuser.

Diffuser Passage

One static pressure tap was located on each of the hub and shroud sidewalls of the diffuser, one-half the distance between the diffuser's throat and exit plane.

Diffuser Exit Plane

Three static pressure taps were located at the diffuser outlet: one on the pressure surface, one on the hub side, and one on the shroud side of the diffuser.

Two 3-element and two 2-element total pressure rakes were located at the diffuser exit. The location of the diffuser exit instrumentation is shown in Figure 22.

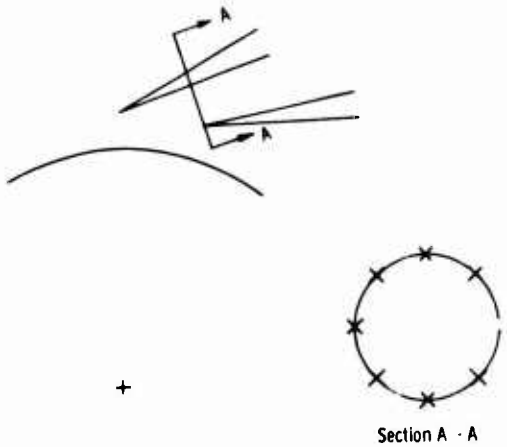

Figure 21. Throat pressure taps.

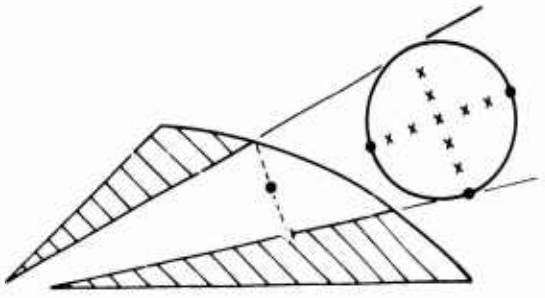

x Total pressures (or temperatures)

• Static

Note: Each passage contains only two or three probes: Pattern shown is a superposition of all the instrumentation in one passage.

Figure 22. Diffuser exit plane instrumentation.

An identical arrangement with thermocouples instead of pressure rakes was also included at the diffuser exit. No more than one of the rakes was positioned at any diffuser passage exit. Thus there were rakes positioned behind eight of the twenty-seven diffuser passages.

Collector Outlet

Three 3-element thermocouple rakes were located at the collector outlet in the pattern indicated in Figure 23.

Impeller Outlet Traverse Data

Two specially designed total pressure probes were used to traverse the vaneless space at a radius 7.7% outboard of the impeller tip radius (i.e., at the diffuser "tangency" radius). These probes were located 180 deg apart, so they were one-half passage apart with respect to a diffuser passage. The probes were steel cylinders of 0.032 in. dia, with a single 0.007-in.-dia sensing hole. These probes were yawed at each axial traverse station until the maximum pressure reading was obtained and recorded. The probes were then yawed in one direction until a suitable lower pressure was obtained, and this yaw angle was recorded. The probes were then rotated in the opposite direction until this last pressure was duplicated, and the angle was recorded again. The measured flow angle was taken to be the average of the two last recorded angles. However, the angle level was modified in the data reduction program to match continuity, thus accounting for zero point calibration errors and circumferential angle variations. In addition, two special thermocouple probes were subsequently substituted for these pressure

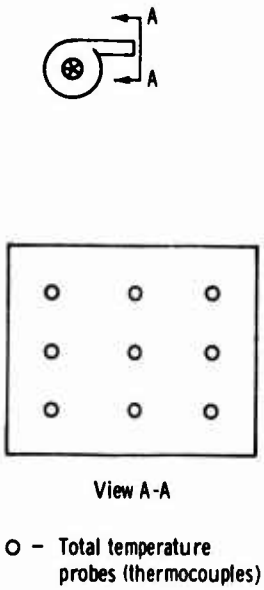

Figure 23. Collector outlet instrumentation.

probes and used to obtain the flow total temperature distribution at the same two locations as the total pressure traverses. These temperature probes consisted of steel cylinders of 0.032 in. outer diameter, with two 0.015-in.-dia holes 1 ° deg apart and axially displaced by 0.032 in. A thermocouple was located halfway between these two holes. The thermocouple was formed by laser-welding two 0.001-in.-dia wires (iron and constantan) together. No attempt was made to modify the readings of these probes for recovery factor and wire correction effects. The traverse data were deleted from the 17-deg inlet guide vane test of RC-2.5 for economic reasons.

RC-2.6 Instrumentation

The RC-2.6 compressor test included all the instrumentation described for the RC-2.5 test, except that no temperature traverses were obtained.

RC-2.7 Instrumentation

The RC-2.7 compressor test included all the instrumentation described for the RC-2.5 test, except that no temperature traverses were obtained.

Additional instrumentation was provided the compressor for this test in the region of the impeller tip, the diffuser throat, and the collector exit as follows:

- The impeller tip additional instrumentation consisted of five static pressure taps distributed circumferentially to span one diffuser passage (i.e., 13.33 deg) at the new impeller outlet radius of 3.91 in.
- The diffuser inlet throat additional instrumentation consisted of:
  - Seven static pressure taps 0.08 in. apart, with the center one at the throat and the others along the pipe centerline on the shroud side
  - Four static pressure taps duplicating the one 0.08 in. upstream of the throat in four other passages
  - Three special removable total pressure probes located 0.05 in. behind the throat along the pipe centerline. These total pressure probes were removable and could be replaced by "blanks" (see Figure 24).
- The added instrumentation at the collector exit consisted of a single total pressure probe and a single static pressure tap.

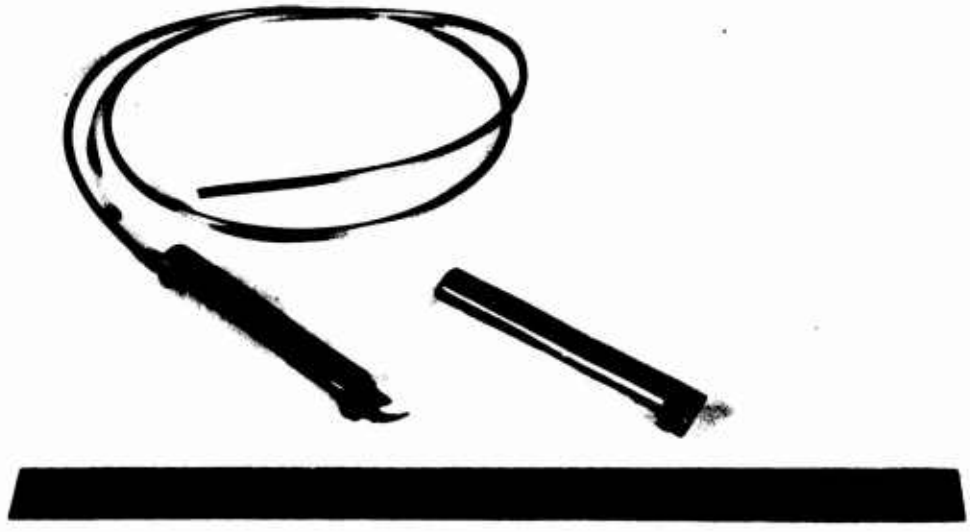

Figure 24. Removable throat total pressure probe (left).

Performance Measurements

The compressor's performance was defined in terms of airflow rate, pressure ratio, speed, and efficiency. The compressor performance is shown later.

The airflow rate was measured by means of an ASME square-edge orifice plate and was corrected to standard conditions. This orifice meter was calibrated and shown to conform to the ASME standards[17] and had an accuracy of ±1/2% of the flow.

The compressor's pressure ratio was the ratio of the arithmetic average of the measured diffuser exit total pressure to the arithmetic average of the measured inlet pressure. This measurement has an accuracy of better than ±1/4%. The quoted compressor efficiency was the true adiabatic efficiency (i.e., calculated from the enthalpy tables rather than using a constant specific heat ratio). The efficiency calculated using a constant $\gamma = 1.4$ would be higher than the true value by about 1% at a pressure ratio of 8:1.

$$\eta_{\text{adiabatic}} = \frac{(H_2 - H_1)_{\text{ideal}}}{(H_2 - H_1)_{\text{actual}}}$$

$$= \frac{H_{2\ \text{ideal}} - H_1}{H_{2\ \text{actual}} - H_1}$$

The ideal enthalpy rise $H_{2\ \text{ideal}} - H_1$ was obtained for the achieved pressure ratio from the gas tables in Reference 18; the actual enthalpy rise $H_{2\ \text{actual}} - H_1$ was obtained from the measured arithmetic average temperatures at the inlet and the collector outlet. To ensure that no heat was lost between the diffuser exit and the collector exit, the entire compressor was wrapped in fiberglass insulation. The diffuser exit temperatures were not used to calculate efficiencies because of the large and varied thermocouple recovery corrections required at the diffuser exit, where the transverse Mach number gradients are very large. However, the corrected temperature measurements taken at the diffuser exit do in fact agree fairly closely with those taken at the collector exit.

The accuracy of the efficiency measurement is approximately ±1/2% at design speed.

The speed of rotation at the compressor is measured by a digital tachometer mounted on the control panel in the test stand. The accuracy of this instrument is better than ±1/10 of 1% of the reading.

---

[17] Flow Measurement. ASME Power Test Code Committee, ASME, New York. 1959.

[18] Keenan, J. H., and Kaye, J. Gas Tables. John Wiley and Sons, Inc., New York. 1961.

RC-2.5 BASELINE TEST

The RC-2.5 compressor was tested for performance with 17, 25, and 33 deg inlet guide vane settings. Yaw/pressure and yaw/temperature traverses of the impeller outlet flow were performed at the 25 and 33 deg inlet guide vane settings. These traverses could be executed for choked flow conditions only, as the compressor surged prematurely with the probes installed. The impeller and diffuser are shown in Figures 25 and 26.

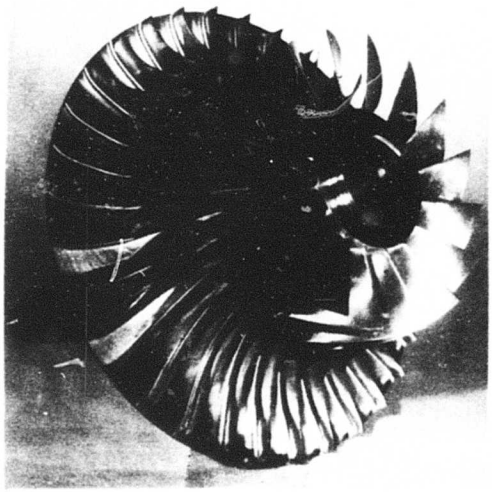

Figure 25. RC-2 impeller (RC-2.5 and RC-2.6 configuration).

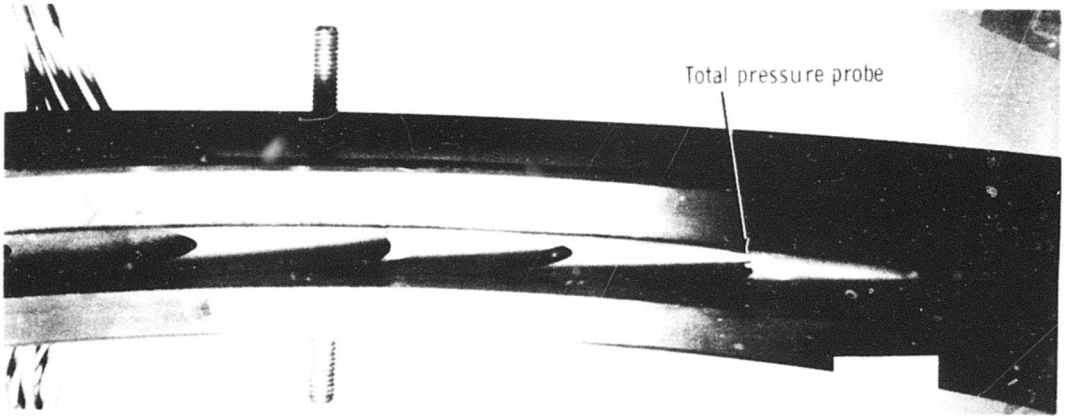

Figure 26. RC-2 diffuser.

The test period was 24 September 1973 to 4 October 1973. The reading numbers were 266 to 460. A configuration summary follows:

Configuration	Baseline RC-2.5 ("as designed")
Impeller	P/N EX-106488
Diffuser	P/N EX-106583 27 Pipe
IGV assy	P/N EX-99257
Collector	P/N EX-99270
Cover	P/N EX-106582
Impeller tip	Cold clearance: 0.035 in.

Compressor Performance Data

Compressor performance maps for each of the three inlet guide vane settings are presented in Figures 27 through 35. The efficiency and pressure ratio plotted in these figures are based on total pressure measurements at the diffuser exit and total temperature measurements at the collector exit.

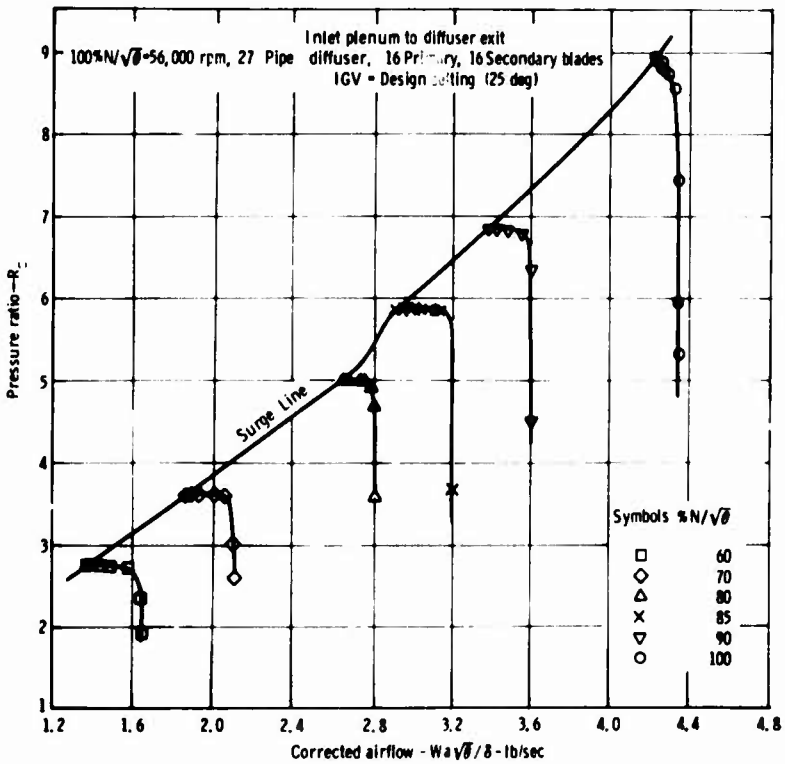

Figure 27. RC-2.5 performance—25 deg IGV setting.

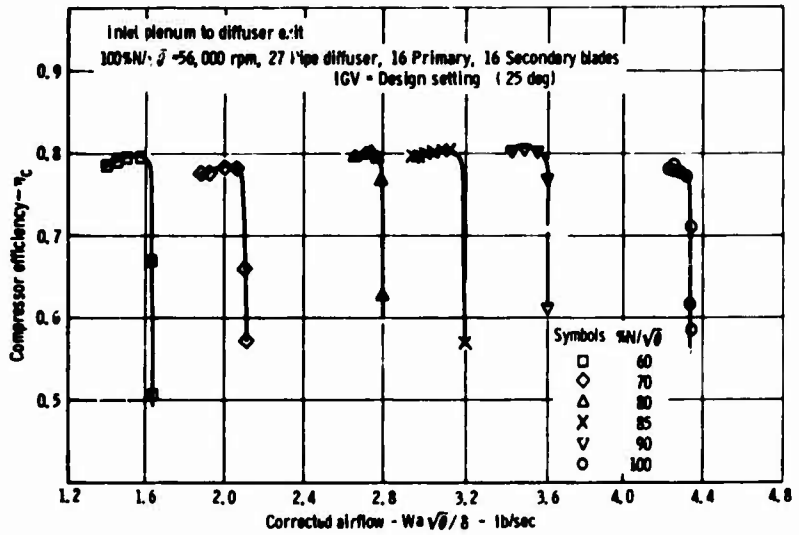

Figure 28. RC-2.5 performance—25 deg IGV setting.

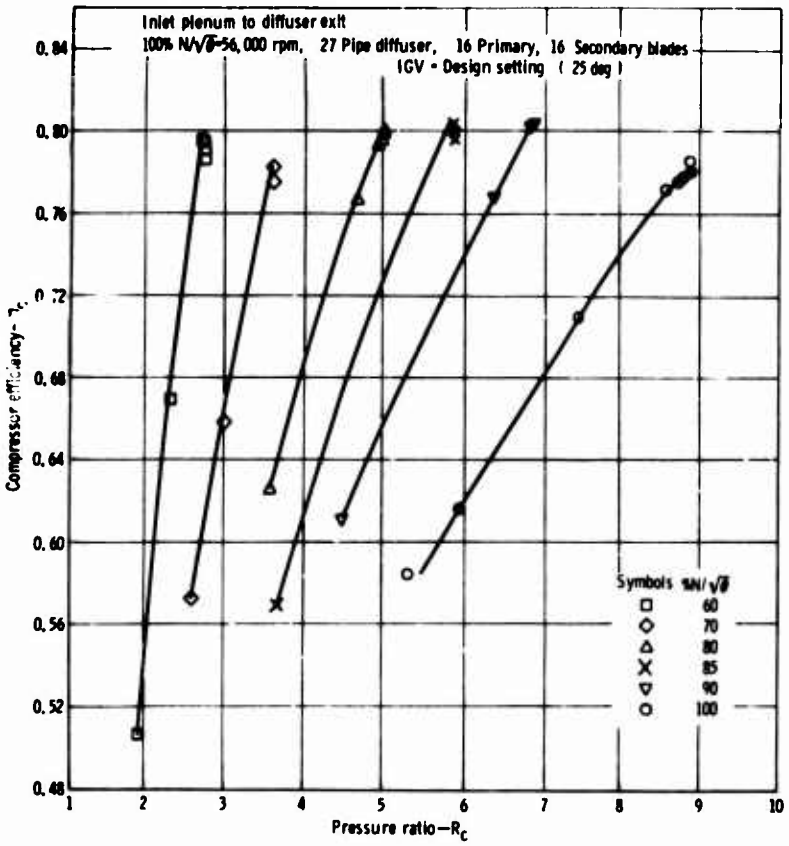

Figure 29. RC-2.5 performance—25 deg IGV setting.

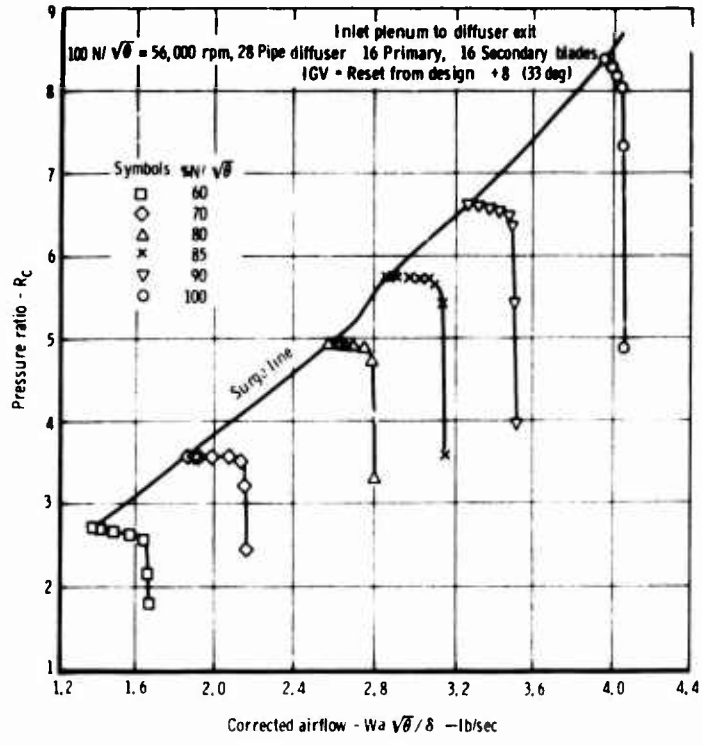

Figure 30. RC-2.5 performance—33 deg IGV setting.

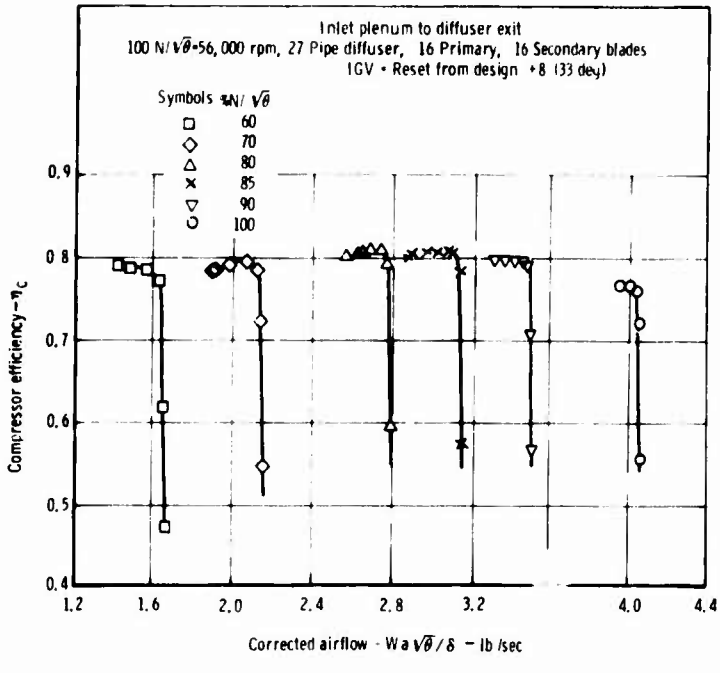

Figure 31. RC-2.5 performance—33 deg IGV setting.

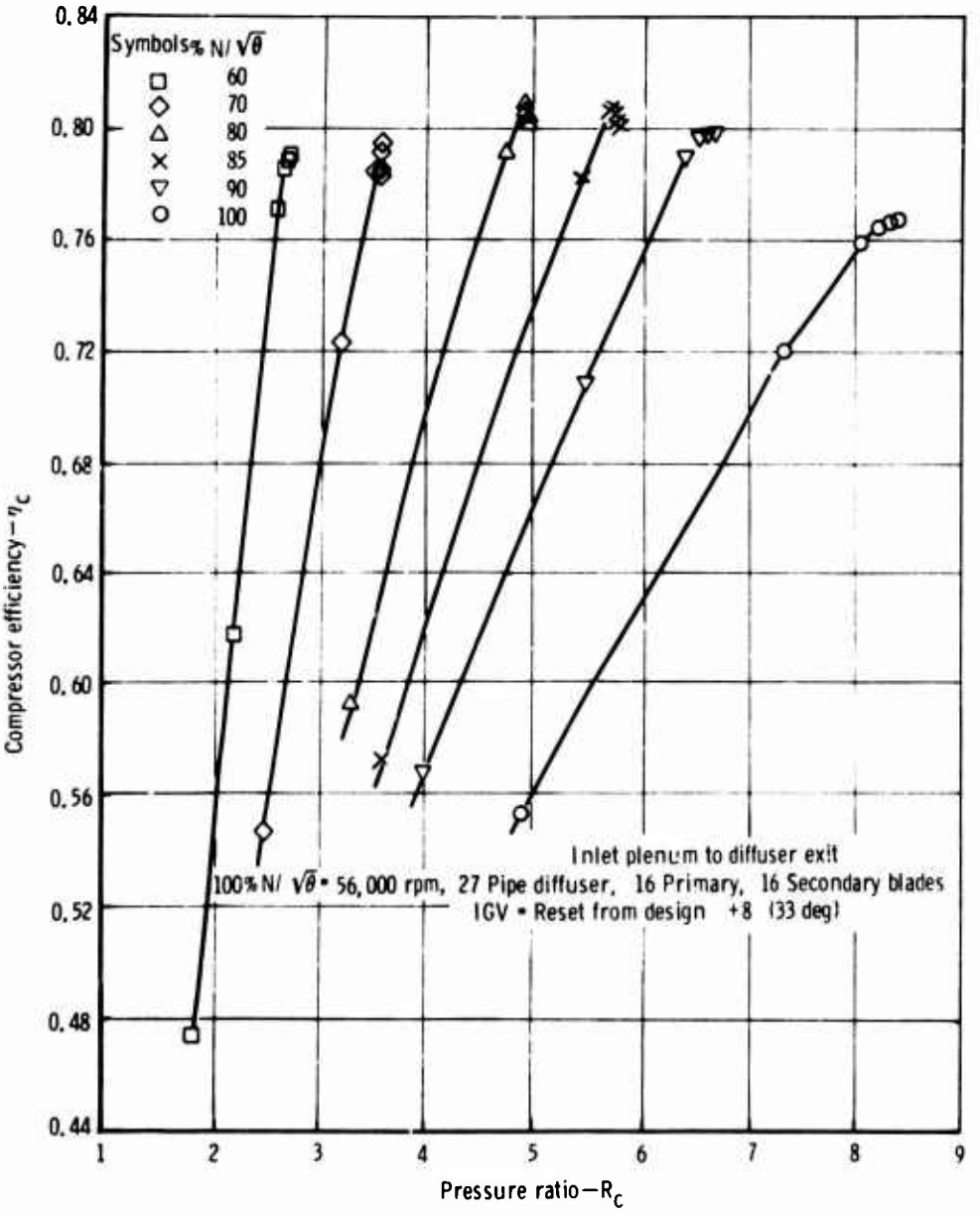

Figure 32. RC-2.5 performance—33 deg IGV setting.

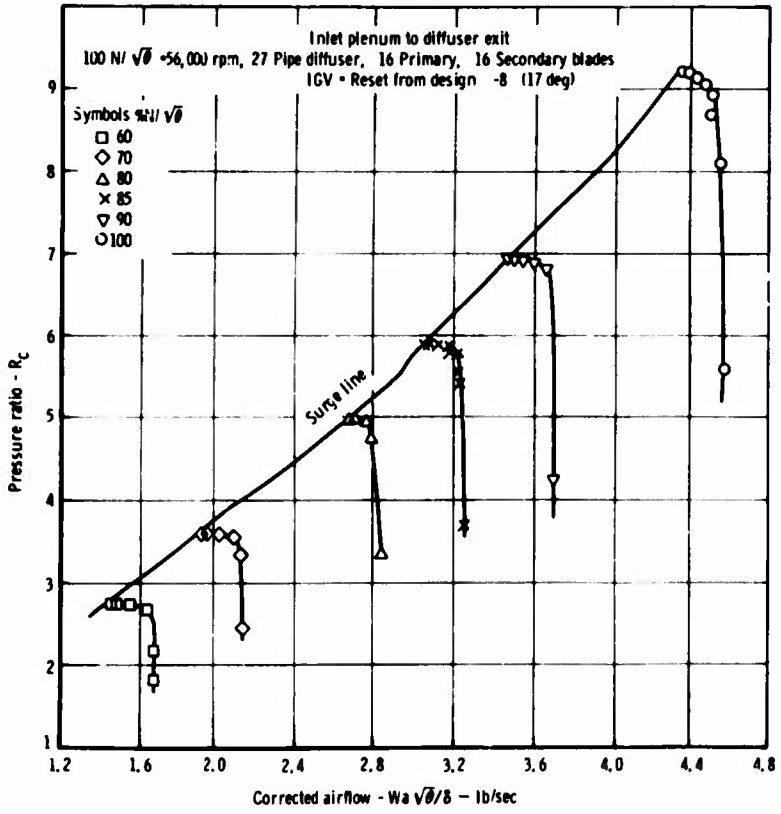

Figure 33. RC-2.5 performance—17 deg IGV setting.

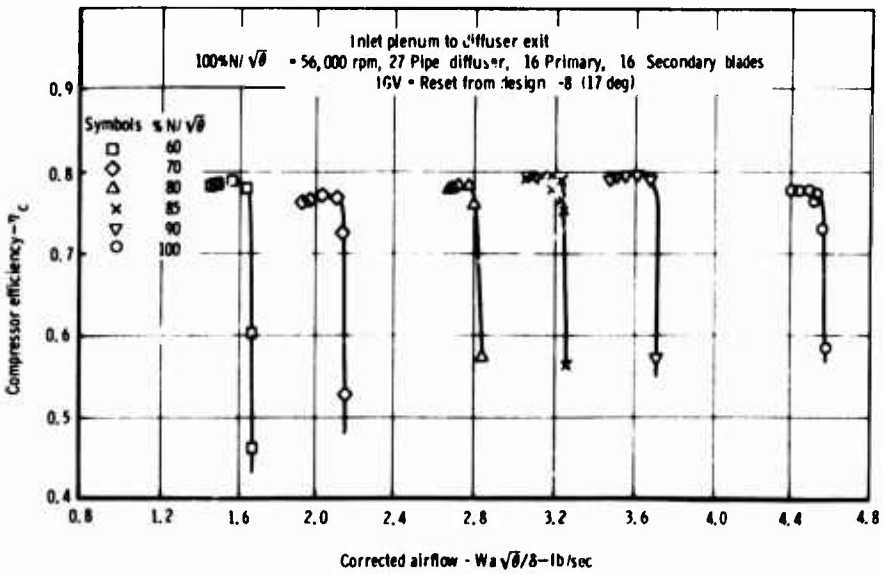

Figure 34. RC-2.5 performance—17 deg IGV setting.

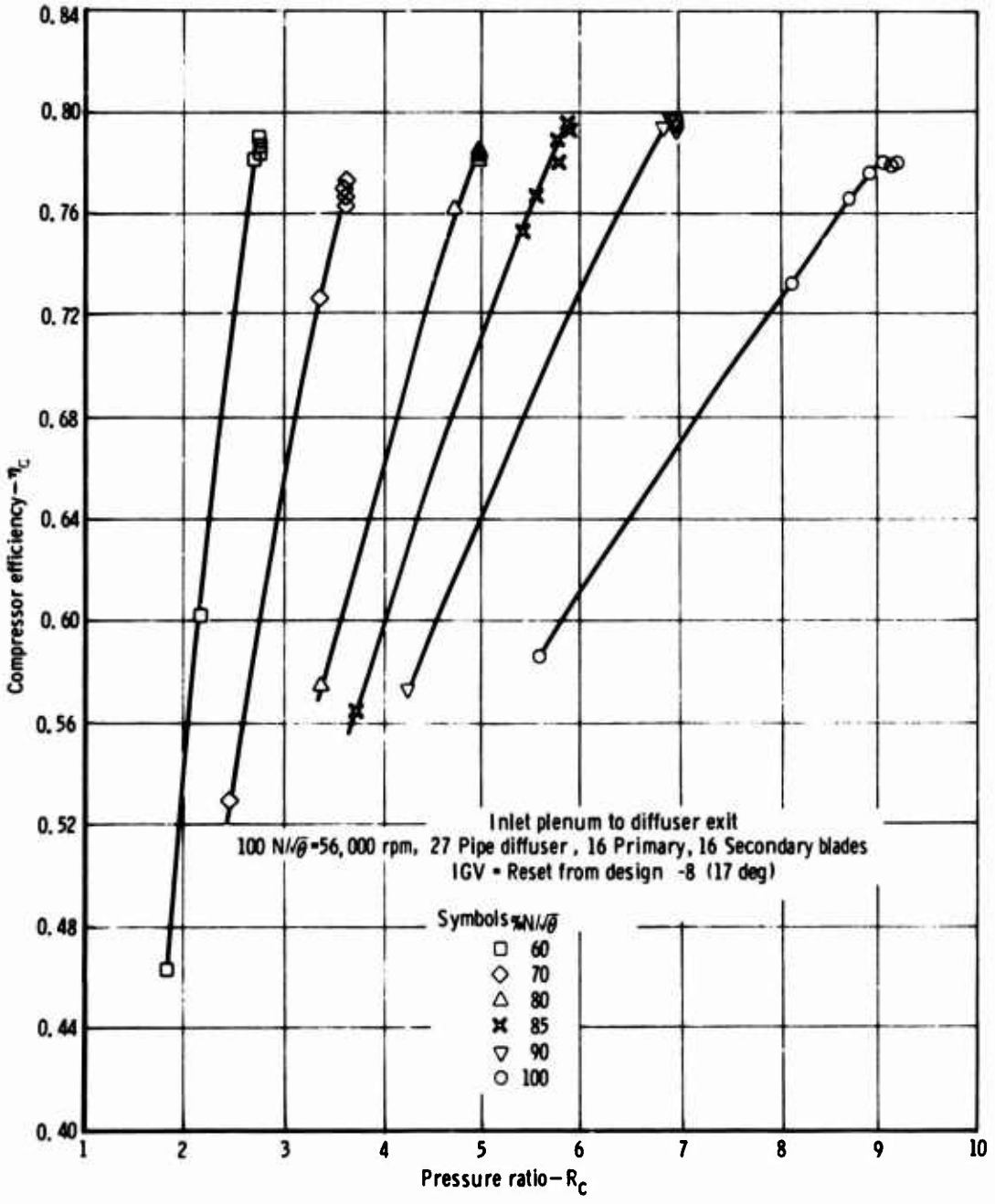

Figure 35. RC-2.5 performance—17 deg IGV setting.

Impeller Outlet Flow Distribution Data

Two traversing yaw/pressure probes were installed after the completion of the performance tests at 25 and 33 deg inlet guide vane settings. Five traverse points were taken between the hub and the shroud of the compressor, and both the flow total pressure and angle were obtained. The traverse data were obtained for a choked flow condition only because the presence of the probes was found to cause the compressor to surge as soon as the flow decreased from its choke value. Inasmuch as these probes did affect the compressor performance, all performance data were obtained prior to installation of these probes.

Following these pressure surveys, the two temperature probes were installed in the place of the pressure probes and the traverse was repeated.

Figures 36 through 40 show the impeller outlet total pressure distribution, total temperature distribution, and a typical flow angle distribution for both the 25 and 33 deg IGV settings.

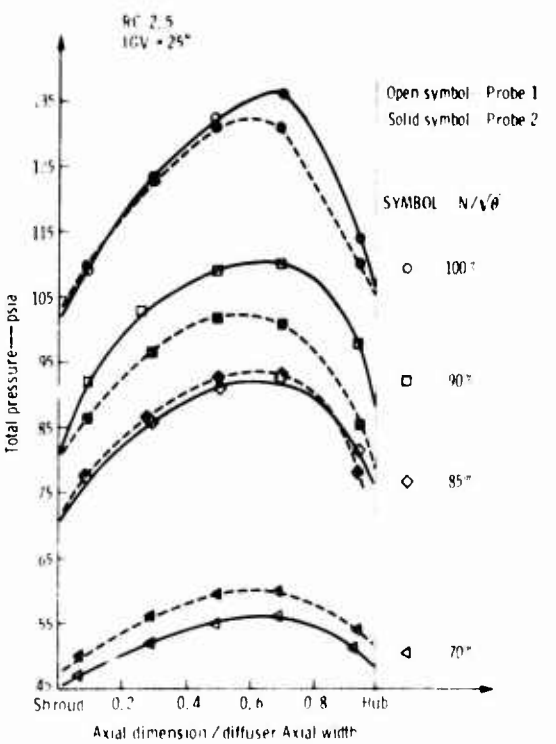

Figure 36. Total pressure distribution at impeller discharge, inlet guide vane setting 25 deg.

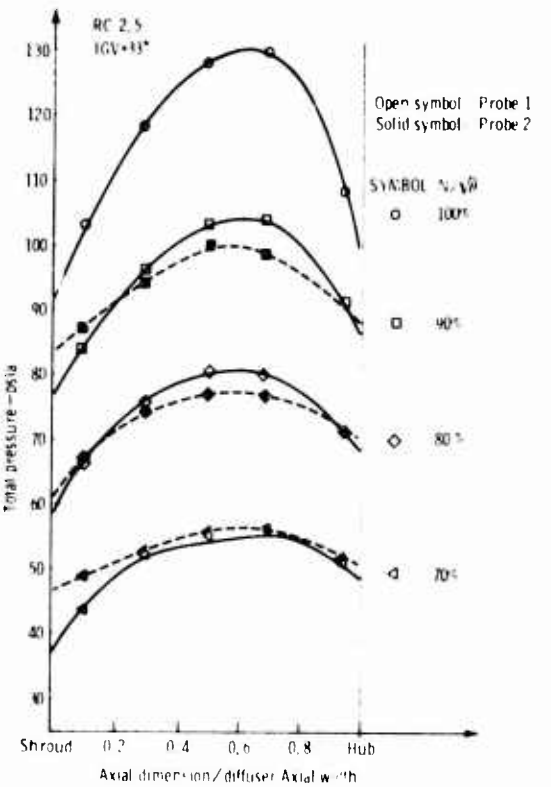

Figure 37. Total pressure distribution at impeller discharge, inlet guide vane setting 33 deg.

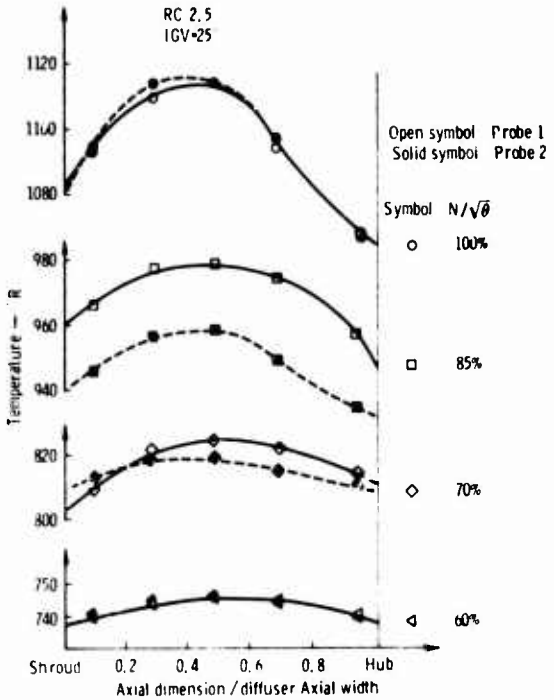

Figure 38. Total temperature distribution at impeller discharge, inlet guide vane setting 25 deg.

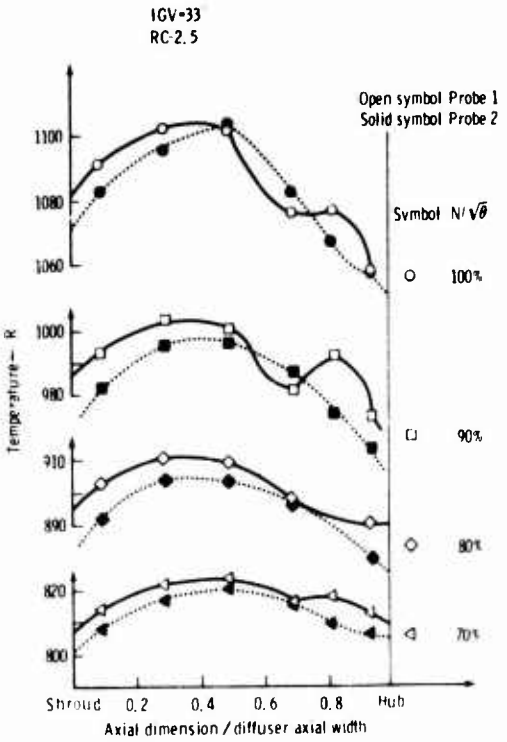

Figure 39. Total temperature distribution at impeller discharge, inlet guide vane setting 33 deg.

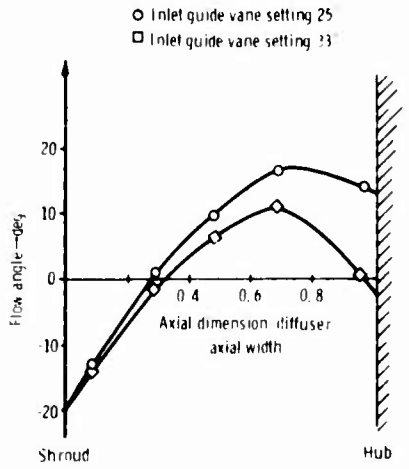

Figure 40. Typical flow angle distribution at impeller discharge (90% corrected speed).

Table 6 is a reduction of the yaw/pressure traverse data obtained by the Traverse Data Reduction program. The nomenclature for this computer output is defined in Table 5.

TABLE 5. TRAVERSE DATA REDUCTION PROGRAM NOMENCLATURE FOR TABLES 6, 7, AND 8.

1st Line: Title

Lines 3-14: Input data obtained from the RC-2.5 run numbers identified in the title

Lines 17-21: Total pressure at probe 1 (PT1), psia; axial traverse location (Z1), in.; flow angle at probe 1 (ALPH1), deg.; total pressure at probe 2 (PTLE), psia; axial traverse location (ZLE), in.; and flow angle at probe 2 (ALPHLE), deg

Note: Probe 1 is identified as INLET STATION PROBE, and probe 2 as LEADING EDGE STATION PROBE.

Line 24: Iteration Count (I)
Averaged total pressure at probe 1 (PTIB)
Averaged flow angle at probe 1 (ALP1)
Averaged static pressure at tangency circle, from first reading number (Choke) (P1)
Averaged Mach number at probe 1 (M1)
Averaged Mach number at diffuser exit, from second reading number (break point) (M2)
Static Pressure Recovery from probe 1 to diffuser exit
(CP = (P2-P1)/(PT1-P1))

Line 26: Averaged total pressure at diffuser exit, from second reading number (break point) (PT2B)
Diffuser exit blockage, as fraction of diffuser exit area (BLOCK)
Airflow corrected to conditions at probe 1 (WAC)
Actual to theoretical flow rate ratio at choke,
$W/WMAX = WA/(.532A^* PT1/\sqrt{T\ T1})$

where A* is the diffuser throat area, and TT1 is the total temperature

Total pressure loss DPT/PT1 = (PT1B-PT2B)/PT1B
Diffuser exit static pressure from second reading number (break point) (P2)
Airflow rate, lbm/sec (WA)
Ratio of diffuser throat area to normal flow area at probe 1 (A*/A1)

Line 29: Same as line 24, except that probe 2 replaces probe 1, and the static pressure P1 is obtained from the second (break point) reading number.

Line 31: Same as line 26, except that probe 2 replaces probe 1.

TABLE 6. YAW/PRESSURF DATA REDUCTION—RC-2.5.

```
    RC2.5, 25 DEG  IGV, 70 PRCNT SPD,        RDG  331,AND BREAK PT  RDG 279
                  INPUT DATA FOLLOWS
5   31.7610   29.4510   31.5920   32.6700   45.4000  829.0001    1.9850
  31.4530   29.4510   31.7150   32.6930
 215.4000   55.3000  261.3000  101.4000
   0.0000   47.0000  201.0000  409.0000    0.0000   50.0000  247.0000  338.0000
   0.0000   52.4000  169.0000  478.0000    0.0000   56.5000  217.0000  414.0000
   0.0000   55.0000  136.0000  513.0001    0.0000   59.5000  187.0000  527.0001
   0.0000   56.3000  102.0000  539.0001    0.0000   60.2000  153.0000  490.0000
   0.0000   51.0000   64.0000  533.0001    0.0000   54.0000  110.0000  493.0000
  52.1000    0.1770   52.8000    0.3541   53.2000    0.3541   51.1300    0.3541
  49.6300    0.3541   52.3000    0.7082   48.3000    0.7082   48.6000    0.7082
  48.8000    0.7082
   0.0000    0.0000    0.0000    0.0000
        INLET STATION PROBE                          LEADING EDGE STATION PROBE

    PT1         Z1      ALPH1                        PTLE      ZLE       ALPHLE
  47.0000    0.0280  -10.9799                      50.0000   0.0278  -26.2799
  52.4000    0.0904    1.4400                      56.5000   0.0863  -12.5999
  55.0000    0.1548    7.7399                      59.5000   0.1448    7.7399
  56.3000    0.2211   12.4200                      60.2000   0.2111    1.0799
  51.0000    0.2952   11.3400                      54.0000   0.2950    1.6199

                  INLET STATION DATA ON AVERAGE BASIS

        I      PT1B      ALP1       P1        M1        M2        CP
        5   54.0470   12.9318   31.3540    0.9174    0.3989    0.6189

    PT2B      BLOCK      WAC      W/WMAX     DPT/PT1      P2         WA        A*/A1
  50.6621    0.2413    0.6829    0.9598    0.0626   45.4000    1.9850    1.0361

                  LEADING EDGE DATA ON AVERAGE BASIS

        I      PT1B      ALP1       P1        M1        M2        CP
        7   58.8421   11.7908   31.3119    0.9937    0.3989    0.5117

    PT2B      BLOCK      WAC      W/WMAX     DPT/PT1      P2         WA        A*/A1
  50.6621    0.2413    0.6273    0.8816    0.1390   45.4000    1.9850    1.1347
```

```
  RC 2.5, 25 DEG IGV, 85 PRCNT SPD, CHOKE RDG 334,AND BREAK PT RDG 312
                  INPUT DATA FOLLOWS
5   44.9400   38.6100   43.1400   47.2900   72.1000  960.2000    2.9460
  44.2000   37.8000   43.4000   47.0000
 215.4000   55.3000  261.3000  101.4000
   0.0000   77.0000  201.0000  410.0000    0.0000   77.5000  247.0000  355.0000
   0.0000   85.5000  169.0000  476.0000    0.0000   87.8000  217.0000  441.0000
   0.0000   91.2000  136.0000  515.0001    0.0000   92.5000  187.0000  476.0000
   0.0000   93.4000  102.0000  552.0001    0.0000   93.0000  153.0000  486.0000
   0.0000   81.5000   64.0000  546.0001    0.0000   78.0000  110.0000  491.0000
  83.3000    0.1770   84.6000    0.3541   84.7000    0.3541   81.3000    0.3541
  79.8000    0.3541   83.1000    0.7082   76.5000    0.7082   74.3000    0.7082
  78.1000    0.7082
   0.0000    0.0000    0.0000    0.0000
        INLET STATION PROBE                          LEADING EDGE STATION PROBE

    PT1         Z1      ALPH1                        PTLE      ZLE       ALPHLE
  77.0000    0.0280  -10.7999                      77.5000   0.0278  -23.2199
  85.5000    0.0904    1.0799                      87.8000   0.0863   -7.7399
  91.2000    0.1548    8.1000                      92.5000   0.1448   -1.4400
  93.4000    0.2211   14.7599                      93.0000   0.2111    0.3600
  81.5000    0.2952   13.6799                      78.0000   0.2950    1.2599
```

TABLE 6. (CONT)

INLET STATION DATA ON AVERAGE BASIS

I	PT1B	ALP1	[illegible]	M1	M2	CP	
5	88.6841	12.6809	39.[illegible]5	1.1325	0.4031	0.6601	
PT2B	BLOCK	WAC	W/WMAX	DPT/PT1	P2	WA	A*/A1
80.6411	0.2452	0.6648	0.934[illegible]	0.0906	72.1000	2.9460	1.0562

LEADING EDGE DATA ON AVERAGE BASIS

I	PT1B	ALP1	P1	M1	M2	CP	
7	88.5079	12.5859	42.8624	1.0728	0.4031	0.6405	
PT2B	BLOCK	WAC	W/WMAX	DPT/PT1	P2	WA	A*/A1
80.6411	0.2452	0.6661	0.9361	0.0888	72.1000	2.9460	1.0641

RC 2.5 25 DEG IGV.90 PRCNT SPD. CHOKE RDG 343.AND BREAK PT RDG 292

INPUT DATA FOLLOWS

5 48.4400	42.0000	46.2500	52.8000	74.4000	1001.6000	3.2780	
49.7000	42.2000	46.4000	52.9000				
215.0000	55.3000	261.0000	101.4000				
0.0000	92.0000	201.0000	396.0000	0.0000	86.5000	247.0000	380.0000
0.0000	103.0000	169.0000	474.0000	0.0000	96.2000	217.0000	438.0000
0.0000	109.0000	136.0000	521.0001	0.0000	101.5000	187.0000	472.0000
0.0000	110.0000	102.0000	560.0001	0.0000	100.8000	153.0000	493.0000
0.0000	97.8000	64.0000	551.0001	0.0000	85.0000	110.0000	474.0000
90.9000	0.1770	91.9000	0.3541	90.1000	0.3541	88.6000	0.3541
86.5000	0.3541	86.5000	0.7082	79.8000	0.7082	81.3000	0.7082
84.1000	0.7082						
0.0000	0.0000	0.0000	0.0000				

INLET STATION PROBE

PT1	Z1	ALPH1
92.0000	0.0273	-13.3199
103.0000	0.0896	0.7200
109.0000	0.1540	9.1800
110.0000	0.2203	16.2000
97.8000	0.2944	14.5799

LEADING EDGE STATION PROBE

PTLE	ZLE	ALPHLE
86.5000	0.0273	-18.7200
96.2000	0.0858	-8.2800
101.5000	0.1443	-2.1599
100.8000	0.2106	1.6199
85.0000	0.2944	-1.7999

INLET STATION DATA ON AVERAGE BASIS

I	PT1B	ALP1	P1	M1	M2	CP	
6	106.2073	12.0551	47.0055	1.1450	0.4598	0.4627	
PT2B	BLOCK	WAC	W/WMAX	DPT/PT1	P2	WA	A*/A1
86.0063	0.2746	0.6308	0.8866	0.1902	74.4000	3.2780	1.1102

LEADING EDGE DATA ON AVERAGE BASIS

I	PT1B	ALP1	P1	M1	M2	CP	
6	96.1033	13.1589	47.5557	1.0550	0.4598	0.5529	
PT2B	BLOCK	WAC	W/WMAX	DPT/PT1	P2	WA	A*/A1
86.0063	0.2746	0.6972	0.9798	0.1050	74.4000	3.2780	1.0185

TABLE 6. (CONT)

```
  RC295 25 DEG IGV•100 PRCNT SPD• CHOKE RDG 339•AND BREAK PT RDG 301
                    INPUT DATA FOLLOWS
5    58.8000    ɔ0.2000    54.6000    55.3000   101.0000 1102.8501     3.8730
  59.4000    50.0000    54.6000    56.3000
 215.0000    55.3000   261.0000   101.4000
 109.0000   109.0000   201.0000   408.0000     0.0000   110.0000   247.0000   323.0000
 109.0000   123.0000   169.0000   518.0001     0.0000   123.0000   217.0000   448.0000
   0.0000   132.0000   136.0000   563.0001     0.0000   131.0000   187.0000   527.0001
   0.0000   136.0000   102.0000   565.0001     0.0000   131.0000   153.0000   563.0001
   0.0000   114.0000    64.0000   500.0000     0.0000   110.0000   110.0000   460.0000
 116.4000     0.1770   121.4000     0.3541   118.2000     0.3541   113.1000     0.3541
 113.1000     0.3541   120.3000     0.7082   106.2000     0.7082   106.0000     0.7082
 110.7000     0.7082
   0.0000     0.0000     0.0000     0.0000
        INLET STATION PROBE                              LEADING EDGE STATION PROBE

    PT1          Z1       ALPH1                            PTLE       ZLE        ALPHLE
 109.0000     ɔ.0273   -11.1599                         110.0000     0.0273   -28.9799
 123.0000     0.0896     8.6399                         123.0000     0.0858    -6.4799
 132.0000     0.1540    16.7400                         131.0000     0.1443     7.7399
 136.0000     0.2203    17.0999                         131.0000     0.2106    14.2199
 114.0000     0.2944     5.3999                         110.0000     0.2944    -4.3199

                   INLET STATION DATA ON AVERAGE BASIS

         I      PT1B       ALP1        P1         M1         M2         CP
         6   129.8408    12.3485    54.5900     1.1851     0.4240     0.6167

   PT2B       BLOCK      WAC       W/WMAX      DPT/PT1      P2         WA         A*/A1
 114.2947     0.2794     0.6398     0.8991     0.1197   101.0000     3.8730     1.0842

                   LEADING EDGE DATA ON AVERAGE BASIS

         I      PT1B       ALP1        P1         M1         M2         CP
         8   128.3320    12.3989    56.1546     1.1540     0.4240     0.6213

   PT2B       BLOCK      WAC       W/WMAX      DPT/PT1      P2         WA         A*/A1
 114.2947     0.2794     0.6473     0.9097     0.1093   101.0000     3.8730     1.0799

  RC2.5• 33 DEG IGV••70 PRCNT SPD• CHOKE RDG 394•AND BREAK PT RDG 360
                    INPUT DATA FOLLOWS
5    31.4800    29.4900    30.6900    32.5900    44.6000   817.1000     2.0230
  31.5700    29.4900    31.5300    32.6000
 215.4000    55.3000   261.3000   101.4000
   0.0000    49.0000   201.0000   438.0000     0.0000    44.0000   247.0000   353.0000
   0.0000    53.0000   169.0000   483.0000     0.0000    52.5000   217.0000   477.0000
   0.0000    56.0000   136.0000   523.0001     0.0000    55.0000   187.0000   513.0001
   0.0000    56.5000   102.0000   543.0001     0.0000    56.0000   153.0000   535.0001
   0.0000    50.0000    64.0000   507.0000     0.0000    51.0000   110.0000   518.0001
  51.8500     0.1770    52.8200     0.3541    53.2000     0.3541    50.9000     0.3541
  49.1000     0.3541    51.8000     0.7082    47.8000     0.7082    46.1000     0.7082
  44.4000     0.7082
   0.0000     0.0000     0.0000     0.0000
        INLET STATION PROBE                              LEADING EDGE STATION PROBE

    PT1          Z1       ALPH1                            PTLE       ZLE        ALPHLE
  49.0000     0.0280    -5.7600                          44.0000     0.0278   -23.5799
  53.0000     0.0904     2.3400                          52.5000     0.0863    -1.2599
  56.0000     0.1548     9.5399                          55.0000     0.1448     5.2200
  56.5000     0.2211    13.1399                          56.0000     0.2111     9.1800
  50.0000     0.2952     6.6599                          51.0000     0.2950     6.1199
```

TABLE 6. (CONT)

INLET STATION DATA ON AVERAGE BASIS

I	PT1B	ALP1	P1	M1	M2	CP
5	54.0933	13.0580	31.0494	0.9270	0.4263	0.5880

PT2B	BLOCK	WAC	W/WMAX	DPT/PT1	P2	WA	A*/A1
50.5370	0.2704	0.6904	0.9703	0.0657	44.6000	2.0230	1.0262

LEADING EDGE DATA ON AVERAGE BASIS

I	PT1B	ALP1	P1	M1	M2	CP
8	54.7472	12.8926	31.2827	0.9311	0.4263	0.5675

PT2B	BLOCK	WAC	W/WMAX	DPT/PT1	P2	WA	A*/A1
50.5370	0.2704	0.6822	0.9587	0.0769	44.6000	2.0230	1.0392

RC 2.5, 33 DEG IGV, 80 PRCNT SPD, CHOKE RDG 398 AND BREAK PT RDG 366

INPUT DATA FOLLOWS

5 38.8000	34.3000	38.3000	41.0000	58.2000	900.0001	2.5700	
38.9000	34.5000	38.7000	41.2000				
215.4000	55.3000	261.3000	101.4000				
0.0000	67.0000	201.0000	459.0000	0.0000	66.0000	247.0000	413.0000
0.0000	74.0000	169.0000	486.0000	0.0000	76.0000	217.0000	470.0000
0.0000	77.0000	136.0000	521.0001	0.0000	80.5000	187.0000	509.0000
0.0000	76.8000	102.0000	542.0001	0.0000	80.0000	153.0000	524.0001
0.0000	57.0000	64.0000	435.0000	0.0000	71.5000	110.0000	523.0001
69.6000	0.1770	70.6000	0.3541	70.6000	0.3541	67.8000	0.3541
65.5000	0.3541	67.8000	0.7082	62.6000	0.7082	59.9000	0.7082
60.1000	0.7082						
0.0000	0.0000	0.0000	0.0000				

INLET STATION PROBE

PT1	Z1	ALPH1
67.0000	0.0280	-1.9799
74.0000	0.0904	2.8800
77.0000	0.1548	9.1800
76.8000	0.2211	12.9599
57.0000	0.2952	-6.2999

LEADING EDGE STATION PROBE

PTLE	ZLE	ALPHLE
66.0000	0.0278	-12.7799
76.0000	0.0863	-2.5199
80.5000	0.1448	4.5000
80.0000	0.2111	7.1999
71.5000	0.2950	7.0199

INLET STATION DATA ON AVERAGE BASIS

I	PT1B	ALP1	P1	M1	M2	CP
5	73.0926	12.8229	38.0190	1.0132	0.4338	0.5753

PT2B	BLOCK	WAC	W/WMAX	DPT/PT1	P2	WA	A*/A1
66.2359	0.2679	0.6812	0.9574	0.0938	58.2000	2.5700	1.0447

LEADING EDGE DATA ON AVERAGE BASIS

I	PT1B	ALP1	P1	M1	M2	CP
8	77.1701	12.1620	38.2377	1.0539	0.4338	0.5127

PT2B	BLOCK	WAC	W/WMAX	DPT/PT1	P2	WA	A*/A1
66.2359	0.2679	0.6452	0.9068	0.1416	58.2000	2.5700	1.1006

RC2.5 33 DEG IGV,, 90 PERCENT SPD, CHOKE, RDG 401

INPUT DATA FOLLOWS

5 47.0650	40.0800	43.7770	50.3840	50.0000	994.0001	3.1690	
46.5760	40.0800	44.7160	51.1070				
215.4000	55.3000	261.3000	101.4000				
0.0000	87.0000	247.0000	395.0000	0.0000	84.0000	201.0000	404.0000
0.0000	94.0000	217.0000	460.0000	0.0000	96.0000	169.0000	464.0000
0.0000	100.0000	187.0000	503.0000	0.0000	103.0000	136.0000	510.0000

TABLE 6. (CONT)

```
  0.0000    98.0000   153.0000   531.0001     0.0000   104.0000   102.0000   529.0001
  0.0000    91.0000   110.0000   472.0000     0.0000    91.0000    64.0000   510.0000
 84.5000     0.1770    85.7860     0.3541    83.2830     0.3541    82.1680     0.3514
 80.1100     0.3541    76.0660     0.7082    73.5250     0.7082    69.2790     0.7082
 76.2050     0.7082
  0.0000     0.0000     0.0000     0.0000
        INLET STATION PROBE                              LEADING EDGE STATION PROBE

    PT1         Z1       ALPH1                             PTLE       ZLE        ALPHLE
 87.0000    -0.0616   -13.5000                          84.0000    0.1175   -14.3999
 94.0000    -0.0031    -1.799.                          96.0000    0.1799    -3.5999
100.0000     0.0353     5.9399                         103.0000    0.2443     4.6800
 98.0000     0.1216    10.9799                         104.0000    0.3106     8.1000
 91.0000     0.2055     0.3600                          91.0000    0.3847     4.6800

                    INLET STATION DATA ON AVERAGE BASIS

         I      PT1B       ALP1        P1         M1         M2         CP
         4   95.5370    12.8065    44.8928     1.0973     0.8175     0.1008

    PT2B       BLOCK       WAC      W/WMAX     DPT/PT1       P2         WA        A*/A1
 77.5662      0.4394     0.6754     0.9492      0.1881   50.0000     3.1690     1.0461

                    LEADING EDGE DATA ON AVERAGE BASIS

         I      PT1B       ALP1        P1         M1         M2         CP
         7  101.4961    12.1301    45.3663     1.1372     0.8175     0.0825

    PT2B       BLOCK       WAC      W/WMAX     DPT/PT1       P2         WA        A*/A1
 77.5662      0.4394     0.6357     0.8935      0.2357   50.0000     3.1690     1.1034
```

```
 RC2.5  33 DEG IGV.100 PRCT SPD. RDG 404-CHOKE. AND 389 -BREAK PT
                    INPUT DATA FOLLOWS
5   53.1000   46.6400   49.4900   54.0000   96.6000 1097.2001    3.6490
  0.0000    0.0000    0.0000    0.0000
215.0000   55.3000  261.0000  101.4000
  0.0000  103.0000  201.0000  389.0000    0.0000    0.0000    0.0000    0.0000
  0.0000  118.0000  169.0000  457.0000    0.0000    0.0000    0.0000    0.0000
  0.0000  128.0000  136.0000  555.0001    0.0000    0.0000    0.0000    0.0000
  0.0000  130.0000  102.0000  534.0001    0.0000    0.0000    0.0000    0.0000
  0.0000  108.0000   64.0000  511.0000    0.0000    0.0000    0.0000    0.0000
111.2000    0.1770  115.4000    0.3541  111.0000    0.3541  107.7000    0.3541
108.5000    0.3541  114.8000    0.7082  101.4000    0.7082  101.1000    0.7082
105.4000    0.7082
  0.0000    0.0000    0.0000    0.0000
        INLET STATION PROBE                              LEADING EDGE STATION PROBE

    PT1         Z1       ALPH1                             PTLE       ZLE        ALPHLE
103.0000    0.0273   -14.5799                          0.0000    0.5089   -87.1199
118.0000    0.0896    -2.3400                          0.0000    0.5089   -87.1199
128.0000    0.1540    15.2999                          0.0000    0.5089   -87.1199
130.0000    0.2203    11.5200                          0.0000    0.5089   -87.1199
108.0000    0.2944     7.3799                          0.0000    0.5089   -87.1199

                    INLET STATION DATA ON AVERAGE BASIS

         I      PT1B       ALP1        P1         M1         M2         CP
         5  124.4537    12.2121    50.2532     1.2160     0.4166     0.6246

    PT2B       BLOCK       WAC      W/WMAX     DPT/PT1       P2         WA        A*/A1
108.8595      0.2791     0.6272     0.8815      0.1253   96.6000     3.6490     1.0961
```

The progression of the flow from the tangency circle to the diffuser leading edge was calculated by the Radial Vaneless Space program. The flow angle and Mach number variation with radius calculated by this program for the 100% speed data at 25 deg inlet guide vane setting are shown in Figure 41. These curves show that the diffuser is operating at approximately one deg of incidence even in this choke flow condition. The calculated total pressure loss in the vaneless space agrees closely with the loss indicated by the difference in total pressure measurements between the traverse station and the diffuser leading edge.

Rig Mechanical Operation

The mechanical operation of the compressor rig itself was uneventful. However, vibrations in the steam turbine drive train were great enough to prohibit running in the neighborhood of 95% speed.

Six compressor rear bearing support struts were added for this build, with a view to reducing the vibration levels previously recorded on the RC-1 and RC-2 rigs. This configuration exhibited maximum rear bearing vibration levels of 2.25 in./sec compared to 3.6 in./sec in the previous build (RC-2.2). Rotor whip did not exceed 6 mils.

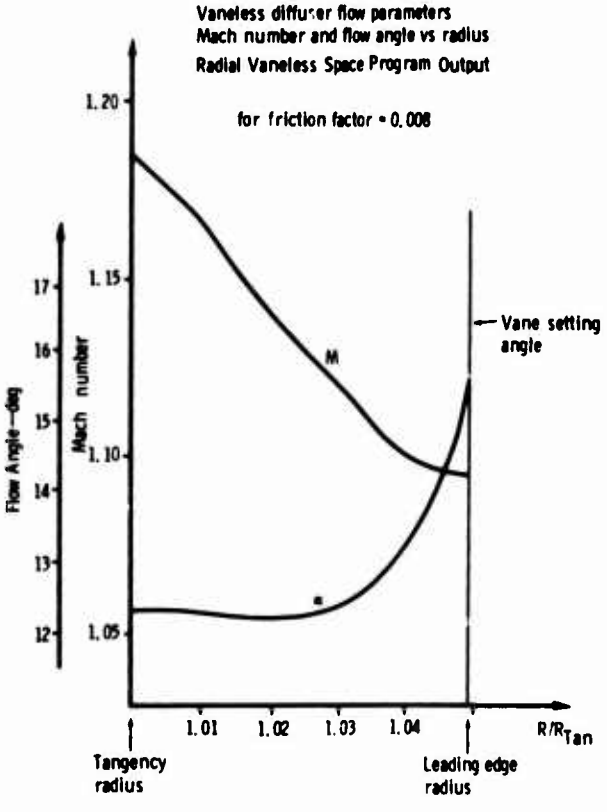

Figure 41. Distribution of Mach number and flow angle in vaneless diffuser.

RC-2.6 FIRST MODIFICATION TEST

The RC-2.6 compressor was modified from the original design by twisting the inlet guide vanes +8 deg at the hub and -8 deg at the tip, and plating the diffuser flow path 0.003 in. The modified compressor was tested for performance, and then yaw/pressure data was obtained in the manner described in the RC-2.5 Baseline Test Report at the 25 deg IGV setting.

The test period was 29 and 30 January 1974. The reading numbers were 461 to 552. A configuration summary follows:

Configuration	Modified RC-2 compressor	
Impeller	P/N EX-106488	
Diffuser	P/N EX-106583-1	Plated 27 Pipe
IGV assy	P/N EX-99257-1	Twisted
Collector	P/N EX-99270	
Cover	P/N EX-106582	
Impeller tip	Cold clearance:	0.035 in.

Compressor Performance Data

The modified compressor performance is shown in Figures 42, 43, and 44. The measuring stations and methods were identical to those described in the RC-2.5 Baseline Test Report. The rig was insulated in the same manner as was RC-2.5.

Impeller Outlet Flow Distribution Data

The two total pressure/yaw probes described in the RC-2.5 Baseline Test subsection were used to obtain traverse data in the manner described previously.

Figures 45 and 46 show, respectively, the impeller outlet total pressure distribution and typical flow angle distributions.

Table 7 is a reduction of the yaw/pressure traverse data obtained by the Traverse Data Reduction program. The nomenclature for this computer output is defined in Table 5.

Rig Mechanical Operation

The mechanical operation of the rig itself was uneventful. However, vibrations in the steam turbine drive train were great enough to prohibit running at 85% speed. Data were obtained at 86% speed since the vibration level there was acceptable.

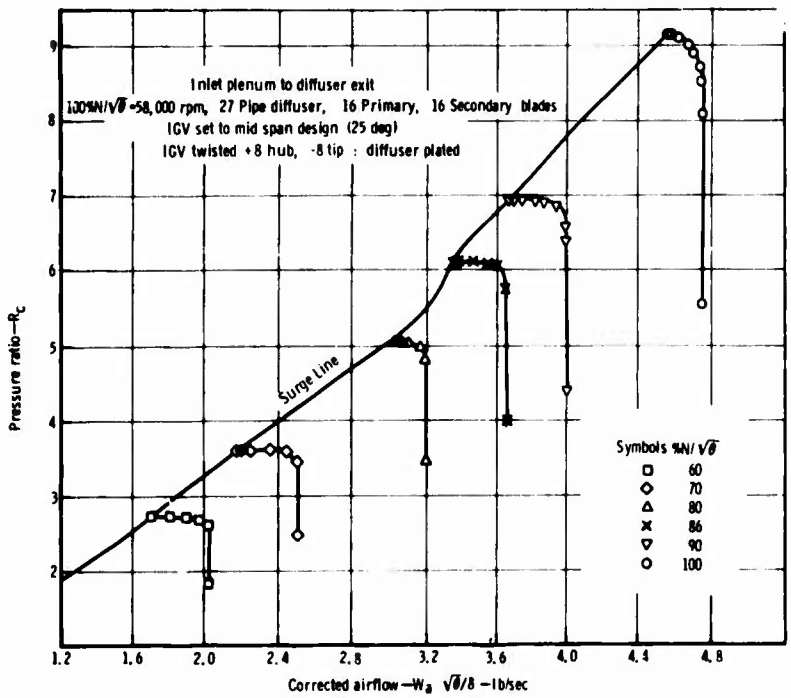

Figure 42. RC-2.6 performance.

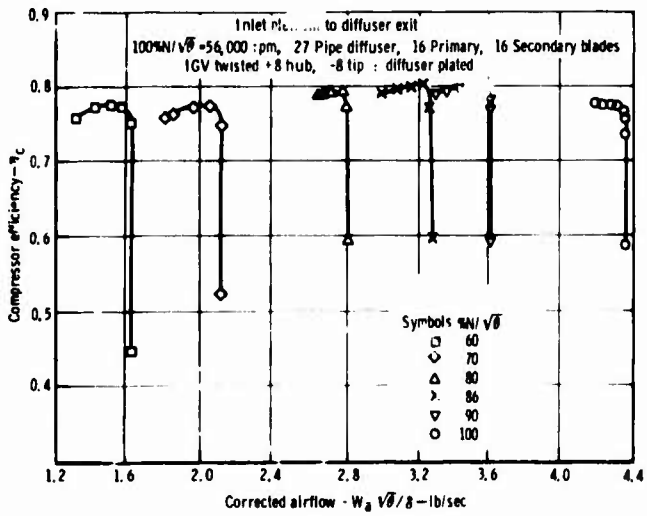

Figure 43. RC-2.6 performance.

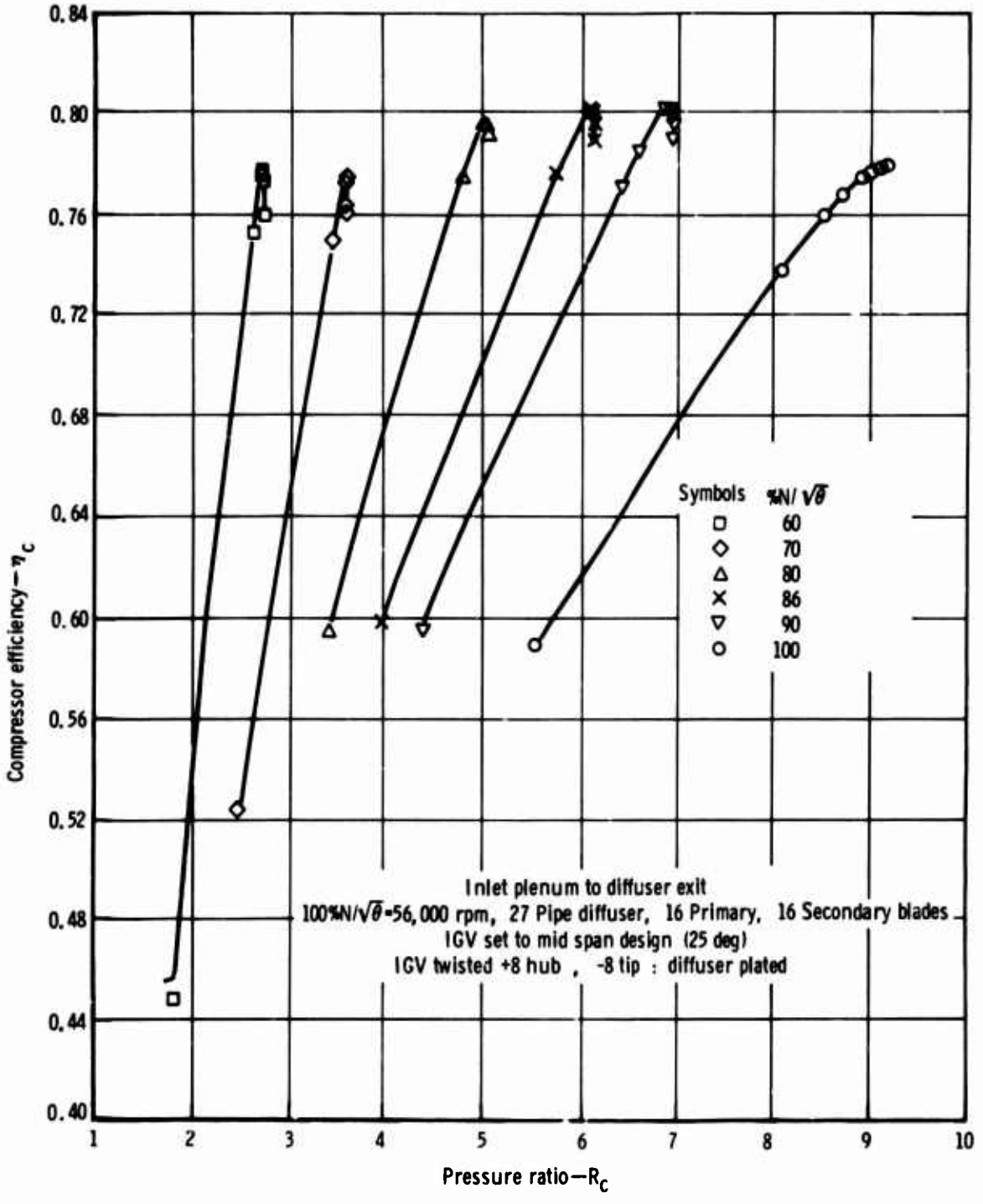

Figure 44. RC-2.6 performance.

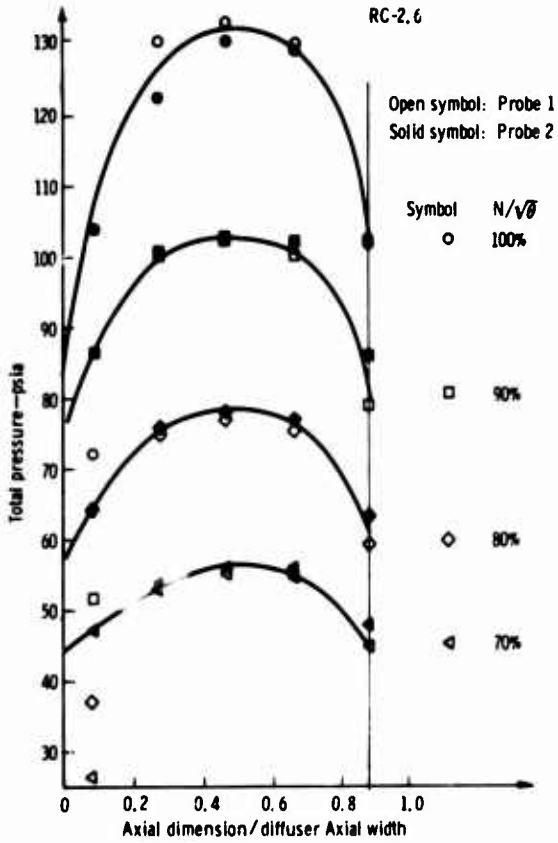

Figure 45. Impeller outlet total pressure distribution.

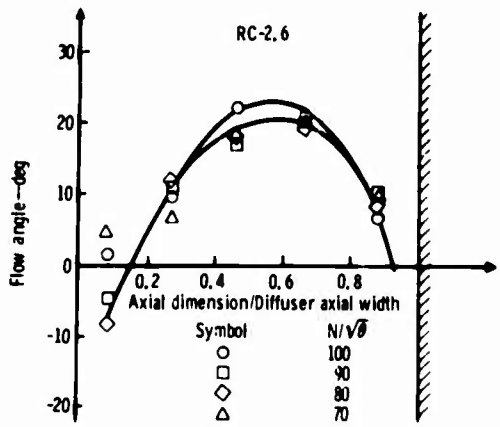

Figure 46. Flow angle at impeller discharge.

TABLE 7. YAW/PRESSURE DATA REDUCTION—RC-2.6.

```
 RC 2.6 , 70 PRCNT  SPEED     RDG 544
                INPUT DATA FOLLOWS
5   33.1890   31.1980   32.7270   33.1510   42.6075  794.5700    2.0150
  32.8970   31.9950   31.9930   33.1510
 215.4000   55.3000  261.3000  101.4000
   0.0000   26.5000  201.0000  494.0000    0.0000   47.1000  247.0000  366.0000
   0.0000   53.0000  169.0000  501.5000    0.0000   54.0000  217.0000  422.0000
   0.0000   55.2000  136.0000  572.0001    0.0000   56.1000  187.0000  447.0000
   0.0000   54.9000  102.0000  580.0001    0.0000   56.1000  153.0000  471.0000
   0.0000   45.0000   64.0000  525.5001    0.0000   48.0000  110.0000  425.5000
  51.4500    0.1770   50.7680    0.3541   51.9520    0.3541   49.9850    0.3541
  48.0160    0.3541   47.9780    0.7082   45.4930    0.7082   43.0430    0.7082
  46.7530    0.7082
   0.0000    0.0000    0.0000    0.0000
        INLET STATION PROBE                          LEADING EDGE STATION PROBE

    PT1         Z1       ALPH1                      PTLE       ZLE       ALPHLE
  26.5000    0.0280    4.3199                     47.1000    0.0278   -21.2399
  53.0000    0.0904    5.6700                     54.0000    0.0863   -11.1599
  55.2000    0.1548   18.3600                     56.1000    0.1448    -6.6599
  54.9000    0.2211   19.7999                     56.1000    0.2111    -2.3400
  45.0000    0.2952    9.9899                     48.0000    0.2950   -10.5299

                INLET STATION DATA ON AVERAGE BASIS
        I      PT1B      ALP1       P1        M1        M2        CP
        6    51.7647   13.9223   32.4629    0.8444    0.4304    0.5255

   PT2B      BLOCK      WAC     W/WMAX     DPT/PT1      P2        WA        A*/A1
  48.3934    0.2373    0.7086    1.0353    0.0651   42.6075    2.0150    0.9451

              LEADING EDGE DATA ON AVERAGE BASIS

        I      PT1B      ALP1       P1        M1        M2        CP
        5    53.6357   13.3109   32.5056    0.8770    0.4304    0.4780

   PT2B      BLOCK      WAC     W/WMAX     DPT/PT1      P2        WA        A*/A1
  48.3934    0.2373    0.6839    0.9992    0.0977   42.6075    2.0150    0.9877
```

```
  RC 2.6,  80 PRCNT  SPEED ,  RDG 547
                INPUT DATA FOLLOWS
5   42.6100   38.6620   41.4680   42.6300   59.3000  873.2200    2.6200
  41.9690   40.0970   39.7520   42.6300
 215.4000   55.3000  261.3000  101.4000
   0.0000   37.2000  201.0000  424.0000    0.0000   64.2000  247.0000  346.0000
   0.0000   75.0000  169.0000  535.0001    0.0000   75.5000  217.0000  412.0000
   0.0000   77.0000  136.0000  569.0001    0.0000   78.1000  187.0000  437.0000
   0.0000   75.5000  102.0000  578.0001    0.0000   77.1000  153.0000  460.5000
   0.0000   59.4000   64.0000  517.5001    0.0000   63.1000  110.0000  414.5000
  71.0000    0.1770   70.8080    0.3541   72.0900    0.3541   66.9470    0.3541
  66.4570    0.3541   67.3080    0.7082   63.3810    0.7082   59.5940    0.7082
  64.9510    0.7082
   0.0000    0.0000    0.0000    0.0000
        INLET STATION PROBE                          LEADING EDGE STATION PROBE

    PT1         Z1       ALPH1                      PTLE       ZLE       ALPHLE
  37.2000    0.0280   -8.2800                     64.2000    0.0278   -24.8400
  75.0000    0.0904   11.6999                     75.5000    0.0863   -12.9599
  77.0000    0.1548   17.8199                     78.1000    0.1448    -8.4599
  75.5000    0.2211   19.4399                     77.1000    0.2111    -4.2299
  59.4000    0.2952    8.5499                     63.1000    0.2950   -12.5100
```

TABLE 7. (CONT)

INLET STATION DATA ON AVERAGE BASIS

I	PT1B	ALP1	P1	M1	M2	CP	
7	73.0763	13.1695	41.1068	0.9451	0.4261	0.5690	
PT2B	BLOCK	WAC	W/WMAX	DPT/PT1	P2	WA	A*/A1
67.1864	0.2453	0.6842	0.9997	0.0806	59.3000	2.6200	0.9981

LEADING EDGE DATA ON AVERAGE BASIS

I	PT1B	ALP1	P1	M1	M2	CP	
5	73.7850	13.0306	41.0991	0.9538	0.4261	0.5568	
PT2B	BLOCK	WAC	W/WMAX	DPT/PT1	P2	WA	A*/A1
67.1864	0.2453	0.6777	0.9901	0.0894	59.3000	2.6200	1.0086

RC 2.6 , 90 PRCNT SPEED , RDG 550 AND BREAK PT. RDG. 504 CORRECTED

INPUT DATA FOLLOWS

5	53.6290	46.3230	51.3190	53.4890	83.4900	959.6700	3.3220
	52.9580	49.0670	48.9540	53.4890			
	215.4000	55.3000	261.3000	101.4000			
	0.0000	51.9000	201.0000	442.0000	0.0000	86.4000	247.0000	337.5000
	0.0000	100.5000	169.0000	529.5001	0.0000	100.3000	217.0000	406.5000
	0.0000	102.5000	136.0000	564.5001	0.0000	103.0000	187.0000	434.0000
	0.0000	100.2000	102.0000	588.0001	0.0000	102.2000	153.0000	458.5000
	0.0000	78.9000	64.0000	527.5001	0.0000	86.0000	110.0000	417.0000
	97.8300	0.1770	98.2890	0.3541	97.6800	0.3541	95.2760	0.3541
	93.4100	0.3541	93.9300	0.7082	88.0220	0.7082	84.8800	0.7082
	91.6400	0.7820						
	0.0000	0.0000	0.0000	0.0000				

INLET STATION PROBE

PT1	ZI	ALPH1
51.9000	0.0280	-5.0399
100.5000	0.0904	10.7099
102.5000	0.1548	17.0099
100.2000	0.2211	21.2399
78.9000	0.2952	10.3500

LEADING EDGE STATION PROBE

PTLE	ZLE	ALPHLE
86.4000	0.0278	-26.3699
100.3000	0.0863	-13.9499
103.0000	0.1448	-9.0000
102.2000	0.2111	-4.5900
86.0000	0.2950	-12.0599

INLET STATION DATA ON AVERAGE BASIS

I	PT1B	ALP1	P1	M1	M2	CP	
7	96.5595	13.2148	50.7612	1.0041	0.4029	0.7146	
PT2B	BLOCK	WAC	W/WMAX	DPT/PT1	P2	WA	A*/A1
93.3690	0.2450	0.6883	1.0056	0.0330	83.4900	3.3220	0.9947

LEADING EDGE DATA ON AVERAGE BASIS

I	PT1B	ALP1	P1	M1	M2	CP	
5	98.1946	12.9926	51.0766	1.0132	0.4029	0.6879	
PT2B	BLOCK	WAC	W/WMAX	DPT/PT1	P2	WA	A*/A1
93.3690	0.2450	0.6769	0.9889	0.0491	83.4900	3.3220	1.0115

TABLE 7. (CONT)

RC 2.6 • 100 PRCNT SPEED• RDG• 552 AND BREAK PT RDG 513 CORRECTED
INPUT DATA FOLLOWS.

```
5   63.9940   54.3740   59.1560   56.7090   99.8700 1053.8801    3.9330
  64.1710   58.7210   58.2490   56.7090
 215.4000   55.3000  261.2000  101.4000
   0.0000   72.0000  201.0000  479.0000    0.0000  104.0000  247.0000  306.0000
   0.0000  130.5000  169.0000  523.0001    0.0000  122.5000  217.0000  392.0000
   0.0000  133.0000  136.0000  593.0001    0.0000  130.5000  187.0000  412.0000
   0.0000  130.0000  102.0000  589.0001    0.0000  129.0000  153.0000  459.0000
   0.0000  102.0000   64.0000  508.0000    0.0000  102.5000  110.0000  404.0000
 120.4000    0.1770  121.6800    0.3541  121.6300    0.3541  116.1800    0.3541
 115.7200    0.3541  115.4400    0.7082  108.2440    0.7082  105.8700    0.7082
 113.6900    0.7820
   0.0000    0.0000    0.0000    0.0000
```

INLET STATION PROBE

PT1	Z1	ALPH1
72.0000	0.0280	1.6199
130.5000	0.0904	9.5399
133.0000	0.1548	22.1399
130.0000	0.2211	21.4199
102.0000	0.2952	6.8399

LEADING EDGE STATION PROBE

PTLE	ZLE	ALPHLE
104.0000	0.0278	-32.0400
122.5000	0.0863	-16.5600
130.5000	0.1448	-12.9599
129.0000	0.2111	-4.5000
102.5000	0.2950	-14.3999

INLET STATION DATA ON AVERAGE BASIS

I	PT1B	ALP1	P1	M1	M2	CP
7	125.3422	12.7351	58.2386	1.1064	0.4505	0.6204

PT2B	BLOCK	WAC	W/WMAX	DPT/PT1	P2	WA	A*/A1
114.7942	0.3024	0.6579	0.9612	0.0841	99.8700	3.9330	1.0216

LEADING EDGE DATA ON AVERAGE BASIS

I	PT1B	ALP1	P1	M1	M2	CP
5	122.8547	12.9376	59.4180	1.0738	0.4505	0.6376

PT2B	BLOCK	WAC	W/WMAX	DPT/PT1	P2	WA	A*/A1
114.7942	0.3024	0.6712	0.9806	0.0656	99.8700	3.9330	1.0157

RC-2.7 FINAL TEST

The RC-2.7 compressor was modified from the RC-2.6 configuration by cutting off the outside 7.5% of the rotor (from the original radius of 4.224 in. to the new radius of 3.91 in.). The impeller blade exit angle is now 5 deg from radial at the hub and zero deg (radial) at the shroud, instead of the original 35 deg at the hub and 30 deg at the shroud. The modified impeller is shown in Figure 47. This compressor was tested for performance, and then yaw/pressure data were obtained in the manner described in the RC-2.5 Baseline Test Report.

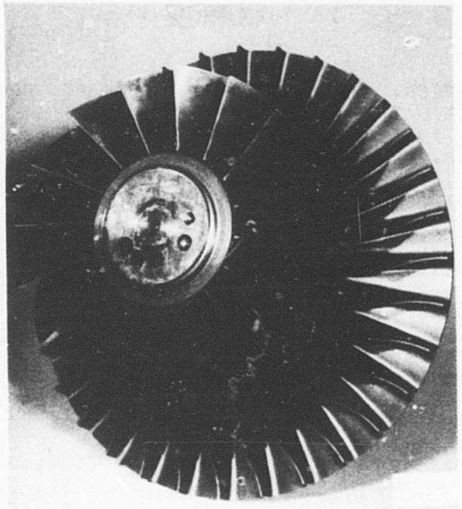

Figure 47. Modified impeller—RC-2.7 configuration.

The test period was 4 through 10 April 1974. The reading numbers were 553 to 635. A configuration summary follows.

Configuration — Baseline compressor with the following modifications:

- Diffuser plated as in RC-2.6
- Inlet guide vanes twisted as in RC-2.6
- Rotor cut down 7.5% radially

Impeller:	P/N EX-106488-1 Cut down
Diffuser:	P/N EX-106583-1 Plated
IGV assy:	P/N EX-99257-1 Twisted
Collector:	P/N EX-99270
Cover:	P/N EX-106582
Impeller tip:	Cold clearance: 0.022 in.

Compressor Performance Data

The modified compressor performance is shown in Figures 48, 49, and 50. The measuring stations and methods were identical to those described in the RC-2.5 Baseline Test subsection. The rig was insulated in the same manner as were RC-2.5 and RC-2.6.

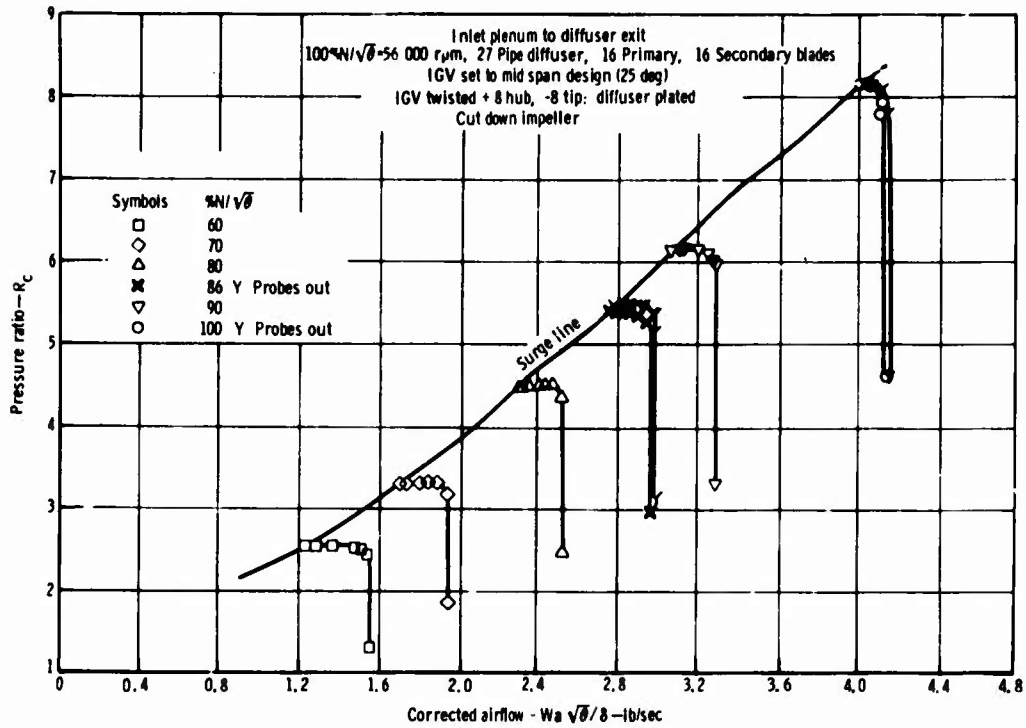

Figure 48. RC-2.7 performance.

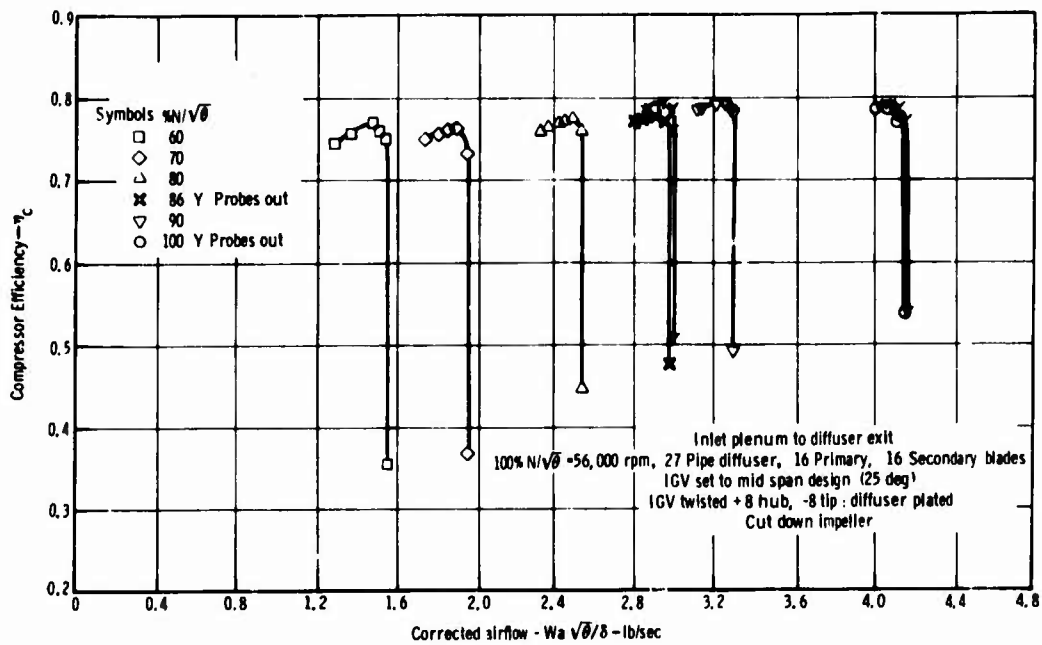

Figure 49. RC-2.7 performance.

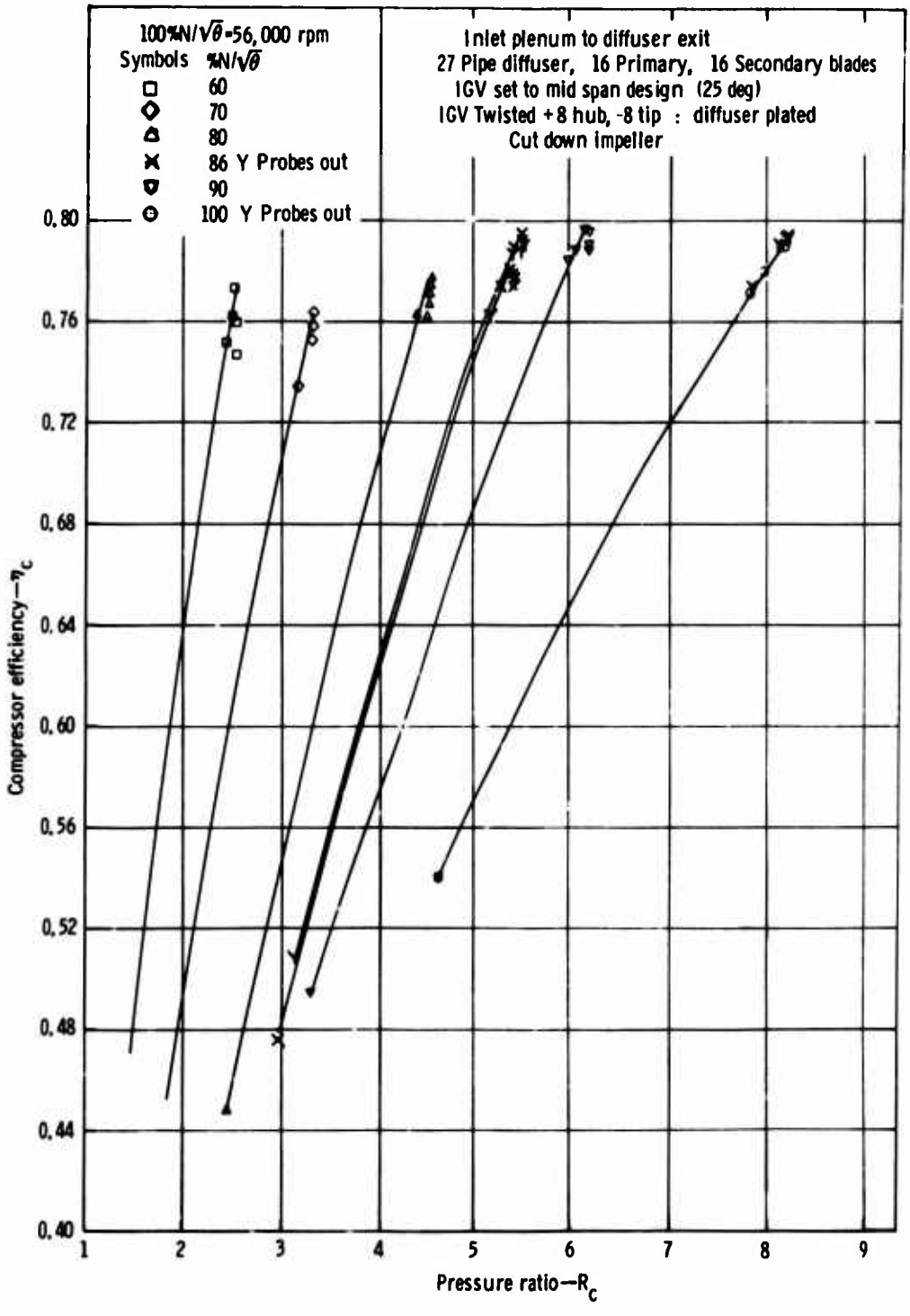

Figure 50. RC-2.7 performance.

New Instrumentation

The RC-2.7 compressor test included all the instrumentation described for the RC-2.5 test, except that no temperature traverses were obtained. Additional instrumentation was provided the compressor for this test in the region of the impeller tip, the diffuser throat, and the collector exit as previously discussed under RC-2.7 Instrumentation. The three removable throat total pressure probes were removed after completion of the initial part of the test and were replaced by the "blanks," and the 86% and 100% design speed lines were repeated to check the effect of the probes on the flow. The comparison at 86% speed is not quite straightforward, however, because the impeller rubbed the shroud at 100% speed, thus removing material from the shroud, and increasing the clearance when the 86% speed was repeated as compared to the original clearance. The main effect of the throat probes at 100% speed was to decrease the efficiency by less than 0.3%.

Impeller Outlet Flow Distribution Data

The two total pressure/yaw probes described in the RC-2.5 Baseline Test subsection were used to obtain traverse data in the manner described previously. Because of the reduced impeller radius, these probes were 16.5% outboard of the impeller, instead of 7.7% as in the previous tests.

Some difficulty was experienced in yawing probe 2, so only partial data were obtained with that unit. The problem was caused by a mechanical bind in the actuator mechanism.

Figures 51 and 52 show, respectively, the impeller outlet total pressure distribution and a typical flow angle distribution.

Table 8 is a reduction of the yaw/pressure traverse data obtained by the Traverse Data Reduction program. The nomenclature for this computer output has been defined in Table 5.

Rig Mechanical Operation

The mechanical operation of the compressor rig itself was uneventful. However, vibrations in the steam turbine drive train were great enough to prohibit running at 85% speed. Data were obtained at 86% speed instead. The lower of the two drive turbines was replaced during this test because its vibrations exceeded normal limits at 90% speed. No further problems were encountered after installation of the new turbine.

After teardown of the compressor rig, evidence was observed of a light rub between the rotor exducer and the shroud. This slight contact was anticipated in view of the low tip clearance used in the buildup.

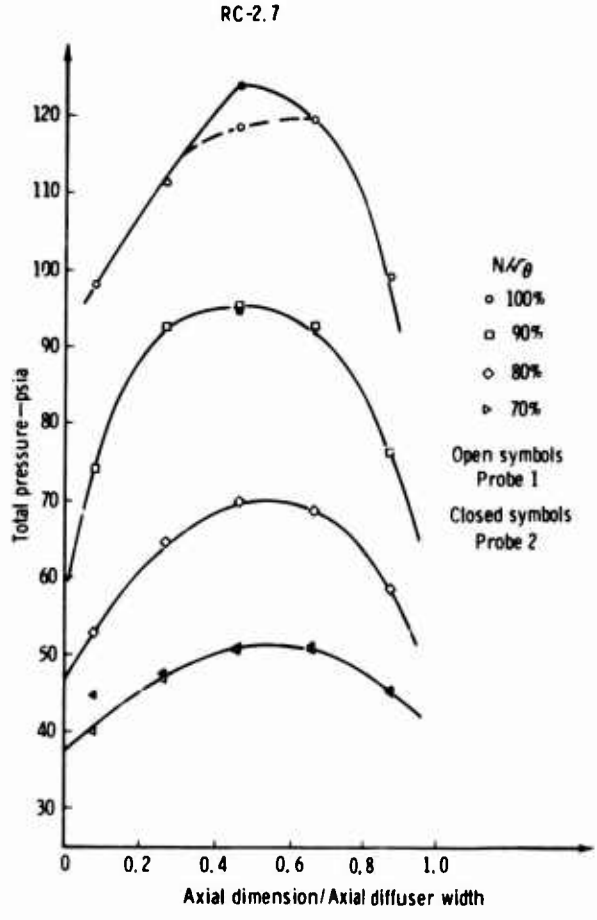

Figure 51. Impeller outlet total pressure profile.

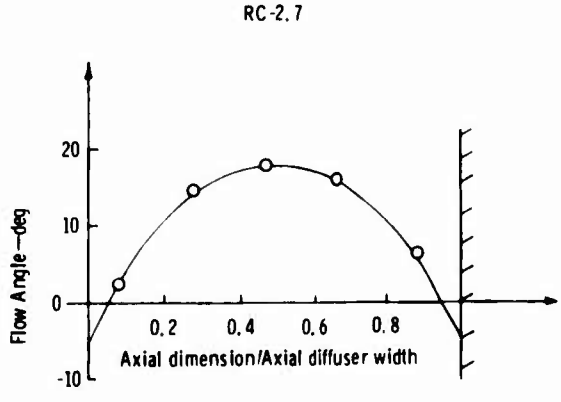

Figure 52. Impeller cutlet flow angle profile.

TABLE 8. YAW/PRESSURE DATA REDUCTION—RC-2.7.

```
 RC 2.7   70( SPEED, RDG 627
                    INPUT DATA FOLLOWS
5   32.1960   30.6450   31.9440   33.0610   40.8000  784.3400    1.8640
  32.0320   31.2200   31.5230   32.3700
 215.4000   55.3000  261.3000  101.4000
   0.0000   39.8000  201.0000  436.5000    0.0000   44.5000  247.0000  441.5000
   0.0000   46.8000  169.0000  495.0000    0.0000   47.5000  217.0000  471.5000
   0.0000   50.4000  136.0000  565.0001    0.0000   51.2000  187.0000  513.0001
   0.0000   50.8000  102.0000  569.5001    0.0000   50.5000  153.0000  504.5000
   0.0000   45.0000   64.0000  539.0001    0.0000   45.0000  110.0000  474.0000
  47.9460    0.1770   46.9350    0.3541   49.3110    0.3541   48.0440    0.3541
  45.4960    0.3541   42.8950    0.7082   41.9440    0.7082   42.5860    0.7082
  44.3270    0.7028
   0.0000    0.0000    0.0000    0.0000
        INLET STATION PROBE                          LEADING EDGE STATION PROBE

    PT1         Z1       ALPH1                        PTLE       ZLE       ALPHLE
  39.8000    0.0280   -6.0299                       44.5000    0.0278   -7.6499
  46.8000    0.0904    4.5000                       47.5000    0.0863   -2.2500
  50.4000    0.1548   17.0999                       51.2000    0.1448    5.2200
  50.8000    0.2211   17.9099                       50.5000    0.2111    3.6899
  45.0000    0.2952   12.4200                       45.0000    0.2950   -1.7999

                  INLET STATION DATA ON AVERAGE BASIS

        I      PT1B      ALP1       P1        M1        M2        CP
        6   48.7784   13.7786   31.9473    0.8016    0.3930    0.5259

    PT2B      BLOCK      WAC     W/WMAX    DPT/PT1      P2        WA       A*/A1
  45.3845    0.1959    0.6912    1.0098    0.0695   40.8000    1.8640    0.9548

                LEADING EDGE DATA ON AVERAGE BASIS

        I      PT1B      ALP1       P1        M1        M2        CP
        7   48.5907   13.8257   31.7833    0.8029    0.3930    0.5364

    PT2B      BLOCK      WAC     W/WMAX    DPT/PT1      P2        WA       A*/A1
  45.3845    0.1959    0.6939    1.0137    0.0659   40.8000    1.8640    0.9516
```

```
 RC 2.7 , 79.73 (  SPEED, RDG 630
                    INPUT DATA FOLLOWS
5   39.7970   37.2260   39.4990   41.3770   51.4000  870.2900    2.3890
  39.4550   38.0650   38.7880   40.1540
 215.4000   55.3000  261.3000  101.4000
   0.0000   52.9000  201.0000  476.5000    0.0000    0.0000    0.0000    0.0000
   0.0000   64.3000  169.0000  533.5001    0.0000    0.0000    0.0000    0.0000
   0.0000   59.6000  136.0000  575.5001    0.0000    0.0000    0.0000    0.0000
   0.0000   68.7000  102.0000  572.5001    0.0000    0.0000    0.0000    0.0000
   0.0000   58.5000   64.0000  514.5001    0.0000    0.0000    0.0000    0.0000
  60.9600    0.1770   59.1400    0.3541   61.1900    0.3541   59.4040    0.3541
  59.7310    0.3541   53.8340    0.7082   53.2040    0.7082   54.3860    0.7082
  57.4380    0.7028
   0.0000    0.0000    0.0000    0.0000
        INLET STATION PROBE                          LEADING EDGE STATION PROBE

    PT1         Z1       ALPH1                        PTLE       ZLE       ALPHLE
  52.9000    0.0280    1.1700                        0.0000    0.5095  -87.1199
  64.3000    0.0904   11.4300                        0.0000    0.5095  -87.1199
  69.6000    0.1548   18.9899                        0.0000    0.5095  -87.1199
  68.7000    0.2211   18.4500                        0.0000    0.5095  -87.1199
  58.5000    0.2952    8.0100                        0.0000    0.5095  -87.1199

                  INLET STATION DATA ON AVERAGE BASIS

        I      PT1B      ALP1       P1        M1        M2        CP
        6   65.6673   13.4688   39.4500    0.8852    0.4022    0.4558

    PT2B      BLOCK      WAC     W/WMAX    DPT/PT1      P2        WA       A*/A1
  57.4599    0.1586    0.6931    1.0127    0.1249   51.4000    2.3890    0.9763
```

TABLE 8. (CONT)

```
 RC2.7    89.79 (   SPEED .  RDG.632
                  INPUT DATA FOLLOWS
5   50.7200   48.1090   48.7590   51.4150   71.9000  950.2800    3.0470
  51.9580   46.9420   50.4540   54.0100
 215.4000   55.3000  261.3000  101.4000
   0.0000   73.8000  201.0000  483.5000    0.0000    0.0000    0.0000    0.0000
   0.0000   92.1000  169.0000  549.5001    0.0000    0.0000    0.0000    0.0000
   0.0000   95.5000  136.0000  568.0001    0.0000    0.0000    0.0000    0.0000
   0.0000   92.5000  102.0000  558.0001    0.0000    0.0000    0.0000    0.0000
   0.0000   76.1000   64.0000  505.0000    0.0000    0.0000    0.0000    0.0000
  85.5810    0.1770   83.8690    0.3541   86.8750    0.3541   83.8620    0.3541
  81.7310    0.3541   74.8990    0.7082   73.9180    0.7082    0.0000    0.7082
   0.0000    0.7028
   0.0000    0.0000    0.0000    0.0000
        INLET STATION PROBE                          LEADING EDGE STATION PROBE

    PT1         Z1       ALPH1                        PTLE      ZLE       ALPHLE
  73.8000    0.0280    2.4299                        0.0000    0.5095  -87.1199
  92.1000    0.0904   14.3099                        0.0000    0.5095  -87.1199
  95.5000    0.1548   17.6399                        0.0000    0.5095  -87.1199
  92.5000    0.2211   15.8399                        0.0000    0.5095  -87.1199
  76.1000    0.2952    6.2999                        0.0000    0.5095  -87.1199

                  INLET STATION DATA ON AVERAGE BASIS

         I      PT1B      ALP1       P1        M1        M2        CP
         6   89.7259   12.9954   49.7365    0.9581    0.4276    0.5542

    PT2B      BLOCK      WAC      W/WMAX     DPT/PT1      P2        WA        A*/A1
  81.5354    0.2477    0.6761    0.9878    0.0912   71.9000    ..  70      1.0112
```

```
    RC 2.7 .100(  SPEED.  RDG 635        FIXED    STATION 3
                  INPUT DATA FOLLOWS
5   63.3210   56.6020   58.1000   63.8730   93.5600 1044.5300    3.7370
  63.9340   54.6680   60.8550   66.4910
 215.4000   55.3000  261.3000  101.4000
   0.0000   98.0000  201.0000  446.5000    0.0000    0.0000    0.0000    0.0000
   0.0000  111.0000  169.0000  505.0000    0.0000    0.0000    0.0000    0.0000
   0.0000  124.0000  136.0000  586.0001    0.0000    0.0000    0.0000    0.0000
   0.0000  119.5000  102.0000  576.5001    0.0000    0.0000    0.0000    0.0000
   0.0000   99.0000   64.0000  523.0001    0.0000    0.0000    0.0000    0.0000
 110.7400    0.1770  106.7600    0.3541  112.9480    0.3541  109.5970    0.3541
 106.5450    0.3541   97.7920    0.7082   96.2360    0.7082   97.9420    0.7082
 103.5530    0.7028
   0.0000    0.0000    0.0000    0.0000
        INLET STATION PROBE                          LEADING EDGE STATION PROBE

    PT1         Z1       ALPH1                        PTLE      ZLE       ALPHLE
  98.0000    0.0280   -4.2299                        0.0000    0.5095  -87.1199
 111.0000    0.0904    6.2999                        0.0000    0.5095  -87.1199
 124.0000    0.1548   20.8800                        0.0000    0.5095  -87.1199
 119.5000    0.2211   19.1699                        0.0000    0.5095  -87.1199
  99.0000    0.2952    9.5399                        0.0000    0.5095  -87.1199

                  INLET STATION DATA ON AVERAGE BASIS

         I      PT1B      ALP1       P1        M1        M2        CP
         6  116.1180   12.8929   60.4002    1.0132    0.3994    0.5951

    PT2B      BLOCK      WAC      W/WMAX     DPT/PT1      P2        WA        A*/A1
 104.4340    0.2022    0.6717    0.9814    0.1006   93.5600    3.7370    1.0191
```

IV. COMPARISON OF THEORY AND EXPERIMENT

The test data obtained for the RC-2.5, -2.6, and -2.7 compressor builds were analyzed and compared with the CCP calculation predictions. The calculation was then rerun with different values of some of the input parameters in order to "match" the test data. The data matching procedure was used to diagnose the compressor and to recommend modifications for the subsequent tests.

DATA ANALYSIS

The compressor test data were analyzed to obtain the intrastage performance parameters. A short discussion of each of the measurements and its analysis follows. For comparison purposes, all pressure values were nondimensionalized by dividing by the compressor inlet (plenum) pressure.

DIFFUSER VANELESS SPACE

Inlet Static Pressure

This is the arithmetic average of eight static pressure taps distributed circumferentially so as to span one diffuser passage at a radius 3% outboard of the original impeller and 11.3% outboard of the modified impeller used in the RC-2.7 test. Half the taps were located on the hub side of the compressor, and the other half on the shroud side.

Traverse Station Static Pressure

This is the arithmetic average of eight static pressure taps distributed as previously stated, except that they were located at a radius 7.7% outboard of the original impeller and 16.5% outboard of the RC-2.7 impeller.

Traverse Station Total Pressure

The "raw" value of this parameter is calculated from the data obtained in choke and as described in the RC-2.5 Test subsection.

A correction was then made to the raw value to reflect the value which the traverse data would have yielded had the compressor been capable of stable operation at other than choked flow conditions with the traversing probes in place. The correction is performed by multiplying the raw value of the traverse pressure by the ratio of the maximum diffuser exit pressure at the operating point in question to the same pressure at the "break" point at that speed. The value of the break point pressure is illustrated in Figure 53. In the case of RC-2.7, the value

of the throat total pressure readings could be substituted for the maximum diffuser exit pressure; this method would give a result differing by less than 0.2% from the method actually used. The value of the traverse total pressure obtained in this manner is used in the calculation of the pressure ratio, Mach number, and efficiency to the traverse stations of Tables 9, 10, 11, and 12 shown later in this section.

The method of obtaining the operating point traverse total pressure clearly involves the assumption that only minor (and negligible) profile changes occur at the traversing station as the compressor is loaded. Some substantiation for this assumption has been presented by S. Baghdadi.[19]

The Diffuser Leading-Edge Static Pressure

The value of this parameter is obtained by averaging the readings of four static pressure taps. Two of these pressure taps are located on the hub and two on the shroud side of the compressor as illustrated in Figure 54. Because of the very large pressure gradients in this region, the value of the leading-edge pressure obtained in this manner is felt to be accurate only to within ±5%.

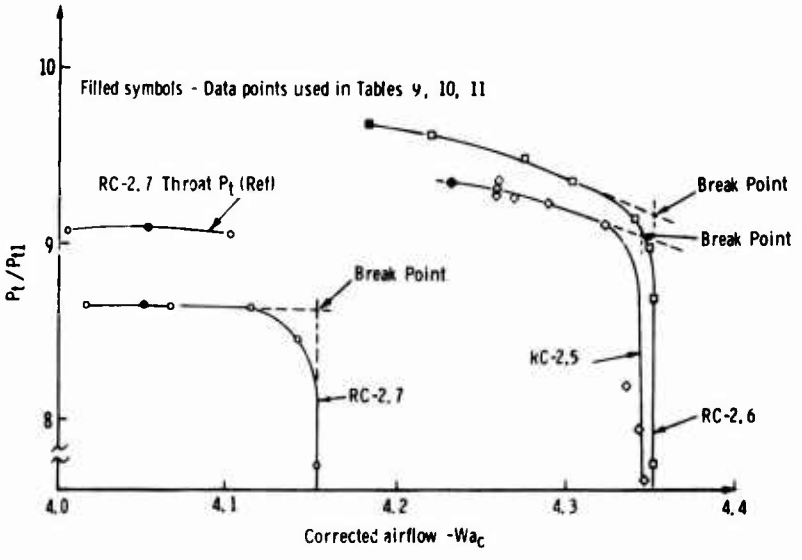

Figure 53. Diffuser exit peak total pressure ratio—"Break Point".

[19] Baghdadi, S. A Study of Vaned Radial Diffusers Using Swirling Transonic Flow Produced by a Vortex Nozzle. PhD. Thesis, Purdue University, Lafayette, Indiana. December 1973.

The Diffuser Leading-Edge Total Pressure

The diffuser leading-edge centerline total pressure read lower than the maximum diffuser exit static pressure throughout the RC-2 program. The other two leading-edge total pressure probes, which were in place and intact only for the RC-2.5 test, appeared to read a realistic value. The average reading of these two probes was used in Table 2. These probes were damaged in the plating process used to decrease the throat area for the RC-2.6 tests and were not used.

The Diffuser Throat Static Pressure

The value of this parameter is obtained by arithmetically averaging the readings of the static pressure taps distributed around the diffuser throat as shown in Figure 21. All seven of the tap readings were used in the RC-2.6 data analysis; in the case of RC-2.5 and -2.7, however one of the taps was disregarded in the averaging as it read suspiciously high.

The Diffuser Throat Total Pressure

Diffuser throat total pressure data were obtained only for the RC-2.7 test, as previously discussed. The arithmetic average of the readings of the three probes located at the centerline of the three different diffuser passages was used* to obtain the diffuser throat centerline total pressure. The value of the area-averaged (or "one-dimensional") throat total pressure was then computed by multiplying the centerline total pressure by the blockage factor obtained from a one-dimensional continuity calculation at the throat. This is the throat total pressure listed in Table 11.

Impeller Tip Static Pressure

The RC-2.5 and -2.6 builds did not have static pressure taps exactly at the impeller tip radius. It was therefore necessary to interpolate the impeller tip static pressure value from the radial static pressure distribution measured along the shroud and in the diffuser. The arithmetic average of the five taps 4% radially inboard and the eight taps 3% radially outboard of the impeller tip were included in that distribution.

In the case of RC-2.7, the arithmetic average of the five taps located at the new impeller tip radius was used as the impeller tip static pressure.

*All three centerline probes read within 1% of the average value.

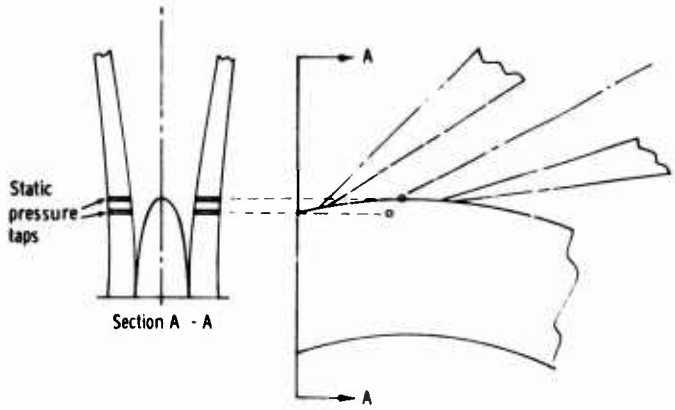

Figure 54. Leading-edge static pressure tap location.

APPLICATION OF CCP TO THE RC-2 COMPRESSOR

RC-2.5

Table 9 compares the predicted and measured values of the intrastage and overall compressor performance parameters. The predicted value of the rotor work, $\Delta H/H$, is seen to be low by 6.6% compared with the measured value. Two factors are of importance in understanding this significant discrepancy. First, the CCP calculation had only recently been modified to account for back-curved exducer blading at the time of the original prediction, and no substantial background for this type of compressor had been acquired. Second, the back-curved section of the RC-2 impeller is an unusual, "no work" section added to the tip of a basically radial design. This approach led to rapid curvature changes in the exducer which, according to the analysis of the test data, resulted in flow separation along the exducer pressure surfaces. (The slip factor works out to be greater than unity if the actual metal angle of 32.5 deg at the rotor exit is used.) The analysis of the test data indicates that, in actuality, the maximum justifiable value of the effective blade exit angle is 28 deg.

Figure 55 compares the original slip factor prediction to the most recent computations used in predicting the slip factor for RC-2.7 as a function of the rotor exit blade angle. The most recent theory produces a much higher value of the slip factor than did the original theory.

Table 9 shows that the CCP calculation was within 1% of the test data in its computation of the pressure ratio and flow rate, but that the calculated efficiency was 4.5% higher than the measurement.

TABLE 9. COMPARISON OF PREDICTED AND MEASURED VALUES—RC-2.5.

	Calculated	Measured
Impeller		
η traverse	0.863	0.834
η adiabatic	0.890	
η hydraulic	0.940	
η mixed	0.864	
$\Delta H/U^2/Jg$	0.763	
C_θ/U	0.780	
Impeller tip static pressure	3.716	3.640
Vaneless space		
Inlet (1.03 R/R_{IT})		
P_s/P_{T_1}	4.290	4.028
P_T/P_{T_1}	9.777	
M	1.150	
Traverse station (1.077 R/R_{IT})		
P_s/P_T	4.600	4.306
P_T/P_{T_1}	9.750	9.995
M	1.094	1.166
Diffuser		
Leading edge		
P_s/P_{T_1}	4.895	4.231
P_T/P_{T_1}	9.542	9.468
M	1.025	1.138
Throat		
P_s/P_{T_1}		5.781
Exit		
P_T/P_{T_1}	8.857	8.883
P_s/P_{T_1}	8.138	8.018
M	0.350	0.385
$C_{PLE\text{-exit}}$	0.700	0.723
$C_{P\text{traverse-exit}}$	0.687	0.653
Overall compressor (to diffuser exit)		
$\Delta H/H$	1.048	1.117
Wa_c	4.184	4.230
η	0.825	0.781
R_c	8.857	8.883

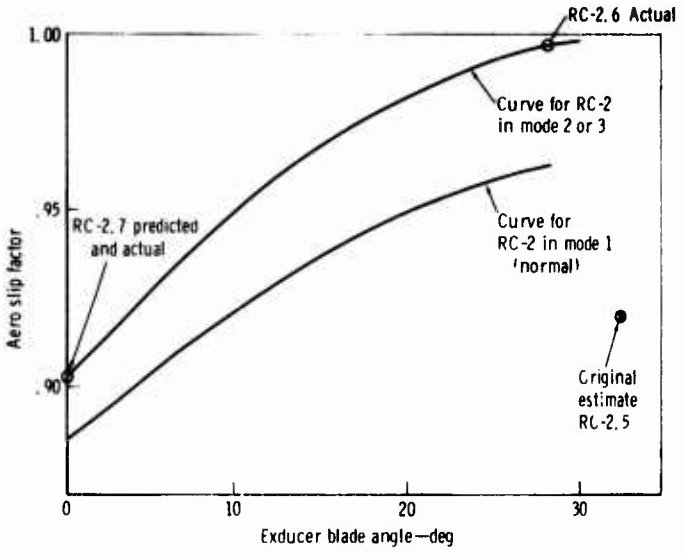

Figure 55. Variation of slip factor with exducer blade angle.

RC-2.6

The RC-2.5 test data indicated that the diffuser inlet flow profile was weak on the shroud side and that the inducer was choking at the maximum flow at design speed. For RC-2.6, the first of these problems was attacked by twisting the inlet guide vanes—-3 deg (open) at the tip, +8 deg (closed) at the hub—in such a manner as to strengthen the shroud flow by redistributing the work at the impeller outlet. The second problem was tackled by plating the diffuser to reduce the throat area by 3%.

The data obtained during the RC-2.6 tests are plotted together with the a priori (predicted) CCP calculations in Figures 56 and 57.

The a priori input to the CCP calculation involved a variation in the impeller axial blockage input with speed which was similar to that deduced from the RC-2.5 a posteriori analysis. The change in the "flow quality" mode which was input for the 70% speed line was likewise anticipated from the RC-2.5 data analysis. Figure 56 shows that the CCP calculation successfully predicted the test data at all speeds except 100%.

To match the 100% speed test data a posteriori, the value of the impeller exit axial blockage was increased over the value used a priori, and the diffuser choking coefficient was modified. In addition, the flow quality mode of the rotor was changed from Mode 1 to Mode 3, indicating

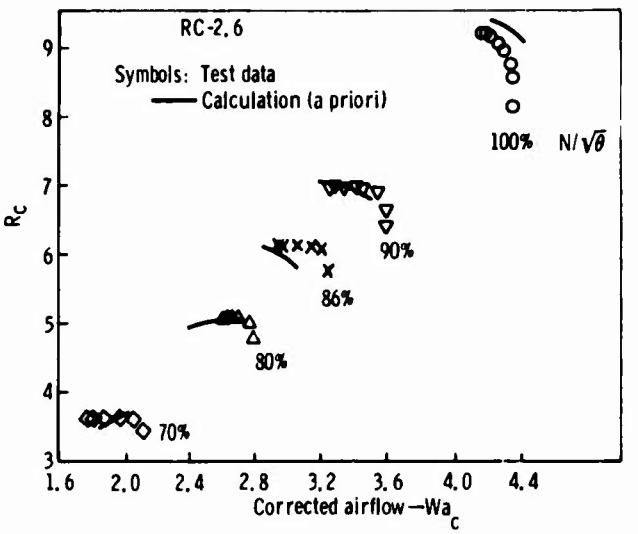

Figure 56. Predicted and measured performance—RC-2.6.

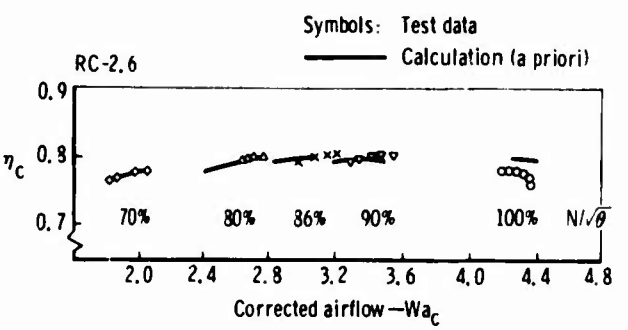

Figure 57. Predicted and measured performance—RC-2.6.

a degraded rotor performance. These changes result from the fact that the RC-2.6 rotor with the twisted IGV's behaved similarly to the RC-2.5, 33 deg IGV setting instead of similarly to the 17 deg setting as anticipated. In other words, it would appear that the hub value of the IGV setting dominated over the tip value.

Table 10 compares the a priori calculated and measured values of the intrastage and overall performance parameters of RC-2.6 near the design point. This table shows that the calculation was within 0.1% of the measured pressure ratio, but was 1.5% high in efficiency and 6.6% high in flow.

TABLE 10. COMPARISON OF PREDICTED AND MEASURED VALUES—RC-2.6

	Calculated	Measured
Impeller		
$\eta_{traverse}$	0.864	0.821
$\eta_{adiabatic}$	0.885	
$\eta_{hydraulic}$	0.926	
η_{mixed}	0.852	
$\Delta H/U^2/Jg$	0.811	
$C\theta/U$	0.836	
Impeller tip static pressure	3.959	3.930
Vaneless space		
Inlet (1.03 R/R_{IT})	4.320	4.398
P_s/P_{T_1}	10.760	
P_T/P_{T_1}	1.210	
M		
Traverse station (1.077 R/R_{IT})		
P_s/P_{T_1}	4.680	4.582
P_T/P_{T_1}	10.033	9.996
M	1.142	1.118
Diffuser		
Leading edge		
P_s/P_{T_1}	4.984	4.630
P_T/P_{T_1}	10.306	
M	1.074	
Throat		
P_s/P_{T_1}	5.421	6.284
Exit		
P_T/P_{T_1}	9.173	9.169
P_s/P_{T_1}	8.425	8.368
M	0.350	0.364
$C_{p\ I\ E\text{-}exit}$	0.618	
$C_{p_{traverse\text{-}exit}}$	0.640	0.699
Overall compressor (to diffuser exit)		
$\Delta H/H$	1.112	1.135
Wa_c	4.460	4.184
η	79.460	78.000
R_c	9.173	9.169

RC-2.7

The analysis of the RC-2.5 and -2.6 data indicated that the rotor outlet flow deviated (i.e., was separated) from the pressure surface in an unusual manner. This deviation was ascribed to the rapid curvature used in the exducer design, so the back-curved portion of the exducer had to be removed to remedy the situation. This modification entailed the insertion of an extended vaneless space to replace the outboard 8% of the rotor which was removed, so the diffuser leading edge was now 22% outboard of the rotor tip.

The predicted and measured values of the RC-2.7 performance (both overall and intrastage) near the design point are shown in Table 11. The calculated value of the mass flow in Table 11 is that which yielded the maximum overall efficiency. However, the program showed very little variation of the overall efficiency with flow rate, so the a priori calculated performance at the increased flow rate differed significantly from the value shown in Table 11 only with respect to the diffuser throat static pressure and Mach number. The calculation is seen to be high by 3.6% in flow, 0.7% in efficiency, and 1.78% in pressure ratio.

The adjustment required to "match" the calculation to the test data consisted of varying the diffuser choking coefficient; this change lowered the pressure and shifted the compressor's choke flow to a lower value. The resulting map is compared to the test data in Figures 58 and 59. The only aerodynamic program input which is varied with speed is the diffuser choking coefficient. If an average value of this coefficient were used*, the maximum deviation from the data resulting would be ±1% in efficiency and ±2% in pressure ratio. The computer runs used to produce Figures 58 and 59 are shown in the Appendix, together with the input-output nomenclature. The compressor running clearance, which is included in the rotor hub to shroud dimension BH, is input, and varies with rotor rpm.

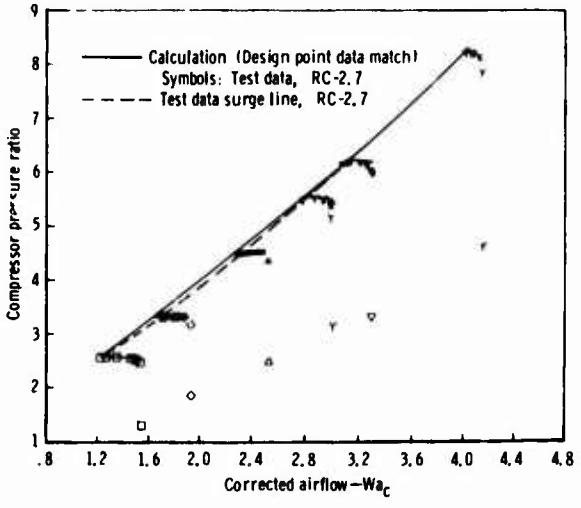

Figure 58. Measured and matched performance—RC-2.7.

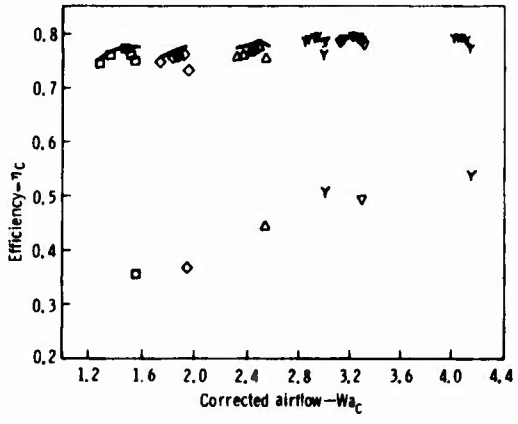

Figure 59. Measured and matched performance—RC-2.7.

*Obviously, until a more accurate diffuser choking relationship is found, the a priori or design mode of the program will use such a constant coefficient.

TABLE 11. COMPARISON OF PREDICTED AND MEASURED VALUES—RC-2.7.

	Calculated	Measured
Impeller		
η traverse	0.866	0.820
η adiabatic	0.898	
η hydraulic	0.940	
η mixed	0.853	
$\Delta H/U^2/Jg$	0.879	
C_θ/U		
Impeller tip static pressure	3.166	3.300
Vaneless space		
Inlet (1.116 R/R_{IT})		
P_S/P	4.225	4.539
P_T/P_{T_1}	9.424	
M	1.135	
Traverse station (1.168 R/R_{IT})		
P_S/P_{T_1}	4.535	4.605
P_T/P_{T_1}	9.436	8.639
M	1.079	0.992
Diffuser		
Leading edge		
P_S/P_{T_1}	4.825	4.583
P_T/P_{T_1}	9.230	
M	1.009	
Throat		
P_T/P_{T_1}	8.880	8.490
P_S/P_{T_1}	5.030	5.137
Exit		
P_T/P_{T_1}	8.334	8.188
P_S/P_{T_1}	7.657	7.473
M	0.350	0.364
$C_{pLE\text{-}exit}$	0.641	
$C_{ptraverse\text{-}exit}$	0.637	0.708
Overall compressor (to diffuser exit)		
$\Delta H/H$	1.041	1.042
Wa_c	4.200	4.053
η	0.800	0.793
R_c	8.334	8.188

DISCUSSION

Tables 9, 10, and 11 may be interpreted to indicate that the CCP program has difficulty in separating the subcomponent performance. The reason for this may be the very complex relationship between the impeller and the diffuser.* Table 12 lists the measured subcomponent efficiencies of the various RC-2 configurations. The pressure ratio at the traverse station for the 17 deg IGV setting of RC-2.5 was not measured, and is deduced by comparing the leading-edge total pressures to those of the 25 and 33 deg IGV settings of this build. Table 12 indicates that, when the IGV's were twisted, the impeller efficiency was reduced and the diffuser's pressure recovery coefficient increased. This increase in the diffuser performance can be at least partly traced to the improvement in the impeller outlet flow profile which in turn can be traced to the work redistribution effect of twisting the inlet guide vanes. Since improving the flow profile into the diffuser was the motivation for twisting the inlet guide vanes, this result was expected. Unfortunately, the loss in impeller efficiency was not expected. The explanation for the decrease in impeller performance in going from RC-2.5 (25 deg IGV) to RC-2.6 cannot be explained solely in terms of an increased inducer tip Mach number, for the RC-2.5, 17 deg IGV build, which has the highest impeller efficiency listed in Table 12, also has the highest inducer tip Mach number. In fact, the only parameter that separates the higher efficiency impellers (RC-2.5, IGV=17 deg and IGV=25 deg) from the lower efficiency impellers (RC-2.5, IGV=33 deg, RC-2.6 and RC-2.7) is the hub value of the inlet guide vane setting, which was 33 deg for the lower efficiency rotors and 17 and 25 deg for the high efficiency rotors. The differences in rotor efficiencies can thus be tentatively attributed to a sensitivity to the inducer inlet flow incidence profile.

TABLE 12. INTRASTAGE EFFICIENCIES OF VARIOUS RC-2 CONFIGURATIONS.

	RC-2.5			RC-2.6	RC-2.7
	IGV = 17	IGV = 25	IGV = 33	IGV = 25	IGV = 25
Impeller					
Inducer tip Mach No.	1.220	1.112	1.034	1.218	1.191
$R_{c_{traverse}}$	10.431	9.995	9.541	9.996	8.639
$\eta_{traverse}$	0.840	0.834	0.823	0.821	0.820
$M_{traverse}$	1.170	1.166	1.181	1.118	0.992
Diffuser					
$C_{P_{traverse-exit}}$	0.643	0.653	0.651	0.699	0.708
$R_{c\ exit}$	9.187	8.883	8.399	9.169	8.188
M_{exit}	0.383	0.385	0.376	0.364	0.364
Overall					
η	0.780	0.781	0.767	0.780	0.793

*The vaneless space up to the traversing station is considered to be part of the impeller, since this is the performance measuring station closest to the rotor.

It is important to note that the "impeller" efficiencies listed in Table 12 actually include losses up to the traverse station. Thus, the actual impeller efficiency (not including vaneless space losses) must have increased in RC-2.7 as compared to RC-2.6, because the traverse station is 13% outboard of the impeller in the former case and only 7.7% in the latter.* This is important because it implies that the removal of the bent back section of the rotor decreased the rotor losses, thus lending credibility to the theory that the exducer pressure surface was separated in RC-2.5 and RC-2.6. In fact, the a posteriori CCP calculations show the rotor loss to have decreased from 50.9% of the total losses in RC-2.6 to only 38.4% in RC-2.7.

The RC-2.7 compressor showed an efficiency improvement of 1.3% in spite of the fact that the diffuser leading edge was 22% outboard of the modified impeller. If the current design practices at DDA and elsewhere can be used as a guide (ref: D. P. Kenny[2], an ASME publication,[6] and D. P. Kenny [20]), the RC-2.7 radius ratio is excessive—the optimum radius ratios used vary from 5% to 13% for high-pressure-ratio machines. Thus, a further efficiency improvement may be realized if the modified rotor were tested with a new, rematched, smaller radius ratio diffuser. However, the magnitude of the improvement is difficult to assess without recourse to a performance prediction calculation (such as CCP) which takes into account both the decreased losses due to the lower leading-edge Mach number and the increased "frictional" loss because of the large vaneless space radius ratio. Contrary to expectations, the CCP calculation does not show a performance decrement in the case of this particular diffuser as the leading-edge radius ratio is increased from 1.13 to 1.22. Because of the lack of sufficient test data at the higher radius ratios, only a specific test can confirm the CCP prediction in this regard.

*Obviously, this comment assumes that the losses in the vaneless space are proportional to the extent of the vaneless space.

[20]Kenny, D. P. A Comparison of the Predicted and Measured Performance of High Pressure Ratio Centrifugal Compressor Diffusers. ASME Paper No. 72-GT-54. 1972.

V. CONCLUSIONS

1. The CCP calculation successfully predicted the flow and pressure ratio, but it did not accurately predict the efficiency measured in the first test of the RC-2 compressor because of the unusual exducer blading used in this design. Indications are that the flow was separated from the pressure surface at the rotor exit. Certain "flow quality" parameters, which are input to the calculation, had to be adjusted to account for the deviation of the flow from the blade pressure surface.

2. Once a machine has been tested, the CCP calculation can be used to deduce the appropriate "flow quality" parameters, and thus helps point out the weaknesses in the rotor design.

3. Once the calculation has been matched to the data at design point, the entire map can be reproduced by varying only one aerodynamic coefficient in the case of the radial rotor (RC-2.7) and three coefficients in the case of a back-curved rotor (RC-2.6 and RC-2.5). In no case are coefficients varied along a given speed line.

4. The CCP calculation will not predict "bumps" in surge lines as were measured in the case of RC-2.5 and RC-2.6. The predicted surge line will be nearly straight, as was measured for RC-2.7.

5. The CCP calculation fairly accurately predicts the effects of minor modifications to the compressor.

6. Both the rotor and the diffuser were sensitive to the flow profile at their respective inlets.

VI. RECOMMENDATIONS

1. The diffuser loss models used in the CCP calculation should be updated to take into account the recent data of References 3 and 4.

2. An effort should be directed toward finding a relationship between the impeller "flow quality" and the blading distribution; in particular, a relationship is required that would express the rotor "flow quality" in terms of the gradients in the impeller blade angle distribution and certain diffuser parameters. Such a relationship would obviate the necessity for inputting the "flow quality" into the calculation.

3. The RC-2.7 rotor should be equipped with a properly matched diffuser and tested for performance to ascertain the compressor's true potential.

VII. REFERENCES

1. Balje, O.E. A Study on Design Criteria and Matching of Turbo Machines. Part B—Compressor and Pump Performance and Matching of Turbo Components. ASME Paper 60-WA-231.

2. Kenny, D.P. A Novel, Low-Cost Diffuser for High Performance Centrifugal Compressors. ASME 68/GT-38.

3. Dean, R. C., Jr., and Runstadler, P. W., Jr. Straight Channel Diffuser Performance at High Inlet Mach Numbers. Creare, Inc., Hanover, New Hampshire.

4. Dolan, F. X., and Runstadler, P. W., Jr. Pressure Recovery Performance of Conical Diffusers at High Subsonic Mach Numbers. Creare Report TN-165, Hanover, New Hampshire. July 1973.

5. Rodgers, C. A Cycle Analysis Technique for Small Gas Turbines; Technical Advances in Gas Turbine Design. Paper No. 5, Institution of Mechanical Engineers. April 1969.

6. Advanced Centrifugal Compressors. ASME Turbomachinery Committee, Gas Turbine Division, New York. 1971.

7. Dallenbach, F. The Aerodynamic Design and Performance of Centrifugal and Mixed-Flow Compressors; Symposium on Centrifugal Compressors. ASME. 1962.

8. Davis, D.M. Radial Flow Compressor and Turbine Design Program. Mathematics Sciences Report. Detroit Diesel Allison Division, General Motors. August 1971.

9. Stanitz, J.D. Some Theoretical Aerodynamic Investigations of Impellers in Radial and Mixed-Flow Centrifugal Compressors. Trans. ASME, Vol 74, pp 473-497. 1952.

10. Katsantis, T. Computer Program for Calculating Velocities and Streamlines on a Blade-to-Blade Stream Surface of a Turbomachine. NASA TN D-4525. April 1968.

11. Hopkins, B.A. Inlet Guide Vane Design for Centrifugal Compressor. Research Note RN 69-79, Detroit Diesel Allison Division, General Motors. December 1969.

12. Morris, R. E., and Kenny, D. P. High-Pressure Ratio Centrifugal Compressors for Small Gas Turbine Engines. Report No. 6, 31st Meeting of the Propulsion and Energetics Panel of AGARD, Ottawa, Canada. June 1968.

13. Trent, R. Dynamic Analysis RC-2 Compressor Rotor Case System. Engineering Department Report TDR AX.0220-016, Detroit Diesel Allision Division, General Motors. June 1972.

14. Burns, L. Vibration Analysis of the RC-2 Impeller. Engineering Department Report TDR AX.0201-037, Detroit Diesel Allison Division, General Motors. July 1972.

15. Clute, M. Stress Analysis of the RC-2 Impeller. Engineering Department Report TDR AX.0201-036, Detroit Diesel Allison Division, General Motors. July 1972.

16. Colborn, J.H. Temperature Distributions in the RC-2 Impeller. Engineering Department Report TDR AX.0201-035, Detroit Diesel Allison Division, General Motors. May 1972.

17. Flow Measurement. ASME Power Test Code Committee, ASME, New York. 1959.

18. Keenan, J. H., and Kaye, J. Gas Tables. John Wiley and Sons, Inc., New York. 1961.

19. Baghdadi, S. A Study of Vaned Radial Diffusers Using Swirling Transonic Flow Produced by a Vortex Nozzle. Ph.D Thesis, Purdue University, Lafayette, Indiana. December 1973.

20. Kenny, D.P. A Comparison of the Predicted and Measured Performance of High Pressure Ratio Centrifugal Compressor Diffusers. ASME Paper No. 72-GT-54. 1972.

APPENDIX
CENTRIFUGAL COMPRESSOR PERFORMANCE PROGRAM

Input

TRIG	Choking flow coefficient acting directly on Δq_{ri} (Normally for no choking = 1.0)
DELSF	Perturbation on slip factor; used only for study
CC	Coefficient acting on (M_{RIT} - M_{RIC}) where M_{RIT} = Inlet shroud rel Mach No. M_{RIC} = Critical rel Mach No.
C3	Coefficient determining the dependence (explicit) of secondary recirculation losses on inlet flow coefficient (0 = no dependence)
C1	Not used
C5	Coefficient acting on abs (M_1 - M_{ICR}), i.e., (M_T - CMT)
C6	Inducer tip coefficient
TRIGR	Scale parameter on the overall diffuser loss from LE to M = 0.15 (collector)
D1	Inducer inlet hub diameter—ft
D1/D2	Inducer hub/tip ratio
N	RPM
W	Mass flow—lb/sec
D_3	Impeller tip diameter—ft
ALPHA	Effective IGV exit angle—deg
IGV	Loss parameter. 0 = no losses. If equal to ALPHA = guide vane correlation losses. If any other number correlation is off by (ALPHA - IGV).
BH	Impeller blade tip width including shroud clearance—ft
BFI	Optional parameter used in conjunction with TRIGR for study only
BLH	Impeller exit wall blockage factor
BLM	Impeller exit metal blockage factor
BLTH	Impeller exit wake blockage factor
RR	Radius ratio of vaneless space
VRATD	Parameter entering a diffusion factor calculation—not used
CPA	Diffuser incidence coefficient
C2	Not used
No. of blades	Impeller tip blade number
AD	Total diffuser throat area—ft^2
BH2	Gap width at diffuser LE—ft
UD	Match or design point speed—ft/sec
PHIPD	Match or design point flow coefficient
WD	Fixed parameter in diffuser calculation-universal

ALPS	Diffuser LE mean blade angle from tangential—deg
C7	Diffuser parameter acting on C_D $P_{DLE}/PTTHT$ V_S M_{DLE} curve
C8	Coefficient entering equation of blockage influence in the impeller on secondary losses
C9	First-order incidence coefficient for diffuser. Same value for all pipes
C10	Diffuser incidence parameter describing the transition from subsonic to supersonic
C11	Universal factor on friction formula in the vaneless space
C12	Factor entering calculation for negative incidence loss on inducer
C13	Factor entering calculation for inducer tip incidence effect on wall blockage
RNMCR	Inducer tip relative critical Mach No. 0.87 is the state-of-the-art number
CMT	Critical absolute inlet Mach No. acting on IGV and inducer

Output

POP	Rotor inlet total head pressure after IGV losses—lb/ft^2
PRTTE	Total/total pressure rise inducer tip to exducer tip in the rotor (before mixing)
HE	Euler head = U^2/gJ
W/A	Flux entering rotor with fixed standard 0.985 blockage factor—lb/ft^2
MT	Absolute inducer inlet Mach No., max when there are no IGV
GG	$(1 + \frac{\gamma-1}{2} MT^2)$
RHOS	Static density—lb/ft^3
MAX	Axial component of MT
PHI	V_{axial} (referring to MT)/$U_{(impeller\ exit\ tip)}$ = flow factor
AI	Sonic speed at MT—ft/sec
VT	Absolute velocity at MT—ft/sec
CTHT	Tangential velocity at inducer RMS—ft/sec
BETAG	Gas angle at inducer tip—deg
PHIP	Inducer inlet flow coefficient V_{ABS}/U_{RMS}
First column of subprints	Gives top column C_D x $P_{DLE}/TTHRT$
(Without incidence)	Bottom column C_D x $P_{DLE}/TTHRT$
(With incidence)	
The remaining subprints are calculation check points.	
URMS	Inducer speed at RMS—ft/sec

PF	Prewhirl factor at U_{RMS} normalized to HE
PSI	Rotor overall total/total pressure coefficient related to PRTTE
EFFH	Rotor isentropic efficiency just before dump
DQ	Internal loss coefficient normalized to HE
RNMIT	Rel inducer inlet tip Mach No.
TO4	Total discharge temp of diffuser—°R
TO3D	Total temperature dumped at impeller tip—°R
TO3	Total temperature at impeller tip before dump—°F
PO3	Total pressure at impeller tip—lb/ft^2
U	Speed at impeller tip—ft/sec
DRMS	Inducer RMS diameter—ft
EPS	D3/DRMS
CSF	Slip factor at impeller tip
PRDLE	Pressure ratio total/total diffuser LE
CPT35	Diffuser static recovery throat to exit (M = 0.35)
RC 35	Pressure ratio total/total at diffuser exit (M = 0.35) to ambient
ET 35	Overall compressor efficiency total/total at discharge (M = 0.35)
DP 35	$\left(\frac{\Delta P_T}{P_T}\right)_{0.35}$ from diffuser LE to exit
DPQ	$\frac{\Delta P \text{ (static)}}{q_{LE}}$ from diffuser LE to throat
PSTH	Static pressure ratio at throat as referred to ambient
ETS	Total-to-static efficiency based on given collector dump loss
NS	Specific speed
RCS	Pressure ratio diffuser exit static to ambient
MEXIT	Correlated guess as an iteration helper to calculate MDEX
MDLE	Mach number at diffuser LE
DQX	External loss coefficient normalized to HE
TRF	Rotor work coefficient – enthalpy rise across impeller normalized to ambient stagnation enthalpy
EFFI	Impeller adiabatic efficiency (unmixed) including IGV losses
DPOP	Total pressure loss in vaneless space normalized to impeller tip total head pressure
PSLE	Static pressure ratio at diffuser LE normalized to ambient
DIBF	Blockage factor in vaneless space at BH2 (not including metal)
EFFM	Rotor efficiency after mixing at diffuser LE (includes vaneless space loss)
MG	Mach No. in rotor just before dump
MDEX	Mach No. (dumped)
DPOD	$\Delta P_o/P_o$ (dump loss)
ALPHD	Mean gas angle from tangential as dumped—deg

ALPLE	Gas angle at diffuser LE—deg
A*/A	Adiabatic efficiency diffuser LE to throat
ET15	Overall stage efficiency to M = 0.15
VTH_4	Whirl at diffuser LE—ft/sec
VR	Radial velocity at discharge to rotor—ft/sec
MTHR	Throat Mach No.
BTHR	Throat blockage factor
RDPTH	$\Delta P_T/P_{T(LE)}$ from LE to throat
POEXIT	Pressure ratio referred to ambient at M = 0.15
RDPEX	$\Delta P_T/P_T$(LE to 0.15 M)
CCPA	Static pressure recovery coefficient LE to M = 0.15

PERMANENT DATA

GAMMA	1.4 at standard inlet conditions; varies with conditions at compressor outlet
CP	0.24 Btu/(lb°R) at standard inlet conditions; n conditions at compressor outlet
H_O	124.03 Btu
RHOST	0.07651 lb/ft^3
PO	2116 lb/ft^2
TO	518.7°R
BF2	wheel throat (at inducer) blockage factor = 0.9
BETAM	Not used
C30	Not used
C31	Iteration step size
C32	Iteration step size
TMW	Iteration limit
C4	Enters collector dump formula for static efficiency

CCP program RC-2.7 output data is listed in Table A-1.

TABLE A-1, CCP PROGRAM RC-2.7 OUTPUT DATA

CENT COMP INLET CALC RC-2.7 100

DATA

TRIG	DELSF	CC	C3	C1	C5	C6	TRIGR
0.1000E 01	0.0	0.2000E 01	0.1200E 01	0.5000E-02	0.2500E 01	0.5850E 02	0.1500E 01
D1	D1/D2	N	W	D3	ALPHA	IGV	RH
0.2000E 00	0.4630E 00	0.5599E 05	0.4115E 01	0.6520E 00	0.2200E 02	0.2200E 02	0.2942E-01
BFI	BLH	BIM	BLTH	RR	VRATD	CPA	C2
0.0	0.8500E 00	0.9400E 00	0.7300E 00	0.1221E 01	0.6000E 00	0.1000E-01	0.0
NO OF BLADES	AD	RH2	UO	PHIPD	WD	ALPS	C7
0.3200E 02	0.1410E-01	0.2600E-01	0.1918E 04	0.6250E 00	0.9950E 00	0.1640E 02	0.1030E 01
C8	C9	C10	C11	C12	C13	RNMCR	CMT
0.1050E 01	0.1500E 00	0.1900E 01	0.6500E-01	0.4500E-01	0.5000E-01	0.8700E 00	0.5440E 00

RESULTS

POP	PRTTE	HE	W/A	MT	GG	RHOS	MAX
0.2087E 04	0.9855E 01	0.1459E 03	0.3629E 02	0.5565E 00	0.1062E 01	0.6491E-01	0.5160E 00
PHI	AI	VT	CTHT	BETAG	PHIP		
0.2925E 00	0.1083E 04	0.6029E 03	0.2259E 03	0.6175E 02	0.6110E 00		

0.9456	0.9772	0.8856	0.7236	0.3296	0.6003	1.0000
0.9318	0.9734	0.8956	0.7236	0.3296	0.6003	1.0000

*** CHOKE ***

STANDARD FIXUP TAKEN , EXECUTION CONTINUING

URMS	PF	PSI	EFFH	DQ	RNMIT	T04	T03D
0.9867E 03	0.6101E-01	0.7843E 00	0.9302E 00	0.5887E-01	0.1090E 01	0.1048E 04	0.1037E 04
T03	P03	U	DRMS	EPS	CSF	PRDLF	CPT35
0.1024E 04	0.2057E 05	0.1911E 04	0.3366E 00	0.1937E 01	0.9042E 00	0.9003E 01	0.6982E 00
RC35	ET35	DP35	DPQ	PSTH	ETS	NS	RCS
0.8065E 01	0.7859E 00	0.1043E 00	-0.4685E-01	0.4570E 01	0.7306E 00	0.9251E 07	-0.7171E 01
MEXIT	MDLE	DQX	TRF	EFFI	DPQP	PSLE	DI8F
0.1276E 01	0.1005E 01	0.4083E-01	0.8843E 00	0.8872E 00	0.7966E-01	0.4726E 01	0.6306E 00
EFFIM	MG	MDEX	DPTO	ALPHD	ALPLE	A*/A	ET15
0.8401E 00	0.1396E 01	0.1310E 01	0.2930E-01	0.1600E 02	0.1870E 02	-0.4448E 01	0.7583E 00
VTH4	V2	MTHR	RTHF	RDPTH	PDEXIT	RDPEX	CCPA
0.1683E 04	0.6974E 03	0.9989E 00	0.9711E 00	0.4040E-01	0.7626E 01	0.1529E 00	0.6274E 00

TABLE A-1 (CONT)

CENT COMP INLET CALC PR=2.7 100

DATA

TRIG	DELSE	CC	C3	C1	C5	C6	TRIGR
0.1000E 01	0.0	0.2000E 01	0.1700E 01	0.5000E-02	0.2500E 01	0.5850E 02	0.1500E 01
D1	D1/D2	N	W	D3	ALPHA	IGV	BH
0.2000E 00	0.4630E 00	0.5590E 05	0.4107E 01	0.6520E 00	0.2200E 02	0.2200E 02	0.2942E-01
BET	BLH	BLM	BLTH	RR	VRATD	CPA	C2
0.0	0.8500E 00	0.9400E 00	0.7300E 00	0.1271E 01	0.6000E 00	0.1000E-01	0.0
NO OF BLADES	AD	BH2	UC	PHIPD	WD	ALPS	C7
0.3200E 02	0.1410E-01	0.2600E-01	0.1918E 04	0.6250E 00	0.9950E 00	0.1640E 02	0.1030E 01
C8	C9	C10	C11	C12	C13	RNMCP	CMT
0.1050E 01	0.1500E 00	0.1900E 01	0.6500E-01	0.4500E-01	0.5000E-01	0.8700E 00	0.5440E 00

RESULTS

POP	PRTTF	HE	W/A	MT	GG	RHOS	MAX
0.2087E 04	0.9858E 01	0.1459E 03	0.3621E 02	0.5548E 00	0.1062E 01	0.6497E-01	0.5144E 00
PHI	AI	VT	CTHT	RETAG	PHIP		
0.2916E 00	0.1084E 04	0.6011E 03	0.2252E 03	0.6183E 02	0.6093E 00		
0.9456 0.9711	0.9862	0.7225 0.0327	0.5996	1.0000			
0.9323 0.9731	0.9862	0.7225 0.0327	0.5996	1.0000			

URMS	PF	PSI	EFFH	DQ	RNMIT	T04	T03
0.9866E 03	0.6093E-01	0.7846E 00	0.9302E 00	0.5887E-01	0.1090E 01	0.1048E 04	0.1037E 04
T03	P03	U	DPMS	EPS	CSF	PRDLE	CPT35
0.1024E 04	0.2058E 05	0.1911E 04	0.3366E 00	0.1937E 01	0.9044E 00	0.9005E 01	0.6811E 00
PC35	ET35	DP35	DP0	PSTH	ETS	NS	RCS
0.8095E 01	0.7876E 00	0.1011E 00	0.3085E-01	0.4833E 01	0.7177E 00	0.9342E 02	0.7017E 01
MEXIT	MDLE	DQX	TRE	EFFI	DPOP	PSLE	DIBE
0.1276E 01	0.1005E 01	0.4054E-01	0.8845E 00	0.8872E 00	0.7979E-01	0.4730E 01	0.6306E 00
EFFIM	MG	MDEX	DPTD	ALPHD	ALPLE	A*/A	ET15
0.8400E 00	0.1386E 01	0.1310E 01	0.2933E-01	0.1596E 02	0.1866E 02	0.3527E 00	0.7611E 00
VTH4	VR	MTHR	RTHP	RDPTH	PDEXIT	RDPEX	CCPA
0.1683E 04	0.6865E 03	0.9521E 00	0.9697E 00	0.3849E-01	0.7672E 01	0.1480E 00	0.6333E 00

TABLE A-1 (CONT)

CENT COMP INLET CALC PC-2.7 100

DATA

TRIG	DELSF	CC	C3	C1	C5	C6	TRIGR
0.1000E 01	0.0	0.2000E 01	0.1200E 01	0.5000E-02	0.2500E 01	0.5850E 02	0.1500E 01
D1	D1/D2	N	W	D3	ALPHA	IGV	BH
0.2000E 00	0.4630E 00	0.5598E 05	0.4068E 01	0.6520E 00	0.2200E 02	0.2200E 02	0.2942E-01
BFI	BLH	BLM	BLTH	RR	VRATD	CPA	C2
0.0	0.8500E 00	0.9400E 00	0.7300E 00	0.1221E 01	0.6000E 00	0.1000E-01	0.0
NO OF BLADES	AD	BH2	HD	PHIPD	WD	ALPS	C7
0.3200E 02	0.1410E-01	0.2600E-01	0.1918E 04	0.6250E 00	0.9950E 00	0.1640E 02	0.1030E 01
C8	C9	C10	C11	C12	C13	RNMCR	CMT
0.1050E 01	0.1500E 00	0.1900E 01	0.6500E-01	0.4500E-01	0.5000E-01	0.8700E 00	0.5440E 00

RESULTS

POP	PRTTE	HE	W/A	MT	GG	RMS	MAX
0.2088E 04	0.9891E 01	0.1459E 03	0.3587E 02	0.5463E 00	0.1060E 01	0.6529E-01	0.5065E 00
PHI	AI	VT	CTHT	BETAG	PHIP		
0.2875E 00	0.1085E 04	0.5925E 03	0.2220E 03	0.6225E 02	0.6005E 00		
0.9459	0.9697	0.8887	0.7164	0.0478	0.5946	1.0000	
0.9342	0.9719	0.8987	0.7164	0.0478	0.5946	1.0000	
URMS	PF	PSI	EFFH	DQ	RNMIT	TO4	TO3D
0.9866E 03	0.5996E-01	0.7862E 00	0.9302E 00	0.5899E-01	0.1088E 01	0.1050E 04	0.1038E 04
TO3	PO3	U	DRMS	EPS	CSF	PRDLE	CPT35
0.1025E 04	0.2066E 05	0.1911E 04	0.3366E 00	0.1937E 01	0.9052E 00	0.9035E 01	0.6450E 00
RC35	ET35	DP35	DPQ	PSTH	ETS	NS	RCS
0.8190E 01	0.7915E 00	0.9350E-01	0.1781E 00	0.5349E 01	0.7539E 00	0.8943E 02	0.7590E 01
MEXIT	MDLE	DQX	TRE	EFFI	DPOP	PSLE	DIBF
0.1276E 01	0.1004E 01	0.4147E-01	0.8967E 00	0.5867E 00	0.8050E-01	0.4752E 01	0.6287E 00
EFFIM	MG	MDEX	DPTD	ALPHD	ALPLE	A*/A	ETIS
0.8396E 00	0.1384E 01	0.1309E 01	0.2942E-01	0.1567E 02	0.1849E 02	0.7685E 00	0.7670E 00
VTH4	VP	MTHR	RTHR	RDPTH	POEXIT	RDPEX	CCPA
0.1684E 04	0.6804E 03	0.8661E 00	0.9674E 00	0.3427E-01	0.7796E 01	0.1371E 00	0.6475E 00

TABLE A-1 (CONT)

CENT COMP INLET CALC RC-2.7 100

DATA

TRIG	DELSF	CC	C3	C1	C5	C6	TRIGR
0.1000E 01	0.0	0.2000E 01	0.1200E 01	0.5000E-02	0.2500E 01	0.5850E 02	0.1500E 01
D1	D1/D2	N	W	D3	ALPHA	IGV	BH
0.2000E 00	0.4630E 00	0.5595E 05	0.4053E 01	0.6520E 00	0.2200E 02	0.2200E 02	0.2942E-01
BFI	BLH	BLW	BLTH	RR	VRATD	CPA	C2
0.0	0.8500E 00	0.9400E 00	0.7300E 00	0.1221E 01	0.6000E 00	0.1000E-01	0.0
NO OF BLADES	AD	RH2	UC	PHIPD	WD	ALPS	C7
0.3200E 02	0.1410E-01	0.2600E-01	0.1919E 04	0.6250E 00	0.9950E 00	0.1640E 02	0.1030E 01
C8	C9	C10	C11	C12	C13	RNMCR	CMT
0.1050E 01	0.1500E 00	0.1900E 01	0.6500E-01	0.4500E-01	0.5000E-01	0.8700E 00	0.5440E 00

RESULTS

POP	PRTTE	HE	W/A	MT	GG	RHOS	MAX
0.2089E 04	0.9884E 01	0.1457E 03	0.3574E 02	0.5431E 00	0.1059E 01	0.6541E-01	0.5036E 00
PHI	AI	VT	CTHT	BETAG	PHIP		
0.2860E 00	0.1085E 04	0.5892E 03	0.2207E 03	0.6239E 02	0.5975E 00		
0.9460	0.9674	0.8897	0.7147	0.0540	0.5932	1.0000	
0.9348	0.9716	0.8897	0.7147	0.0540	0.5932	1.0000	

URMS	PE	PSI	EFFH	DQ	RNMIT	TO4	TO3D
0.9861E 03	0.5966E-01	0.7866E 00	0.9301E 00	0.5910E-01	0.1087E 01	0.1050E 04	0.1038E 04
TO3	PO3	U	DRMS	EPS	CSF	PRDLE	CPT35
0.1025E 04	0.2064E 05	0.1910E 04	0.3366E 00	0.1937E 01	0.9054E 00	0.9028E 01	0.6390E 00
RC35	ET35	DP35	DPQ	PSTH	ETS	NS	RCS
0.8198E 01	0.7921E 00	0.9192E-01	0.2009E 00	0.5425E 01	0.7558E 00	0.8907E 02	0.7617E 01
MEXIT	MDLE	DQX	TRE	EFFI	DPOP	PSLE	DIBF
0.1276E 01	0.1003E 01	0.4165E-01	0.8974E 00	0.8865E 00	0.8066E-01	0.4753E 01	0.6283E 00
EFFIM	MG	MDEX	DPTD	ALPHD	ALPLE	A*/A	ET15
0.8394E 00	0.1383E 01	0.1307E 01	0.2943E-01	0.1560E 02	0.1844E 02	0.7915E 00	0.7680E 00
VTH4	VR	MTHP	RTHR	RDPTH	PDEXIT	RDPEX	CCPA
0.1684E 04	0.6785E 03	0.8529E 00	0.9671E 00	0.3347E-01	0.7809E 01	0.1351E 00	0.6502E 00

TABLE A-1 (CONT)

CENT COMP INLET CALC RC-2.7 100

DATA

TRIG	DELSF	CC	C3	C1	C5	C6	TRIGR
0.1000E 01	0.0	0.2000E 01	0.1200E 01	0.5000E-02	0.2500E 01	0.5850E 02	0.1500E 01
D1	D1/D2	N	W	D3	ALPHA	IGV	BH
0.2000E 00	0.4630E 00	0.5595E 05	0.4018E 01	0.6520E 00	0.2200E 02	0.2200E 02	0.2942E-01
REI	BLH	BLM	BLTH	RR	VRATO	CPA	C2
0.0	0.8500E 00	0.9400E 00	0.7300E 00	0.1221E 01	0.6000E 00	0.1000E-01	0.0
NO OF BLADES	AD	BH2	UD	PHIPD	WD	ALPS	C7
0.3200E 02	0.1410E-01	0.2600E-01	0.1918E 04	0.6250E 00	0.9950E 00	0.1640E 02	0.1030E 01
C8	C9	C10	C11	C12	C13	RNMCR	CMT
0.1050E 01	0.1500E 00	0.1900E 01	0.6500E-01	0.4500E-01	0.5000E-01	0.8700E 00	0.5440E 00

RESULTS

POP	PRTTE	HE	W/A	MT	GG	RHOS	MAX
0.2090E 04	0.9871E 01	0.1457E 03	0.3543E 02	0.5359E 00	0.1057E 01	0.6568E-01	0.4969E 00
PHI	AI	VT	CTHT	BETAG	PHIP		
0.2824E 00	0.1086E 04	0.5818E 03	0.2179E 03	0.6276E 02	0.5900E 00		
0.9461 0.9671	0.8920	0.7092 0.0675	0.5918	1.0000			
0.9359 0.9711	0.8920	0.7092 0.0676	0.5918	1.0000			
URMS	PF	PSI	EFFH	DQ	RNMIT	TO4	TO3D
0.9861E 03	0.5890E-01	0.7861E 00	0.9279E 00	0.6111E-01	0.1085E 01	0.1051E 04	0.1039E 04
TO3	PO3	U	DRMS	EPS	CSF	PRDLF	CPT35
0.1026E 04	0.2063E 05	0.1910E 04	0.3366E 00	0.1937E 01	0.9061E 00	0.9013E 01	0.6240E 00
RC35	ET35	DP35	DPQ	PSTH	ETS	NS	RCS
0.8201E 01	0.7907E 00	0.9007E-01	0.2445E 00	0.5566E 01	0.7562E 00	0.8851E 02	0.7648E 01
MEXIT	MDLF	DQX	TRF	EFFI	DPOP	PSLE	DIBF
0.1276E 01	0.1002E 01	0.4199E-01	0.8892E 00	0.8841E 00	0.8160E-01	0.4749E 01	0.6277E 00
EFFIM	MG	MDEX	DPTD	ALPHD	ALPLE	A*/A	ET15
0.8368E 00	0.1383E 01	0.1306E 01	0.2093E-01	0.1542E 02	0.1834E 02	0.8261E 00	0.7672E 00
VTH4	VR	MTHR	BTHR	RDPTH	PDEXIT	RDPEX	CCPA
0.1684E 04	0.6769E 03	0.8278E 00	0.9667E 00	0.3197E-01	0.7821E 01	0.1322E 00	0.6535E 00

TABLE A-1 (CONT)

CENT COMP INLET CALC RC-2.7 90

DATA

TRIG	DELSF	CC	C3	C1	C5	C6	TRIGR
0.1000E 01	0.0	0.2000E 01	0.1200E 01	0.5000E-02	0.2500E 01	0.5850E 02	0.1500E 01
D1	D1/D2	N	W	D3	ALPHA	IGV	BH
0.2000E 00	0.4630E 00	0.5044E 05	0.3301E 01	0.6520E 00	0.2200E 02	0.2200E 02	0.3010E-01
BFI	BLH	BLM	BLTH	RR	VRATD	CPA	C2
0.0	0.8500E 00	0.9400E 00	0.7300E 00	0.1221E 01	0.6000E 00	0.1000E-01	0.0
NO OF BLADES	AD	BH2	UD	PHIPD	WD	ALPS	C7
0.3200E 02	0.1410E-01	0.2600E-01	0.1918E 04	0.6250E 00	0.9950E 00	0.1640E 02	0.1050E 01
C8	C9	C10	C11	C12	C13	RNMCR	CMT
0.1050E 01	0.1500E 00	0.1900E 01	0.6500E-01	0.4500E-01	0.5000E-01	0.8700E 00	0.5440E 00

RESULTS

POP	PRTTE	HE	W/A	MT	GG	RHOS	MAX
0.2101E 04	0.7047E 01	0.1184E 03	0.2911E 02	0.4087E 00	0.1033E 01	0.6994E-01	0.3790E 00
PHI	AI	VT	CTHT	BETAG	PHIP		
0.2417E 00	0.1098E 04	0.4489E 03	0.1681E 03	0.6684E 02	0.5049E 00		
0.9733 0.9667 0.9269 0.7309 0.5156 0.5588 1.0000							
*** CHOKE ***							
0.9683 0.9888 0.9269 0.7309 0.5156 0.5588 1.0000							
*** CHOKE ***							

URMS	PF	PSI	EFFH	DQ	RNMIT	TO4	TO3D
0.3890E 03	0.5041E-01	0.7823E 00	0.9173E 00	0.7053E-01	0.9634E 00	0.9584E 03	0.9473E 03
TO3	PO3	U	DRMS	EPS	CSF	PRDLE	CPT35
0.9356E 03	0.1480E 05	0.1722E 04	0.3366E 00	0.1937E 01	0.9032E 00	0.6572E 01	0.7439E 00
RC35	ET35	DP35	DPQ	PSTH	ETS	NS	RCS
0.6180E 01	0.7959E 00	0.5963E-01	-0.1258E 00	0.3440E 01	0.1547E 00	0.2754E 03	0.1546E 01
MEXIT	MDLE	DQX	TRF	EFFI	DPOP	PSLE	DIBF
0.1229E 01	0.9375E 00	0.4776E-01	0.9006E 00	0.8687E 00	0.6448E-01	0.3729E 01	0.6602E 00
EFFIM	MG	MDEX	DPTD	ALPHD	ALPLE	A*/A	ET15
0.8286E 00	0.1261E 01	0.1205E 01	0.1949E-01	0.1529E 02	0.1884E 02	0.1298E 01	0.7651E 00
VTH4	VR	MTHR	BTHR	RDPTH	POEXIT	RDPEX	CCPA
0.1516E 04	0.5724E 03	0.9919E 00	0.9866E 00	0.1849E-01	0.5847E 01	0.1104E 00	0.6857E 00

TABLE A-1 (CONT)

CENT COMP INLET CALC RC-2.7 90

DATA

TRIG	DELSF	CC	C3	C1	C5	C6	TRIGR
0.1000E 01	0.0	0.2000E 01	0.1200E 01	0.5000E-02	0.2500E 01	0.5850E 02	0.1500E 01
D1	D1/D2	N	W	D3	ALPHA	IGV	BH
0.2000E 00	0.4630E 00	0.5043E 05	0.3261E 01	0.6520E 00	0.2200E 02	0.2200E 02	0.3010E-01
BFI	BLH	BLM	BLTH	RR	VRATU	CPA	C2
0.0	0.8500E 00	0.9400E 00	0.7300E 00	0.1221E 01	0.6000E 00	0.1000E-01	0.0
NO OF BLADES	AD	BH2	UD	PHIPD	WD	ALPS	C7
0.3200E 02	0.1410E-01	0.2600E-01	0.1918E 04	0.6250E 00	0.9950E 00	0.1640E 02	0.1050E 01
C8	C9	C10	C11	C12	C13	RNMCR	CMT
0.1050E 01	0.1500E 00	0.1900E 01	0.6500E-01	0.4500E-01	0.5000E-01	0.8700E 00	0.5440E 00

RESULTS

POP	PRTTE	HE	W/A	MT	GG	RHOS	MAX
0.2101E 04	0.7040E 01	0.1184E 03	0.2875E 02	0.4025E 00	0.1032E 01	0.7012E-01	0.3732E 00
PHI	AI	VT	CTHT	BETAG	PHIP		
0.2382E 00	0.1099E 04	0.4423E 03	0.1657E 03	0.6719E 02	0.4976E 00		
0.9734 0.9866 0.9285 0.7251 0.5384 0.5558 1.0000							
0.9684 0.9880 0.9285 0.7251 0.5384 0.5558 1.0000							
*** CHOKE ***							

URMS	PF	PSI	EFFH	DQ	RNMIT	T04	T03D
0.8888E 03	0.4968E-01	0.7821E 00	0.9155E 00	0.7222E-01	0.9627E 00	0.9592E 03	0.9480E 03
T03	P03	U	DRMS	EPS	CSF	PRDLE	CPT35
0.9361E 03	0.1479E 05	0.1722E 04	0.3366E 00	0.1937E 01	0.9040E 00	0.6563E 01	0.7462E 00
RC35	ET35	DP35	DPQ	PSTH	ETS	NS	RCS
0.6171E 01	0.7936E 00	0.5975E-01	-0.1401E 00	0.3406E 01	0.7925E 00	0.8036E 02	-0.6136E 01
MEXIT	MDLE	DQX	TRF	EFFI	DPOP	PSLE	DIBF
0.1229E 01	0.9367E 00	0.4827E-01	0.9026E 00	0.8665E 00	0.6523E-01	0.3727E 01	0.6572E 00
EFFIM	MG	MDEX	DPTD	ALPHD	ALPLE	A*/A	ET15
0.8262E 00	0.1260E 01	0.1204E 01	0.1974E-01	0.1509E 02	0.1873E 02	0.1259E 01	0.7626E 00
VTH4	VR	MTHR	BTHR	RDPTH	PDEXIT	RDPEX	CCPA
0.1517E 04	0.5655E 03	0.9992E 00	0.9867E 00	0.1854E-01	0.5835E 01	0.1109E 00	0.6851E 00

TABLE A-1 (CONT)

CENT COMP INLET CALC RC-2.7 90

DATA

TRIG	DELSF	CC	C3	C1	C5	C6	TRIGR
0.1000E 01	0.0	0.2000E 01	0.1200E 01	0.5000E-02	0.2500E 01	0.5850E 02	0.1500E 01
D1	D1/D2	N	W	D3	ALPHA	IGV	BH
0.2000E 00	0.4630E 00	0.5044E 05	0.3213E 01	0.6520E 00	0.2200E 02	0.2200E 02	0.3010E-01
BFI	RLH	RLM	RLTH	RR	VRATD	CPA	C2
0.0	0.8500E 00	0.9400E 00	0.7300E 00	0.1221E 01	0.6000E 00	0.1000E-01	0.0
NO OF BLADES	AD	BH2	UC	PHIPD	WD	ALPS	C7
0.3200E 02	0.1410E-01	0.2600E-01	0.1918E 04	0.6250E 00	0.9950E 00	0.1640E 02	0.1050E 01
C8	C9	C10	C11	C12	C13	RNNCR	CMT
0.1050E 01	0.1500E 00	0.1900E 01	0.6500E-01	0.4500E-01	0.5000E-01	0.8700E 00	0.5440E 00

RESULTS

POP	PRTTF	HE	W/A	MT	GG	RHOS	MAX
0.2102E 04	0.7042E 01	0.1184E 03	0.2833E 02	0.3952E 00	0.1031E 01	0.7033E-01	0.3664E 00
PHI	AI	VT	CTHT	BETAG	PHIP		
0.2339E 00	0.1099E 04	0.4344E 03	0.1627E 03	0.6762E 02	0.4887E 00		
0.9735 0.9867 0.9306 0.7173 0.5658 0.5522 1.0000							
0.9686 0.9869 0.9306 0.7173 0.5658 0.5522 1.0000							

URMS	PF	PSI	EFFH	DQ	RNMIT	T04	T03D
0.8890E 03	0.4879E-01	0.7818E 00	0.9131E 00	0.7445E-01	0.9623E 00	0.9607E 03	0.9493E 03
T03	P03	U	DRMS	EPS	CSF	PRDLE	CPT35
0.9373E 03	0.1480E 05	0.1722E 04	0.3366E 00	0.1937E 01	0.9050E 00	0.6559E 01	0.7055E 00
RC35	ETCS	DP35	DPO	PSTH	ETS	NS	RCS
0.6196E 01	0.7932E 00	0.5529E-01	0.6817E-01	0.3883E 01	0.7489E 00	0.8287E 02	0.5718E 01
MEXIT	MDLE	DQX	TRF	EFFI	DPOP	PSLE	DIBF
0.1229E 01	0.9360E 00	0.4890E-01	0.9052E 00	0.8637E 00	0.6630E-01	0.3727E 01	0.6533E 00
EFFIN	MG	MDEX	DPTD	ALPHD	ALPLE	A*/A	ETIS
0.8231E 00	0.1260E 01	0.1203E 01	0.2014E-01	0.1483E 02	0.1859E 02	0.7090E 00	0.7654E 00
VTH4	VR	MTHR	BTHR	RDPTH	POSXIT	RDPEX	CCPA
0.1518E 04	0.5664E 03	0.8833E 00	0.9849E 00	0.1653E-01	0.5803E 01	0.1015E 00	0.6943E 00

TABLE A-1 (CONT)

CENT COMP INLET CALC RC-2.7 90

DATA

TRIG	DELSF	CC	C3	C1	C5	C6	TRIGR
0.1000E 01	0.0	0.2000E 01	0.1200E 01	0.5000E-02	0.2500E 01	0.5850E 02	0.1500E 01
D1	D1/D2	N	W	D3	ALPHA	IGV	BH
0.2000E 00	0.4630E 00	0.5040E 05	0.3126E 01	0.6520E 00	0.2200E 02	0.2200E 02	0.3010E-01
BFI	BLH	BLM	BLTH	RR	VRATD	CPA	C2
0.0	0.8500E 00	0.9400E 00	0.7300E 00	0.1221E 01	0.6000E 00	0.1000E-01	0.0
NO OF BLADES	AR	BH2	UD	PHIPD	WD	ALPS	C7
0.3200E 02	0.1410E-01	0.2600E-01	0.1918E 04	0.6250E 00	0.9950E 00	0.1640E 02	0.1050E 01
C8	C9	C10	C11	C12	C13	RNMCR	CMT
0.1050E 01	0.1500E 00	0.1900E 01	0.6500E-01	0.4500E-01	0.5000E-01	0.8700E 00	0.5440E 00

RESULTS

POP	PRTTF	HE	W/A	MT	GG	RHOS	MAX
0.2102E 04	0.7018E 01	0.1182E 03	0.2756E 02	0.3821E 00	0.1029E 01	0.7070E-01	0.3543E 00
PHI	AI	VT	CTHT	BETAG	PHIP		
0.2266E 00	0.1100E 04	0.4205E 03	0.1575E 03	0.6836E 02	0.4734E 00		
0.9737 0.9849	0.9344	0.7043 0.6191	0.5462	1.0000			
0.9691 0.9859	0.9344	0.7043 0.6191	0.5462	1.0000			

URMS	PF	PSI	EFFH	DQ	RNMIT	T04	T03D
0.8883E 03	0.4726E-01	0.7814E 00	0.9091E 00	0.7809E-01	0.9605E 00	0.9620E 03	0.9504E 03
T03	P03	U	DRMS	EPS	CSF	PRDLE	CPT35
0.9381E 03	0.1475E 05	0.1721E 04	0.3366E 00	0.1937E 01	0.9068E 00	0.6528E 01	0.6665E 00
RC35	ET35	DP35	DPQ	PSTH	ETS	NS	RCS
0.4185E 01	0.7897E 00	0.5260E-01	0.2079E 00	0.4190E 01	0.7527E 00	0.8118E 02	0.5782E 01
MEXIT	MDLE	DQX	TRF	EFFI	DPOP	PSLE	DIBF
0.1230E 01	0.9342E 00	0.5006E-01	0.9096E 00	0.8591E 00	0.6804E-01	0.3718E 01	0.6462E 00
EFFIM	MG	MDEX	DPTO	ALPHD	ALPLE	A*/A	ET15
0.8179E 00	0.1259E 01	0.1200E 01	0.2075E-01	0.1438E 02	0.1838E 02	0.8870E 00	0.7641E 00
VTH4	VR	MTHR	BTHR	RDPTH	PDEXIT	RDPEX	CCPA
0.1519E 04	0.5606E 03	0.9070E 00	0.9837E 00	0.1483E-01	0.5904E 01	0.9558E-01	0.6992E 00

TABLE A-1 (CONT)

CENT COMP INLET CALC RC-2.7 90

DATA

TRIG	DELSF	CC	C3	C1	C5	C6	TRIGR
0.1000E 01	0.0	0.2000E 01	0.1200E 01	0.5000E-02	0.2500E 01	0.5850E 02	0.1500E 01
D1	D1/D2	N	W	D3	ALPHA	IGV	BM
0.2000E 00	0.4630E 00	0.5041E 05	0.3113E 01	0.6520E 00	0.2200E 02	0.2200E 02	0.3010E-01
BFI	BLH	BLM	BLTH	RR	VRATD	CPA	C2
0.0	0.8500E 00	0.9400E 00	0.7300E 00	0.1221E 01	0.6000E 00	0.1000E-01	0.0
NO OF BLADES	AD	BH2	UD	PHIPD	WD	ALPS	C7
0.3200E 02	0.1410E-01	0.2600E-01	0.1918E 04	0.6250E 00	0.9950E 00	0.1640E 02	0.1050E 01
C8	C9	C10	C11	C12	C13	RNMCR	CMT
0.1050E 01	0.1500E 00	0.1900E 01	0.6500E-01	0.4500E-01	0.5000E-01	0.8700E 00	0.5440E 00

RESULTS

POP	PRTTF	HE	W/A	MT	GG	RHOS	MAX
0.2102E 04	0.7022E 01	0.1183E 03	0.2745E 02	0.3802E 00	0.1029E 01	0.7076E-01	0.3525E 00
PHI	AI	VT	CTHT	BETAG	PHIP		
0.2254E 00	0.1101E 04	0.4184E 03	0.1567E 03	0.6847E 02	0.4709E 00		
0.9737 0.9837	0.9350	0.7018 0.6267	0.5454	1.0000			
0.9692 0.9858	0.9350	0.7018 0.6267	0.5454	1.0000			
URMS	PF	PSI	EFFH	QQ	RNMIT	T04	T03D
0.8885E 03	0.4702E-01	0.7813E 00	0.9084E 00	0.7878E-01	0.9606E 00	0.9626E 03	0.9510E 03
T03	P03	U	DRMS	EPS	CSF	PRDLE	CPT35
0.9386E 03	0.1476E 05	0.1721E 04	0.3366E 00	0.1937E 01	0.9071E 00	0.6529E 01	0.6599E 00
RC35	ET35	DP35	DPQ	PSTH	ETS	NS	RCS
0.6188E 01	0.7889E 00	0.5234E-01	0.2276E 00	0.4235E 01	0.7525E 00	0.8096E 02	0.5791E 01
MEXIT	MDLE	DDX	TRF	EFFI	DPOP	PSLE	DIBF
0.1230E 01	0.9341E 00	0.5024E-01	0.9103E 00	0.8583E 00	0.6843E-01	0.3718E 01	0.6450E 00
EFFIM	MG	MDSX	DPTO	ALPHD	ALPLE	A*/A	ET15
0.9170E 00	0.1259E 01	0.1200E 01	0.2091E-01	0.1430E 02	0.1834E 02	0.8966E 00	0.7636E 00
VTH4	VR	MTHR	RTHR	RDPTH	POEXIT	RDPFX	CCPA
0.1520E 04	0.5600E 03	0.7965E 00	0.9836E 00	0.1459E-01	0.5910E 01	0.9486E-01	0.6997E 00

TABLE A-1 (CONT)

CENT COMP INLET CALC RC-2.7 96

DATA

TRIG	DELSF	CC	C3	C1	C5	C6	TRIGR
0.1000E 01	0.0	0.2000E 01	0.1200E 01	0.5000E-02	0.2500E 01	0.5850E 02	0.1500E 01
D1	D1/D2	N	W	D3	ALPHA	IGV	BM
0.2000E 00	0.4630E 00	0.4815E 05	0.2981E 01	0.6520E 00	0.2200E 02	0.2200E 02	0.3020E-01
BFI	BLH	BLM	BLTH	RR	VRATD	CPA	C2
0.0	0.8500E 00	0.9400E 00	0.7300E 00	0.1221E 01	0.6000E 00	0.1000E-01	0.0
NO OF BLADES	AD	RH2	UD	PHIPD	WD	ALPS	C7
0.3200E 02	0.1410E-01	0.2600E-01	0.1918E 04	0.6250E 00	0.9950E 00	0.1640E 02	0.1049E 01
C8	C9	C10	C11	C12	C13	RNMCR	CMT
0.1050E 01	0.1500E 00	0.1900E 01	0.6500E-01	0.4500E-01	0.5000E-01	0.8700E 00	0.5440E 00

RESULTS

POP	PRTTE	HE	W/A	MT	GG	RHOS	MAX
0.2103E 04	0.6177E 01	0.1079E 03	0.2629E 02	0.3609E 00	0.1026E 01	0.7128E-01	0.3346E 00
PHI	AI	VT	CTHT	BETAG	PHIP		
0.2243E 00	0.1102E 04	0.3977E 03	0.1490E 03	0.6858E 02	0.4687E 00		
0.9753	0.9836	0.9359	0.7383	0.7461	0.5404	0.9800	
*** CHOKE ***							
0.9708	0.9896	0.9359	0.7383	0.7461	0.5404	0.9800	
*** CHOKE ***							

URMS	PF	PSI	EFFH	DQ	RNMIT	TO4	TO3D
0.8486E 03	0.4679E-01	0.7844E 00	0.9169E 00	0.7112E-01	0.9162E 00	0.9226E 03	0.9118E 03
TO3	P03	U	DRMS	EPS	CSF	PRDLE	CPT35
0.9004E 03	0.1299E 05	0.1644E 04	0.3366E 00	0.1937E 01	0.9023E 00	0.5798E 01	0.7472E 00
RC35	ET35	DP35	DPQ	PSTH	ETS	NS	RCS
0.5469E 01	0.7946E 00	0.5675E-01	-0.1856E 00	0.3037E 01	0.2305E-01	0.1112E 04	0.1065E 01
MEXIT	MDLE	DQX	TRF	EFFI	DPOP	PSLE	DIBF
0.1209E 01	0.9074E 00	0.5083E-01	0.9063E 00	0.8654E 00	0.5897E-01	0.3401E 01	0.6639E 00
EFFIM	MG	MDEX	DPTD	ALPHD	ALPLE	A*/A	ET15
0.8271E 00	0.1209E 01	0.1141E 01	0.1604E-01	0.1503E 02	0.1890E 02	0.1177E 01	0.7621E 00
VTH4	VR	MTHR	BTHR	RDPTH	PDEXIT	RDPEX	CCPA
0.1446E 04	0.5273E 03	0.9926E 00	0.9876E 00	0.1707E-01	0.5173E 01	0.1077E 00	0.6775E 00

TABLE A-1 (CONT)

CENT COMP INLET CALC RC-2.7 R6

DATA

TRIG	DELSF	CC	C3	C1	C5	C6	TRIGR
0.1000E 01	0.0	0.2000E 01	0.1200E 01	0.5000E-02	0.2500E 01	0.5850E 02	0.1500E 01
D1	D1/D2	N	W	D3	ALPHA	IGV	BH
0.2000E 00	0.4630E 00	0.4821E 05	0.2939E 01	0.6520E 00	0.2200E 02	0.2200E 02	0.3020E-01
BEI	BLH	BLW	BLTH	RR	VRATD	CPA	C2
0.0	0.9500E 00	0.9400E 00	0.7300E 00	0.1221E 01	0.6000E 00	0.1000E-01	0.0
NO OF BLADES	AD	BH2	UD	PHIPD	WD	ALPS	C7
0.3200E 02	0.1410E-01	0.2600E-01	0.1918E 04	0.6250E 00	0.9950E 00	0.1640E 02	0.1049E 01
C8	C9	C10	C11	C12	C13	RNMCR	CMT
0.1050E 01	0.1500E 00	0.1900E 01	0.6500E-01	0.4500E-01	0.5000E-01	0.8700E 00	0.5440E 00

RESULTS

POP	PRTTE	HE	W/A	MT	GG	RHOS	MAX
0.2103E 04	0.6199E 01	0.1082E 03	0.2592E 02	0.3549E 00	0.1025E 01	0.7144E-01	0.3290E 00
PHI	AI	VT	CTHT	BETAG	PHIP		
0.2204E 00	0.1103E 04	0.3913E 03	0.1466E 03	0.6898E 02	0.4604E 00		
0.9753 0.9876	0.9374	0.7301 0.8034	0.5363	0.9969			
0.9707 0.9885	0.9374	0.7301 0.8034	0.5363	0.9969			

URMS	PE	PSI	EFFH	DQ	RNMIT	TO4	TO3D
0.8497E 03	0.4597E-01	0.7842E 00	0.9146E 00	0.7319E-01	0.9171E 00	0.9251E 03	0.9139E 03
TO3	PO3	U	DRMS	EPS	CSF	PRDLE	CPT35
0.9022E 03	0.1304E 05	0.1646E 04	0.3366E 00	0.1937E 01	0.9033E 00	0.5813E 01	0.7360E 00
RC35	ET35	DP35	DPQ	PSTH	ETS	NS	RCS
0.5489E 01	0.7919E 00	0.5572E-01	-0.1213E 00	0.3171E 01	0.6999E 00	0.8501E 02	0.4676E 01
MEXIT	MDLE	DX	TRF	EFFI	DPOP	PSLE	DIBF
0.1210E 01	0.9074E 00	0.5210E-01	0.9095E 00	0.8622E 00	0.6009E-01	0.3409E 01	0.6578E 00
EFFIM	MG	MDFX	DPTD	ALPHD	ALPLE	A*/A	ET15
0.8236E 00	0.1209E 01	0.1160E 01	0.1639E-01	0.1476E 02	0.1878E 02	0.1297E 01	0.7605E 00
VTH4	VR	MTHR	BTHR	RDPTH	PDEXIT	RDPEX	CCPA
0.1449E 04	0.5245E 03	0.9576E 00	0.9871E 00	0.1660E-01	0.5201E 01	0.1052E 00	0.6798E 00

TABLE A-1 (CONT)

CENT COMP INLET CALC RC-2.7 86

DATA

TRIG	DELSF	CC	C3	C1	C5	C6	TRIGR
0.1000E 01	0.0	0.2000E 01	0.1200E 01	0.5000E-02	0.2500E 01	0.2850E 02	0.1500E 01
D1	D1/D2	N	W	D3	ALPHA	IGV	BH
0.2000E 00	0.4633E 00	0.4817E 05	0.2923E 01	0.6520E 00	0.2200E 02	0.2200E 02	0.3020E-01
BFI	BLH	BLM	BLTH	RR	VRATD	CPA	C2
0.0	0.8500E 00	0.9400E 00	0.7300E 00	0.1221E 01	0.6000E 00	0.1000E-01	0.0
NO OF BLADES	AD	PH2	UD	PHIPD	WD	ALPS	C7
0.3200E 02	0.1410E-01	0.2600E-01	0.1918E 04	0.6250E 00	0.9950E 00	0.1640E 02	0.1049E 01
C8	C9	C10	C11	C12	C13	RNNCR	CMT
0.1050E 01	0.1500E 00	0.1900E 01	0.6500E-01	0.4500E-01	0.5000E-01	0.3700E 00	0.5440E 00

RESULTS

POP	PRTTF	HE	W/A	MT	GG	RHOS	MAX
0.2103E 04	0.4183E 01	0.1080E 03	0.2577E 02	0.3526E 00	0.1025E 01	0.7150E-01	0.3269E 00
PHI	AI	VT	CTHT	BETAG	PHIP		
0.2192E 00	0.1103E 04	0.3888E 03	0.1456E 03	0.6910E 02	0.4580E 00		
0.9753 0.9871	0.9378	0.7287 0.8215	0.5353	0.9998			
0.9707 0.9883	0.9378	0.7287 0.8215	0.5353	0.9998			

URMS	PF	PSI	EFFH	DQ	RNMIT	T04	T03D
0.8490E 03	0.4572E-01	0.7842E 00	0.9142E 00	0.7363E-01	0.9162E 00	0.9247E 03	0.9135E 03
T03	P03	U	DRMS	EPS	CSF	PRDLE	CPT35
0.9017E 03	0.1301E 05	0.1644E 04	0.3366E 00	0.1937E 01	0.9035E 00	0.5797E 01	0.7255E 00
RC35	ET35	DP35	DPQ	PSTH	ETS	NS	RCS
0.5481E 01	0.7917E 00	0.5461E-01	-0.6615E-01	0.3273E 01	0.7321E 00	0.8195E 02	0.4943E 01
MEXIT	MDLE	DQX	TRE	EFFI	DPOP	PSLE	DIBF
0.1210E 01	0.9067E 00	0.5244E-01	0.9103E 00	0.8615E 00	0.6020E-01	0.3403E 01	0.6566E 00
EFFIM	MG	MDEX	DPTD	ALPHD	ALPLE	A*/A	ET15
0.8228E 00	0.1209E 01	0.1159E 01	0.1640E-01	0.1471E 02	0.1876E 02	0.1716E 01	0.7612E 00
VT44	VR	MTHP	BTHR	RDPTH	POEXIT	RDPEX	CCPA
0.1448E 04	0.5231E 03	0.9272E 00	0.9866E 00	0.1611E-01	0.5201E 01	0.1028E 00	0.6819E 00

TABLE A-1 (CONT)

CENT COMP INLET CALC RC-2.7 R6

DATA

TRIS	DELSF	CC	C3	C1	C5	C6	TRIGR
0.1000E 01	0.0	0.2000E 01	0.1200E 01	0.5000E-02	0.2500E 01	0.5850E 02	0.1500E 01
D1	D1/D2	N	W	D3	ALPHA	IGV	BH
0.2000E 00	0.4630E 00	0.4824E 05	0.2870E 01	0.6520E 00	0.2200E 02	0.2200E 02	0.3020E-01
BFI	BLH	BLM	BLTH	RR	VRATD	CPA	C2
0.0	0.8500E 00	0.9400E 00	0.7300E 00	0.1221E 01	0.6000E 00	0.1000E-01	0.0
NO OF BLADES	AD	RH2	UD	PHIPD	WD	ALPS	C7
0.3200E 02	0.1410E-01	0.2600E-01	0.1918E 04	0.6250E 00	0.9950E 00	0.1640E 02	0.1049E 01
C8	C9	C10	C11	C12	C13	RNMCR	CMT
0.1050E 01	0.1500E 00	0.1900E 01	0.6500E-01	0.4500E-01	0.5000E-01	0.8700E 00	0.5440E 00

RESULTS

POP	PRTTF	HF	W/A	MT	GG	RHOS	MAX
0.2104E 04	0.6206E 01	0.1383E 03	0.2531E 02	0.3451E 00	0.1024E 01	0.7169E-01	0.3200E 00
PHI	AI	VT	CTHT	BETAG	PHIP		
0.2144E 00	0.1103E 04	0.3807E 03	0.1426E 03	0.6959E 02	0.4478E 00		
0.9753 0.9866	0.9399	0.7182	0.8582	0.5306	1.0000		
0.9708 0.9873	0.9399	0.7182	0.8582	0.5306	1.0000		

URMS	PF	PSI	EFFH	DQ	RNMIT	TO4	TO3D
0.8502E 03	0.4471E-01	0.7839E 00	0.9113E 00	0.7627E-01	0.9172E 00	0.9273E 03	0.9159E 03
T03	P03	U	DRMS	EPS	CSF	PRDLE	CPT35
0.9039E 03	0.1306E 05	0.1647E 04	0.3366E 00	0.1937E 01	0.9049E 00	0.5811E 01	0.6874E 00
RC35	ET35	DP35	DPQ	PSTH	ETS	NS	RCS
0.5514E 01	0.7901E 00	0.5124E-01	0.1044E 00	0.3616E 01	0.7490E 00	0.7955E 02	0.5135E 01
MEXIT	MDLE	DQX	TRF	EFFI	DPQP	PSLE	DIBF
0.1211E 01	0.9067E 00	0.5330E-01	0.9135E 00	0.8582E 00	0.6165E-01	0.3411E 01	0.6496E 00
EFFIM	MG	MDEX	DPTD	ALPHD	ALPLE	A*/A	ET15
0.8189E 00	0.1279E 01	0.1159E 01	0.1688E-01	0.1436E 02	0.1859E 02	0.7974E 00	0.7623E 00
VTH4	VR	MTHR	RTHR	RDPTH	RDEXIT	RDPEX	CCPA
0.1452E 04	0.5199E 03	0.8378E 00	0.9852E 00	0.1456E-01	0.5256E 01	0.9566E-01	0.6894E 00

TABLE A-1 (CONT)

CENT COMP INLET CALC RC=2.7 RO

DATA

TRIG	DELSF	CC	C3	C1	C5	C6	TRIGR
0.1000E 01	0.0	0.7000E 01	0.1200E 01	0.5000E-02	0.2500E 01	0.5950E 02	0.1500E 01
D1	D1/D2	N	W	D3	ALPHA	IGV	BH
0.2000E 00	0.4630E 00	0.4483E 05	0.2526E 01	0.6520E 00	0.2200E 02	0.2200E 02	0.3040E-01
BEI	RLH	RLM	BLTH	RR	VRATO	CPA	C2
0.0	0.8500E 00	0.9400E 00	0.7300E 00	0.1221E 01	0.6000E 00	0.1000E-01	0.0
NO OF BLADES	AD	RH2	UD	PHIPD	WD	ALPS	C7
0.3200E 02	0.1410E-01	0.2400E-01	0.1918E 04	0.6250E 00	0.9950E 00	0.1640E 02	0.1035E 01
C8	C9	C10	C11	C12	C13	RNMCR	CMT
0.1050E 01	0.1500E 00	0.1900E 01	0.6500E-01	0.4500E-01	0.5000E-01	0.8700E 00	0.5440E 00

RESULTS

POP	PRTTE	HE	W/A	MT	GG	RHOS	MAX
0.2105E 04	0.5120E 01	0.9355E 02	0.2227E 02	0.2982E 00	0.1018E 01	0.7289E-01	0.2765E 00

PHI	AI	VT	CTHT	BETAG	PHIP
0.1999E 00	0.1107E 04	0.3300E 03	0.1236E 03	0.7104E 02	0.4176E 00

0.9653********** 0.9441 0.7489 1.1815 0.5089 0.9540

*** CHOKE ***

0.9599 0.9654 0.9441 0.7489 1.1815 0.5089 0.9540

*** CHOKE ***

URMS	PF	PSI	EFFH	DQ	RNMIT	T04	T03D
0.7901E 03	0.4170E-01	0.7883E 00	0.9176E 00	0.7083E-01	0.8508E 00	0.8734E 03	0.8628E 03
T03	P03	U	DRMS	EPS	CSF	PRDLE	CPT35
0.8517E 03	0.1078E 05	0.1530E 04	0.3366E 00	0.1937E 01	0.9009E 00	0.4842E 01	0.7331E 00
RC35	ET35	DP35	DPQ	PSTH	ETS	NS	RCS
0.4504E 01	0.7799E 00	0.6979E-01	-0.3001E 00	0.2521E 01	0.3908E-01	0.7082E 03	0.1097E 01
MEXIT	MDLE	DQX	TRF	EFFI	DPOP	PSLE	DIBF
0.1141E 01	0.9606E 00	0.5692E-01	0.9160E 00	0.8606E 00	0.5193E-01	0.2986E 01	0.6634E 00
EFFIM	MG	MDEX	DPTD	ALPHD	ALPLE	A*/A	ET15
0.8241E 00	0.1131E 01	0.1093E 01	0.1172E-01	0.1447E 02	0.1886E 02	0.1160E 01	0.7448E 00
VTH4	VR	MTHR	DTHR	RDPTH	PDEXIT	RDPEX	CCPA
0.1345E 04	0.4609E 03	0.9920E 00	0.9830E 00	0.2349E-01	0.4261E 01	0.1200E 00	0.6209E 00

TABLE A-1 (CONT)

CENT COMP INLET CALC RC=2.7 80

DATA

TRIG	DELSF	CC	C3	C1	C5	C6	TRIGR
0.1000E 01	0.0	0.2000E 01	0.1200E 01	0.5000E-02	0.2500E 01	0.5850E 02	0.1500E 01
D1	D1/D2	N	W	D3	ALPHA	IGV	BH
0.2000E 00	0.4630E 00	0.4483E 05	0.2485E 01	0.6520E 00	0.2200E 02	0.2200E 02	0.3040E-01
BFI	BLH	BLM	BLTH	RR	VRATD	CPA	C2
0.0	0.8500E 00	0.9400E 00	0.7300E 00	0.1221E 01	0.6000E 00	0.1000E-01	0.0
NO OF BLADES	AD	RH2	UD	PHIPD	WD	ALPS	C7
0.3200E 02	0.1410E-01	0.2600E-01	0.1919E 04	0.6250E 00	0.9950E 00	0.1640E 02	0.1035E 01
C8	C9	C10	C11	C12	C13	RNMCR	CMT
0.1050E 01	0.1500E 00	0.1900E 01	0.6500E-01	0.4500E-01	0.5000E-01	0.8700E 00	0.5440E 00

RESULTS

POP	PRTTE	HE	W/A	MT	GG	RHOS	MAX
0.2105E 04	0.5120E 01	0.9355E 02	0.2191E 02	0.2928E 00	0.1017E 01	0.7292E-01	0.2715E 00

PHI	AI	VT	CTHT	BETAG	PHIP
0.1963E 00	0.1107E 04	0.3241E 03	0.1214E 03	0.7139E 02	0.4102E 00

0.9654	0.9830	0.9450	0.7420	1.2566	0.5047	0.9693
0.9596	0.9837	0.9450	0.7420	1.2566	0.5047	0.9693

URMS	PF	PSI	EFFH	DQ	RNMIT	TO4	TO3D
0.7901E 03	0.4095E-01	0.7983E 00	0.9158E 00	0.7249E-01	0.8508E 00	0.8746E 03	0.8637E 03

TO3	P03	U	DRMS	EPS	CSF	PRDLE	CPT35
0.8523E 03	0.1078E 05	0.1530E 04	0.3366E 00	0.1937E 01	0.9018E 00	0.4839E 01	0.7169E 00

RC35	ET35	DP35	DPQ	PSTH	ETS	NS	RCS
0.4509E 01	0.7779E 00	0.4824E-01	-0.2132E 00	0.2661E 01	0.6988E 00	0.8053E 02	0.3972E 01

MEXIT	MDLE	DQX	TRF	EFFI	DPOP	PSLE	DIBF
0.1142E 01	0.8600E 00	0.5830E-01	0.9191E 00	0.8577E 00	0.5270E-01	0.2986E 01	0.6564E 00

EFFIM	MG	MDEX	DPTD	ALPHD	ALPLE	A*/A	ET15
0.8209E 00	0.1131E 01	0.1092E 01	0.1188E-01	0.1423E 02	0.1877E 02	0.1245E 01	0.7443E 00

VTH4	VR	MTHR	BTHR	RDPTH	POEXIT	RDPEX	CCPA
0.1345E 04	0.4575E 03	0.9449E 00	0.9818E 00	0.2269E-01	0.4275E 01	0.1165E 00	0.6243E 00

TABLE A-1 (CONT)

CENT COMP INLET CALC RC-2.7 80

DATA

TRIG	DELSF	CC	C3	C1	C5	C6	TRIGR
0.1000E 01	0.0	0.2000E 01	0.1200E 01	0.5000E-02	0.2500E 01	0.5850E 02	0.1500E 01
D1	D1/D2	N	W	D3	ALPHA	IGV	BH
0.2000E 00	0.4630E 00	0.4482E 05	0.2448E 01	0.6520E 00	0.2200E 02	0.2200E 02	0.3040E-01
BET	BLH	BLM	BLTH	RR	VRATD	CPA	C2
0.0	0.8500E 00	0.9400E 00	0.7300E 00	0.1221E 01	0.6000E 00	0.1000E-01	0.0
NO OF BLADES	AD	RH2	UD	PHIPD	WD	ALPS	C7
0.3200E 02	0.1410E-01	0.2600E-01	0.1918E 04	0.6250E 00	0.9950E 00	0.1640E 02	0.1035E 01
C8	C9	C10	C11	C12	C13	RNMCR	CMT
0.1050E 01	0.1500E 00	0.1900E 01	0.6500E-01	0.4500E-01	0.5000E-01	0.8700E 00	0.5440E 00

RESULTS

POP	PRTTE	HE	W/A	MT	GG	RHOS	MAX
0.2105E 04	0.5117E 01	0.9351E 02	0.2159E 02	0.2879E 00	0.1017E 01	0.7303E-01	0.2670E 00
PHI	AI	VT	CTHT	BETAG	PHIP		
0.1932E 00	0.1107E 04	0.2188E 03	0.1194E 03	0.7171E 02	0.4036E 00		
0.9654 0.9818	0.9459	0.7358 1.3269	0.5011	0.9830			
0.9595 0.9825	0.9459	0.7358 1.3269	0.5011	0.9830			

URMS	PF	PSI	EFFH	DQ	RNMIT	TO4	TO3D
0.7899E 03	0.4029E-01	0.7883E 00	0.9142E 00	0.7395E-01	0.8507E 00	0.8755E 03	0.8644E 03
TO3	P03	U	DRMS	EPS	CSF	PRDLE	CPT35
0.8527E 03	0.1077E 05	0.1530E 04	0.3366E 00	0.1937E 01	0.9026E 00	0.4833E 01	0.6854E 00
RC35	ET35	DP35	DPQ	PSTH	ETS	NS	RCS
0.4521E 01	0.7775E 00	0.6463E-01	-0.5635E-01	0.2897E 01	0.7296E 00	0.7721E 02	0.4188E 01
MEXIT	MDLE	DQX	TRE	EFFI	DPOP	PSLE	DIBF
0.1142E 01	0.9594E 00	0.5967E-01	0.9220E 00	0.8551E 00	0.5340E-01	0.2984E 01	0.6502E 00
EFFIM	MG	MDEX	DPTO	ALPHD	ALPLE	A*/A	ET15
0.8190E 00	0.1130E 01	0.1091E 01	0.1203E-01	0.1402E 02	0.1870E 02	0.3533E 01	0.7464E 00
VTH4	VR	MTHP	RTHP	RDPTH	PDEXIT	PDPEX	CCPA
0.1346E 04	0.4545E 03	0.8673E 00	0.9801E 00	0.2100E-01	0.4303E 01	0.1097E 00	0.6326E 00

TABLE A-1 (CONT)

CENT COMP INLET CALC PC-2.7 80

DATA

TRIG	DELSF	CC	C3	C1	C5	C6	TRIGR
0.1000E 01	0.0	0.2000E 01	0.1200E 01	0.5000E-02	0.2500E 01	0.5850E 02	0.1500E 01
D1	D1/D2	N	W	D3	ALPHA	IGV	BH
0.2000E 00	0.4630E 00	0.4493E 05	0.2417E 01	0.6520E 00	0.2200E 02	0.2200E 02	0.3040E-01
REI	BLH	BLM	BLTH	RR	VRATD	CPA	C2
0.0	0.8500E 00	0.9400E 00	0.7300E 00	0.1221E 01	0.6000E 00	0.1000E-01	0.0
NO OF BLADES	AD	BH2	UD	PHIPD	WD	ALPS	C7
0.3200E 02	0.1410E-01	0.2600E-01	0.1918E 04	0.6250E 00	0.9550E 00	0.1640E 02	0.1035E 01
C8	C9	C10	C11	C12	C13	RNMCR	CMT
0.1050E 01	0.1500E 00	0.1900E 01	0.6500E-01	0.4500E-01	0.5000E-01	0.8700E 00	0.5440E 00

RESULTS

POP	PRTTE	HE	W/A	MT	GG	RHOS	MAX
0.2105E 04	0.5120E 01	0.9355E 02	0.2131E 02	0.2839E 00	0.1016E 01	0.7311E-01	0.2632E 00
PHI	AI	VT	CTHT	BETAG	PHIP		
0.1905E 00	0.1107E 04	0.3144E 03	0.1178E 03	0.7198E 02	0.3979E 00		
0.9454 0.9801	0.9467	0.7300 1.3901	0.4979	0.9960			
0.9595 0.9818	0.9467	0.7300 1.3901	0.4979	0.9960			

URMS	PF	PSI	EFFH	DO	RNMIT	T04	T03D
0.7901E 03	0.3973E-01	0.7983E 00	0.9128E 00	0.7530E-01	0.8510E 00	0.8766E 03	0.8653E 03
T03	P03	U	DRMS	EPS	CSF	PRDLE	CPI35
0.8534E 03	0.1078E 05	0.1530E 04	0.3366E 00	0.1937E 01	0.9034E 00	0.4833E 01	0.6633E 00
PC35	ET35	DP35	DPO	PSTH	ETS	NS	RCS
0.4527E 01	0.7758E 00	0.6335E-01	0.2636E-01	0.3025E 01	0.7322E 00	0.7634E 02	0.4222E 01
MEXIT	MDLE	DQX	TRF	EFFI	DPOP	PSLE	DI8F
0.1144E 01	0.8592E 00	0.6091E-01	0.9243E 00	0.8527E 00	0.5410E-01	0.2985E 01	0.6443E 00
EFFIM	MG	MDEX	DPTD	ALPHD	ALPLE	A*/A	ET15
0.8153E 00	0.1130E 01	0.1090E 01	0.1218E-01	0.1383E 02	0.1865E 02	0.3997E 00	0.7461E 00
VTH4	VR	MTHR	BTHR	RDPTH	PDEXIT	RDPEX	CCPA
0.1347E 04	0.4521E 03	0.8265E 00	0.9791E 00	0.2002E-01	0.4317E 01	0.1067E 00	0.6355E 00

TABLE A-1 (CONT)

CENT COMP INLET CALC RC-2.7 80

DATA

TRIG	DELSF	CC	C3	C1	C5	C6	TRIGR
0.1000E 01	0.0	0.2300E 01	0.1200E 01	0.5000E-02	0.2500E 01	0.5850E 02	0.1500E 01
D1	D1/D2	N	W	D3	ALPHA	IGV	BH
0.2000E 00	0.4630E 00	0.4482E 05	0.2367E 01	0.6520E 00	0.2200E 02	0.2200E 02	0.3040E-01
BFI	BLH	BLM	BLTH	RR	VRATD	CPA	C2
0.0	0.8500E 00	0.9400E 00	0.7300E 00	0.1721E 01	0.6000E 00	0.1000E-01	0.0
NO OF BLADES	AD	BH2	UD	PHIPD	WD	ALPS	C7
0.3200E 02	0.1410E-01	0.2600E-01	0.1918E 04	0.6250E 00	0.9950E 00	0.1640E 02	0.1035E 01
C8	C9	C10	C11	C12	C13	RNMCP	CMT
0.1050E 01	0.1500E 00	0.1900E 01	0.6500E-01	0.4500E-01	0.5000E-01	0.8700E 00	0.5440E 00

RESULTS

PDP	PRTTF	HE	W/A	MT	GG	RHOS	MAX
0.2106E 04	0.5117E 01	0.9351E 02	0.2087E 02	0.2774E 00	0.1015E 01	0.7325E-01	0.2572E 00

PHI	AI	VT	CTHT	BETAG	PHIP
0.1852E 00	0.1108E 04	0.3073E 03	0.1151E 03	0.7241E 02	0.3891E 00
0.9655 0.9791	0.9481	0.7209 1.4555	0.4931	1.0000	
0.9596 0.9809	0.9481	0.7209 1.4555	0.4931	1.0000	

UBMS	PF	PSI	EFFH	DQ	RNMIT	TO4	TO3D
0.7899E 03	0.3884E-01	0.7883E 00	0.9106E 00	0.7738E-01	0.8509E 00	0.8778E 03	0.8662E 03
TO3	PO3	U	DBMS	EPS	CSF	PRDLE	CPT35
0.8540E 03	0.1077E 05	0.1530E 04	0.3366E 00	0.1937E 01	0.9046E 00	0.4826E 01	0.6309E 00
RC35	ET35	DP35	DPQ	PSTH	ETS	NS	RCS
0.4525E 01	0.7731E 00	0.6227E-01	0.1239E 00	0.3173E 01	0.7328E 00	0.7531E 02	0.4242E 01
MEXIT	MDLE	DQX	T2F	EFFI	DPOP	PSLE	DIAF
0.1145E 01	0.8565E 00	0.4219E-01	0.9279E 00	0.8496E 00	0.5514E-01	0.2982E 01	0.6358E 00
EFFIM	MG	MDEX	DPTO	ALPHD	ALPLE	A*/A	ET15
0.8117E 00	0.1130E 01	0.1089E 01	0.1242E-01	0.1354E 02	0.1855E 02	0.7641E 00	0.7450E 00
VTH4	V2	MTH2	STHR	RDPTH	PDEXIT	RDPEX	CCPA
0.1348E 04	0.4482E 03	0.7785E 00	0.9779E 00	0.1873E-01	0.4326E 01	0.1035E 00	0.6377E 00

TABLE A-1 (CONT)

CENT COMP INLET CALC RC=2.7 RQ

DATA

TRIG	DELSF	CC	C3	C1	C5	C6	TRIGR
0.1000E 01	0.0	0.2300E 01	0.1200E 01	0.5000E-02	0.2500E 01	0.5850E 02	0.1500E 01
D1	D1/D2	N	W	D3	ALPHA	IGV	RH
0.2000E 00	0.4632E 00	0.4483E 05	0.2328E 01	0.6520E 00	0.2200E 02	0.2200E 02	0.3040E-01
BFI	BLH	BLM	BLTH	RR	VRATD	CPA	C2
0.0	0.8500E 00	0.9400E 00	0.7300E 00	0.1221E 01	0.6000E 00	0.1000E-01	0.0
NO OF BLADES	A1	BH2	UD	PHIPD	WD	ALPS	C7
0.2200E 02	0.1410E-01	0.2600E-01	0.1918E 04	0.6250E 00	0.9950E 00	0.1640E 02	0.1035E 01
C8	C9	C10	C11	C12	C13	RNMCR	CMT
0.1050E 01	0.1500E 00	0.1900E 01	0.6500E-01	0.4500E-01	0.5000E-01	0.8700E 00	0.5440E 00

RESULTS

POP	PRTTE	HE	W/A	MT	GG	RHOS	MAX
0.2106E 04	0.5120E 01	0.9355E 02	0.2053E 02	0.2724E 00	0.1015E 01	0.7335E-01	0.2525E 00
PHI	AI	VT	CTHT	BETAG	PHIP		
0.1829E 00	0.1138E 04	0.3018E 03	0.1131E 03	0.7274E 02	0.3820E 00		
0.9655	0.9779	0.9493	0.7130 1.4997	0.4893	1.0000		
0.9598	0.9802	0.9493	0.7130 1.4997	0.4893	1.0000		
URMS	PF	PSI	EFFH	DQ	RNMIT	T04	T03D
0.7901E 03	0.3914E-01	0.7183E 00	0.9088E 00	0.7914E-01	0.8513E 00	0.8789E 03	0.8672E 03
T02	P03	U	DPMS	EPS	CSF	PRDLE	CPT35
0.8549E 03	0.1078E 05	0.1530E 04	0.3366E 00	0.1937E 01	0.9056E 00	0.4824E 01	0.6059E 00
RC35	ET35	DP35	DPQ	PSTH	ETS	NS	RCS
0.4528E 01	0.7710E 00	0.4137E-01	0.1899E 00	0.3274E 01	0.7324E 00	0.7455E 02	0.4256E 01
MEXIT	MDLE	DQX	TRE	EFFI	DPOP	PSLE	DIBF
0.1147E 01	0.8582E 00	0.6308E-01	0.9306E 00	0.8472E 00	0.5611E-01	0.2982E 01	0.6288E 00
EFFIM	MG	MDEX	DPTD	ALPHD	ALPLE	A*/A	ETLS
0.9089E 00	0.1130E 01	0.1089E 01	0.1267E-01	0.1329E 02	0.1846E 02	0.8366E 00	0.7439E 00
VTH4	VR	MTHR	RTHR	RDPTH	POEXIT	RDPEX	CCPA
0.1349E 04	0.4454E 03	0.7462E 00	0.9772E 00	0.1780E-01	0.4336E 01	0.1012E 00	0.6397E 00

TABLE A-1 (CONT)

CENT COMP INLET CALC RC-2.7 70

DATA

TRIG	DELSF	CC	C3	C1	C5	C6	TRIGR
0.1000E 01	0.0	0.2000E 01	0.1200F 01	0.5000E-02	0.2500E 01	0.5850E 02	0.1500E 01
D1	D1/D2	N	W	D3	ALPHA	IGV	BH
0.2000E 00	0.4630F 00	0.3919E 05	0.1939F 01	0.6520E 00	0.2200E 02	0.2200E 02	0.3080E-01
BFI	BLH	BLM	BLTH	RR	VRATD	CPA	C2
0.0	0.8500F 00	0.9400E 00	0.7300F 00	0.1221E 01	0.6000E 00	0.1000F-01	0.0
NO OF BLADES	AD	BH2	HD	PHIPD	WD	ALPS	C7
0.3200E 02	0.1410E-01	0.2600E-01	0.1918F 04	0.6250E 00	0.9950E 00	0.1640E 02	0.1033E 01
C8	C9	C10	C11	C12	C13	RNMCR	CMT
0.1050E 01	0.1500F 00	0.1900E 01	0.6500E-01	0.4500E-01	0.5000E-01	0.8700E 00	0.5440E 00

RESULTS

POP	PRTTF	FE	W/A	MT	GG	RHOS	MAX
0.2106F 04	0.3722F 01	0.7149E 02	0.1710F 02	0.2236E 00	0.1010E 01	0.7426E-01	0.2073E 00

PHI	AI	VT	CTHT	BETAG	PHIP
0.1721E 00	0.1111F 04	0.2483E 03	0.9303F 02	0.7382E 02	0.3595E 00

0.9659	0.9852	0.9486	0.7930	1.9886	0.4686	0.8742

*** CHOKE ***

0.9612	0.9857	0.9486	0.7900	1.9886	0.4686	0.8742

*** CHOKE ***

STANDARD FIXUP TAKEN , EXECUTION CONTINUING

URMS	PF	PSI	EFFH	DQ	RNMIT	TO4	TO3D
0.6907E 03	0.3590F-01	0.7907E 00	0.9199E 00	0.6887E-01	0.7437E 00	0.7936E 03	0.7840E 03
TO3	PO3	U	DPMS	EPS	CSF	PRDLE	CPT35
0.7741F 03	0.7840F 04	0.1338E 04	0.3366F 00	0.1937E 01	0.8954F 00	0.3562E 01	0.7364E 00
RC35	ET35	DP35	DPO	PSTH	ETS	NS	RCS
0.3318F 01	0.7684E 00	0.6833E-01	-0.5432E 00	0.1845E 01	0.1143E 00	0.2943E 03	-0.1229E 01
MEXIT	MDLE	DDX	TRF	EFFI	DPOP	PSLE	DI8F
0.9911E 00	0.7757F 00	0.6629E-01	0.9259F 00	0.8540F 00	0.4016E-01	0.2393E 01	0.6765E 00
EFFIM	MG	MDEX	DPTO	ALPHO	ALPLE	A*/A	ET15
0.9199F 00	0.9999F 00	0.9752F 00	0.6283E-02	0.1407E 02	0.1896F 02	0.1094E 01	0.7266E 00
VTH4	VR	MTHP	RTHP	RDPTH	POEXIT	RDPEX	CCPA
0.1169E 04	0.3674E 03	0.9969F 00	0.9936F 00	0.2277E-01	0.3138E 01	0.1189E 00	0.5613E 00

TABLE A-1 (CONT)

CENT COMP INLET CALC RC-2.7 70

DATA

TRIG	DELSF	CC	C3	C1	C5	C6	TRIGR
0.1000E 01	0.0	0.2000E 01	0.1200E 01	0.5000E-02	0.2500E 01	0.5850E 02	0.1500E 01
D1	D1/D2	N	W	D3	ALPHA	IGV	BH
0.2000E 00	0.4630E 00	0.3918E 05	0.1989E 01	0.6520E 00	0.2200E 02	0.2200E 02	0.3080E-01
REI	BLH	BLM	BLTH	RR	VRATD	CPA	C2
0.0	0.8500E 00	0.9400E 00	0.7300E 00	0.1221E 01	0.6000E 00	0.1000E-01	0.0
NO OF BLADES	AD	BH2	UD	PHIPD	WD	ALPS	C7
0.3200E 02	0.1410E-01	0.2600E-01	0.1918E 04	0.6250E 00	0.9950E 00	0.1640E 02	0.1033E 01
C9	C9	C10	C11	C12	C13	RNMCR	CMT
0.1050E 01	0.1500E 00	0.1900E 01	0.6500E-01	0.4500E-01	0.5000E-01	0.8700E 00	0.5440E 00

RESULTS

POP	PRTTF	HE	W/A	MT	GG	RHOS	MAX
0.2106E 04	0.3720E 01	0.7145E 02	0.1666E 02	0.2174E 00	0.1009E 01	0.7436E-01	0.2016E 00
PHI	AI	VT	CTHT	BETAG	PHIP		
0.1675E 00	0.1111E 04	0.2416E 03	0.9051E 02	0.7428E 02	0.3499E 00		
0.9659 0.9836 0.9486	0.7814 2.1483	0.4616 0.8957					
0.9606 0.9827 0.9486	0.7814 2.1483	0.4616 0.8957					

UPMS	PE	PSI	EFFH	DQ	RNMIT	TO4	TO3D
0.6905E 03	0.3493E-01	0.7907E 00	0.9174E 00	0.7096E-01	0.7439E 00	0.7949E 03	0.7849E 03
TO3	PO3	U	DPMS	EPS	CSF	PRDLE	CPT35
0.7746E 03	0.7836E 04	0.1338E 04	0.3366E 00	0.1937E 01	0.8966E 00	0.3557E 01	0.6834E 00
RC35	ET35	DP35	DPQ	PSTH	ETS	NS	RCS
0.3333E 01	0.7681E 00	0.6302E-01	-0.2383E 00	0.2152E 01	0.7123E 00	0.7335E 02	0.3093E 01
MEXIT	MDLE	DQX	TRF	EFFI	DPOP	PSLE	DIBF
0.9921E 00	0.7750E 00	0.6907E-01	0.9307E 00	0.8496E 00	0.4099E-01	0.2392E 01	0.6635E 00
EFFIM	MG	MDEX	DPTD	ALPHD	ALPLE	A*/A	ET15
0.8151E 00	0.9989E 00	0.9737E 00	0.6346E-02	0.1374E 02	0.1888E 02	0.1237E 01	0.7314E 00
VTH4	VP	MTHR	RTHR	RDPTH	POEXIT	RDPEX	CCPA
0.1169E 04	0.3621E 03	0.8593E 00	0.9804E 00	0.2025E-01	0.3174E 01	0.1078E 00	0.5755E 00

TABLE A-1 (CONT)

CENT COMP INLET CALC RC-2.7 70

DATA

TRIG	DELSF	CC	C3	C1	C5	C6	TRIGR
0.1000E 01	0.0	0.2000E 01	0.1200E 01	0.5000E-02	0.2500E 01	0.5850E 02	0.1500E 01
D1	D1/D2	N	W	D3	ALPHA	IGV	BM
0.2000E 00	0.4630E 00	0.3919E 05	0.1845E 01	0.6520E 00	0.2200E 02	0.2200E 02	0.3080E-01
REI	RLH	RLM	RLTH	RR	VRATD	CPA	C2
0.0	0.8500E 00	0.9400E 00	0.7300E 00	0.1221E 01	0.6000E 00	0.1000E-01	0.0
NO OF BLADES	AD	RH2	UD	PHIPD	WD	ALPS	CT
0.3200E 02	0.1410E-01	0.2630E-01	0.1918E 04	0.6250E 00	0.9950E 00	0.1640E 02	0.1033E 01
C8	C9	C10	C11	C12	C13	RNMCR	CMT
0.1050E 01	0.1500E 00	0.1900E 01	0.6500E-01	0.4500E-01	0.5300E-01	0.8700E 00	0.5440E 00

RESULTS

POP	PRITE	HE	W/A	MT	GG	RHOS	MAX
0.2106E 04	0.3722E 01	0.7149E 02	0.1627E 02	0.2121E 00	0.1009E 01	0.7444E-01	0.1966E 00
PHI	AT	VT	CTHT	BETAG	PHIP		
0.1633E 00	0.1111E 04	0.2357E 03	0.8829E 02	0.7469E 02	0.3413E 00		

STANDARD FIXUP TAKEN , EXECUTION CONTINUING

0.9659	0.9804	0.9436	0.7729	2.3028	0.4555	0.9169
0.9604	0.9814	0.9486	0.7729	2.3029	0.4555	0.9169

URMS	PF	PSI	EFFH	QQ	RNMIT	TO4	TO3D
0.6907E 03	0.3407E-01	0.7907E 00	0.9155E 00	0.7296E-01	0.7446E 00	0.7964E 03	0.7860E 03
TO3	PO3	U	DRMS	EPS	CSF	PRDLE	CPT35
0.7753E 03	0.7843E 04	0.1338E 04	0.3366E 00	0.1937E 01	0.8977E 00	0.3556E 01	0.6433E 00
RC35	ET35	DP35	DPQ	PSTH	ETS	NS	RCS
0.3337E 01	0.7646E 00	0.6174E-01	-0.8784E-01	0.2303E 01	0.7156E 00	0.7196E 02	0.3124E 01
MEXIT	MDLE	DDX	TRE	EFFI	DPDP	PSLE	DIBE
0.6936E 00	0.7747E 00	0.7176E-01	0.9354E 00	0.8453E 00	0.4185E-01	0.2392E 01	0.6510E 00
EFFM	MG	MDEX	DPTO	ALPHO	ALPLE	A*/A	ETLS
0.8104E 00	0.9985E 00	0.9729E 00	0.6435E-02	0.1344E 02	0.1882E 02	0.2009E 01	0.7306E 00
VTH4	VR	MTHP	RTHR	RDPTH	PDEXIT	RDPEX	CCPA
0.1170E 04	0.3578E 03	0.7939E 00	0.5787E 00	0.1975E-01	0.3187E 01	0.1037E 00	0.5789E 00

TABLE A-1 (CONT)

CENT COMP INLET CALC PC-2.7 70

DATA

TRIG	DELSF	CC	C3	C1	C5	C6	TRIGR
0.1000E 01	0.0	0.2000E 01	0.1200E 01	0.5000E-02	0.2500E 01	0.5850E 02	0.1500E 01
D1	D1/D2	N	W	D3	ALPHA	IGV	BH
0.2000E 00	0.4630E 00	0.3919E 05	0.1804E 01	0.6520E 00	0.2200E 02	0.2200E 02	0.3080E-01
RFI	RLM	RLM	RLTH	RR	VRATD	CPA	C2
0.0	0.9500E 00	0.9400E 00	0.7300E 00	0.1221E 01	0.6000E 00	0.1000E-01	0.0
NO OF BLADES	AD	RH2	UD	PHIPD	WD	ALPS	C7
0.3200E 02	0.1410E-01	0.2600E-01	0.1319E 04	0.6250E 00	0.9950E 00	0.1640E 02	0.1033E 01
C8	C9	C10	C11	C12	C13	RNMCR	CMT
0.1050E 01	0.1500E 00	0.1900E 01	0.6500E-01	0.4500E-01	0.5000E-01	0.8700E 00	0.5440E 00

RESULTS

POP	PRTTF	HF	W/A	MT	GG	RHOS	MAX
0.2106E 04	0.3722E 01	0.7149E 02	0.1591E 02	0.2071E 00	0.1009E 01	0.7452E-01	0.1920E 00
PHI	AI	VT	CTHT	BETAG	PHIP		
0.1595E 00	0.1112E 04	0.2302E 03	0.8624E 02	0.7506E 02	0.3333E 00		

STANDARD FIXUP TAKEN , EXECUTION CONTINUING

0.9659	0.9787	0.9487	0.7647	2.4563	0.4500	0.9372
0.9603	0.9805	0.9487	0.7647	2.4563	0.4500	0.9372

URMS	PF	PSI	EFFH	DQ	RNMIT	TO4	TO3D
0.6907E 03	0.3329E-01	0.7907E 00	0.9135E 00	0.7484E-01	0.7450E 00	0.7977E 03	0.7869E 03
TO3	PO3	U	DRMS	EPS	CSF	PRDLE	CPT35
0.7759E 03	0.7840E 04	0.1338E 04	0.3366E 00	0.1937E 01	0.8988E 00	0.3554E 01	0.6095E 00
RC35	ET35	DP35	DPQ	PSTH	ETS	NS	RCS
0.3337E 01	0.7613E 00	0.6090E-01	0.1427E-01	0.2405E 01	0.7150E 00	0.7094E 02	0.3136E 01
MEXIT	MDLE	DQX	TRF	EFFI	DPOP	PSLE	DIBF
0.9948E 00	0.7743E 00	0.7442E-01	0.9399E 00	0.8412E 00	0.4267E-01	0.2391E 01	0.6391E 00
EFFIM	MG	MDEX	DPTO	ALPHD	ALPLE	A*/A	ETLS
0.8059E 00	0.9980E 00	0.9720E 00	0.6522E-02	0.1316E 02	0.1878E 02	0.2503E 00	0.7287E 00
VTH4	VR	MTHR	RTHR	RDPTH	PDEXIT	RDPEX	CCPA
0.1171E 04	0.3539E 03	0.7494E 00	0.9775E 00	0.1766E-01	0.3195E 01	0.1009E 00	0.5809E 00

TABLE A-1 (CONT)

CENT COMP INLET CALC RC-2.7 T_0 DATA

TRIG	DELSF	CC	C3	C1	C5	C6	TRIGR
0.1000E 01	0.0	0.2000E 01	0.1200E 01	0.5000E-02	0.2500E 01	0.5850E 02	0.1500E 01
D1	D1/D2	N	W	D3	ALPHA	IGV	BH
0.2000E 00	0.4630E 00	0.3920E 05	0.1738E 01	0.6520E 00	0.2200E 02	0.2200E 02	0.3080E-01
BFI	BLH	RLM	BLTH	RR	VRATD	CPA	C2
0.0	0.8500E 00	0.9400E 00	0.7300E 00	0.1221E 01	0.6000E 00	0.1000E-01	0.0
NO OF BLADES	*	RH2	UP	PHIPD	WD	ALPS	C7
0.3200E 02	0.1410E-01	0.2600E-01	0.1918E 04	0.6250E 00	0.9950E 00	0.1640E 02	0.1033E 01
C8	C9	C10	C11	C12	C13	RNMCR	CMT
0.1050E 01	0.1500E 00	0.1900E 01	0.6500E-01	0.4500E-01	0.5000E-01	0.8700E 00	0.5440E 00

RESULTS

POP	PRTTF	HE	W/A	MT	GG	RHOS	MAX
0.2106E 04	0.3724E 01	0.7153E 02	0.1533E 02	0.1991E 00	0.1008E 01	0.7464E-01	0.1846E 00
PHI	AI	VT	CTHT	BETAG	PHIP		
0.1534E 00	0.1112E 04	0.2214E 03	0.8295E 02	0.7567E 02	0.3205E 00		

IHC251I SQRT NEGATIVE ARGUMENT=-0.7604599E-02

TRACEBACK	ROUTINE	CALLED FROM ISN	REG. 14	REG. 15	REG. 0	REG. 1
	SQRT		52364884	0036AC70	FFFFFFE4	00362980
	MAIN		00016864	013625A8	FD000008	00386FF8

ENTRY POINT= 013625A8

STANDARD FIXUP TAKEN , EXECUTION CONTINUING

0.9659	0.9775	0.9488	0.7503	2.7293	0.4413	0.9729
0.9601	0.9792	0.9489	0.7503	2.7293	0.4413	0.9729

URMS	PF	PSI	EFFH	DQ	RNMIT	T04	T03D
0.6909E 03	0.3200E-01	0.7906E 00	0.9102E 00	0.7804E-01	0.7460E 00	0.8002E 03	0.7887E 03
T03	P03	U	DRMS	EPS	CSF	PRDLE	CPT35
0.7769E 03	0.7845E 04	0.1338E 04	0.3366E 00	0.1937E 01	0.9007E 00	0.3551E 01	0.5566E 00
RC35	ET35	DP35	DPQ	PSTH	ETS	NS	RCS
0.3339E 01	0.7547E 00	0.5958E-01	0.1462E 00	0.2536E 01	0.7120E 00	0.6941E 02	0.3150E 01
MEXIT	MDLE	DQX	TRF	EFFI	DPOP	PSLE	DI8F
0.6971E 00	0.7740E 00	0.7916E-01	0.9478E 00	0.8341E 00	0.4415E-01	0.2389E 01	0.6186E 00
EFFIM	MG	MDEX	DPTD	ALPHD	ALPLE	A*/A	ET15
0.7981E 00	0.3977E 00	0.9708E 00	0.6705E-02	0.1270E 02	0.1873E 02	0.7829E 00	0.7248E 00
VTH4	VR	MTHP	RTHR	RDPTH	PDEXIT	RDPEX	CCPA
0.1173E 04	0.3479E 03	0.6922E 00	0.9759E 00	0.1619E-01	0.3206E 01	0.9711E-01	0.5844E 00

IHC900I EXECUTION TERMINATING DUE TO ERROR COUNT FOR ERROR NUMBER 217

IHC217I FIOCS - END OF DATA SET ON UNIT 5

TABLE A-1 (CONT)

CENT COMP INLET CALC RC-2.7 60

DATA

TRIG	DELSF	CC	C3	C1	C5	C6	TRIGR
0.1000E 01	0.0	0.2000E 01	0.1200E 01	0.5000E-02	0.2500E 01	0.5850E 02	0.1500E 01
D1	D1/D2	N	W	B3	ALPHA	IGV	BH
0.2000E 00	0.4630E 00	0.3361E 05	0.1545E 01	0.6520E 00	0.2200E 02	0.2200E 02	0.3100E-01
BFI	BLH	BLM	BLTH	RR	VRATD	CPA	C2
0.0	0.8500E 00	0.9400E 00	0.7300E 00	0.1221E 01	0.6000E 00	0.1000E-01	0.0
NO OF BLADES	AD	BH2	UD	PHIPD	WD	ALPS	C7
0.3200E 02	0.1410E-01	0.2600E-01	0.1918E 04	0.6250E 00	0.9950E 00	0.1640E 02	0.1046E 01
C8	C9	C10	C11	C12	C13	RNMCR	CMT
0.1050E 01	0.1500E 00	0.1900E 01	0.6500E-01	0.4500E-01	0.5000E-01	0.8700E 00	0.5440E 00

RESULTS

PDP	PRTTF	HE	V/A	MT	GG	RHOS	MAX
0.2107E 04	0.2762E 01	0.5258E 02	0.1342E 02	0.1761E 00	0.1005E 01	0.7497E-01	0.1633E 00
PHI	AI	VT	CTHT	BETAG	PHIP		
0.1584E 00	0.1113E 04	0.1960E 03	0.7342E 02	0.7518E 02	0.3309E 00		

STANDARD FIXUP TAKEN , EXECUTION CONTINUING

0.9779 0.0000 0.9541 0.8499 2.7125 0.4483 0.7489

*** CHOKE ***

0.9751 0.9907 0.9541 0.8499 2.7125 0.4483 0.7489

*** CHOKE ***

STANDARD FIXUP TAKEN , EXECUTION CONTINUING

URMS	PF	PSI	EFFI	DQ	RNMIT	T04	T03D
0.5923E 03	0.3303E-01	0.7943E 00	0.9296E 00	0.6[illegible]8E-01	0.6383E 00	0.7219E 03	0.7140E 03
T03	P03	U	URMS	EPS	CSF	PRDLE	CPT35
0.7059E 03	0.5817E 04	0.1147E 04	0.3366E 00	0.1937E 01	0.8875E 00	0.2670E 01	0.7541E 00
RC35	ET35	DP35	DPQ	PSTH	ETS	NS	RCS
0.2532E 01	0.7753E 00	0.5175E-01	-0.8719E 00	0.1393E 01	0.3180E 00	0.1315E 03	-0.1508E 01
MEXIT	MDLE	DQX	TRE	EFFI	DPDP	PSLE	DIBF
0.8424E 00	0.6845E 00	0.7345E-01	0.9279E 00	0.8560E 00	0.2961E-01	0.1952E 01	0.7137E 00
EFFIM	MG	MDEX	DPTD	ALPHD	ALPLE	A*/A	ET15
0.8235E 00	0.8687E 00	0.8535E 00	0.3089E-02	0.1423E 02	0.1922E 02	0.1043E 01	0.7227E 00
VTH4	VR	MTHR	BTHR	RDPTH	PDEXIT	RDPEX	CCPA
0.9941E 03	0.2971E 03	0.3979E 00	0.9895E 00	0.1459E-01	0.2395E 01	0.1032E 00	0.5217E 00

TABLE A-1 (CONT)

CENT COMP INLET CALC RC-2.7 60

DATA

TRIG	DELSF	CC	C3	C1	C5	C6	TRIGR
0.1000E 01	0.0	0.2000E 01	0.1200E 01	0.5000E-02	0.2500E 01	0.5850E 02	0.1500E 01
D1	D1/D2	N	W	D3	ALPHA	IGV	BH
0.2000E 00	0.4630E 00	0.3359E 05	0.1538E 01	0.6520E 00	0.2400E 02	0.2200E 02	0.3100E-01
BFI	BLH	BLM	BLTH	RR	VRATD	CPA	C2
0.0	0.8500E 00	0.9400E 00	0.7300E 00	0.1221E 01	0.6000E 00	0.1000E-01	0.0
NO OF BLADES	AD	BH2	UD	PHIPD	HD	ALPS	C7
0.3200E 02	0.1410E-01	0.2600E-01	0.1918E 04	0.6250E 00	0.9950E 00	0.1640E 02	0.1046E 01
C8	C9	C10	C11	C12	C13	RNMCR	CMT
0.1050E 01	0.1500E 00	0.1900E 01	0.6500E-01	0.4500E-01	0.5000E-01	0.8700E 00	0.5440E 00

RESULTS

POP	PRTTE	HE	W/A	PT	GG	RHOS	MAX
0.2107E 04	0.2759E 01	0.5252E 02	0.1356E 02	0.1753E 00	0.1006E 01	0.7498E-01	0.1625E 00
PHI	AI	VT	CTHT	BETAG	PHIP		
0.1577E 00	0.1113E 04	0.1951E 03	0.7308E 02	0.7524E 02	0.3295E 00		

STANDARD FIXUP TAKEN , EXECUTION CONTINUING

0.9779	0.9895	0.9540	0.8493	2.7418	0.4472	0.7509
0.9750	0.9903	0.9540	0.8493	2.7418	0.4472	0.7509

*** CHOKE ***

STANDARD FIXUP TAKEN , EXECUTION CONTINUING

URMS	PF	PSI	EFFH	DQ	RNMIT	TO4	TO3D
0.5920E 03	0.3290E-01	0.7942E 00	0.9293E 00	0.6043E-01	0.6380E 00	0.7218E 03	0.7138E 03
TO3	PO3	U	DRMS	EPS	CSF	PRDLE	CPT35
0.7058E 03	0.5811E 04	0.1147E 04	0.3366E 00	0.1937E 01	0.8876E 00	0.2667E 01	0.7543E 00
RC35	ET35	DP35	DPQ	PSTH	ETS	NS	RCS
0.2529E 01	0.7744E 00	0.5193E-01	-0.9765E 00	0.1390E 01	0.4708E 00	0.7497E 02	-0.2262E 01
MEXIT	MDLE	DQX	TRF	EFFI	DPOP	PSLE	DIBF
0.8420E 00	0.6941E 00	0.7390E-01	0.9286E 00	0.8553E 00	0.2966E-01	0.1950E 01	0.7117E 00
EFFIM	MG	MDEX	DPTD	ALPHD	ALPLE	A*/A	ET1>
0.8228E 00	0.8681E 00	0.8529E 00	0.3080E-02	0.1419E 02	0.1922E 02	0.1044E 01	0.7218E 00
VTH4	VR	MTHR	BTHR	RDPTH	POEXIT	RDPEX	CCPA
0.9935E 03	0.2961E 03	0.9989E 00	0.9895E 00	0.1468E-01	0.2391E 01	0.1035E 00	0.5206E 00

TABLE A-1 (CONT)

CENT COMP INLET CALC RC-2.7 60

DATA

TRIG	DELSF	CC	C3	C1	C5	C6	TRIGR
0.1000E 01	0.0	0.2000E 01	0.1700E 01	0.5000E-02	0.2500E 01	0.5850E 02	0.1500E 01
D1	D1/D2	N	W	D3	ALPHA	IGV	BH
0.2000E 00	0.4630E 00	0.3363E 05	0.1504E 01	0.6520E 00	0.2200E 02	0.2200E 02	0.3100E-01
BFI	BLH	BLM	BLTH	RR	VRATD	CPA	C2
0.0	0.8500E 00	0.9400E 00	0.7300E 00	0.1221E 01	0.6000E 00	0.1000E-01	0.0
NO OF BLADES	AD	BH2	UD	PHIPD	WD	ALPS	C7
0.3200E 02	0.1410E-01	0.2600E-01	0.1918E 04	0.6250E 00	0.9950E 00	0.1640E 02	0.1046E 01
C8	C9	C10	C11	C12	C13	RNMCR	CMT
0.1050E 01	0.1500E 00	0.1900E 01	0.6500E-01	0.4500E-01	0.5000E-01	0.8700E 00	0.5440E 00

RESULTS

PCP	PRTTE	HE	W/A	MT	GG	RHOS	MAX
0.2107E 04	0.2765E 01	0.5264E 02	0.1326E 02	0.1713E 00	0.1006E 01	0.7503E-01	0.1588E 00
PHI	AI	VT	CTHT	BETAG	PHIP		
0.1539E 00	0.1113E 04	0.1906E 03	0.7141E 02	0.7562E 02	0.3216E 00		

IHC251I SQRT NEGATIVE ARGUMENT=-0.3127480E-01

TRACEBACK	ROUTINE	CALLED FROM ISN	REG. 14	REG. 15	REG. 0	REG. 1
	SQRT		52328984	0032CC70	FFFFFFE4	00326980
	MAIN		00016868	013265A8	FD000008	0034AFF8

ENTRY POINT= 013265A8

STANDARD FIXUP TAKEN , EXECUTION CONTINUING

0.9779	0.9895	0.9531	0.8431	2.9119	0.4402	0.7679
0.9747	0.9888	0.9531	0.8431	2.9119	0.4402	0.7679

URMS	PE	PST	EFFH	DQ	RNMIT	TO4	TO3D
0.5927E 03	0.3211E-01	0.7943E 00	0.9276E 00	0.6196E-01	0.6393E 00	0.7232E 03	0.7150E 03
TO3	PO3	U	DRMS	EPS	CSF	PRDLF	CPT35
0.7066E 03	0.5824E 04	0.1148E 04	0.3366E 00	0.1937E 01	0.8884E 00	0.2671E 01	0.6981E 00
RC35	ET35	DP35	DPQ	PSTH	ETS	NS	RCS
0.2545E 01	0.7751E 00	0.4729E-01	-0.4748E 00	0.1649E 01	0.7072E 00	0.7091E 02	0.2367E 01
MEXIT	MDLE	DQX	TRE	EFFI	DPOP	PSLF	DIBF
0.8438E 00	0.6842E 00	0.7666E-01	0.9329E 00	0.9514E 00	0.3026E-01	0.1953E 01	0.6983E 00
EFFIM	MG	MDEX	DPTD	ALPHD	ALPLE	A*/A	ET15
0.8185E 00	0.8681E 00	0.8527E 00	0.3089E-02	0.1389E 02	0.1914E 02	0.1080E 01	0.7297E 00
VT44	VR	MTHR	RTHP	RDPTH	POEXIT	RDPEX	CCPA
0.9951E 03	0.2917E 03	0.8473E 00	0.9873E 00	0.1278E-01	0.2425E 01	0.9231E-01	0.5366E 00

TABLE A-1 (CONT)

CONT COMP INLET CALC RC-2.7 60

DATA

TRIG	DELSF	CC	C3	C1	C5	C6	TRIGR
0.1000E 01	0.0	0.2000E 01	0.1200E 01	0.5000E-02	0.2500E 01	0.5850E 02	0.1500E 01
D1	D1/D2	N	W	D3	ALPHA	IGV	BH
0.2000E 00	0.4630E 00	0.3360E 05	0.1469E 01	0.6520E 00	0.2200E 02	0.2200E 02	0.3100E-01
BFI	BLH	BLM	BLTH	RR	VRATD	CPA	C2
0.0	0.8500E 00	0.9400E 00	0.7300E 00	0.1221E 01	0.6000E 00	0.1000E-01	0.0
NO OF BLADES	AD	BH2	UD	PHIPD	WD	ALPS	C7
0.3200E 02	0.1410E-01	0.2600E-01	0.1918E 04	0.6250E 00	0.9950E 00	0.1640E 02	0.1046E 01
C8	C9	C10	C11	C12	C13	RNMCR	CMT
0.1050E 01	0.1500E 00	0.1900E 01	0.6500E-01	0.4500E-01	0.5000E-01	0.8700E 00	0.5440E 00

RESULTS

POP	PRTTE	HE	W/A	MT	GG	RHOS	MAX
0.2107E 04	0.2760E 01	0.5255E 02	0.1295E 02	0.1671E 00	0.1006E 01	0.7509E-01	0.1550E 00
PHI	AI	VT	CTI*	BETAG	PHIP		
0.1504E 00	0.1113E 04	0.1861E 03	0.6970E 02	0.7597E 02	0.3142E 00		
0.9779 0.9873	0.9524	0.8380	3.0879	0.4341	0.7827		
0.9746 0.9880	0.9524	0.8380	3.0879	0.4341	0.7827		

URMS	PF	PSI	EFFH	DQ	PNMIT	TO4	TO3D
0.5922E 03	0.3137E-01	0.7943E 00	0.9260E 00	0.6344E-01	0.6391E 00	0.7238E 03	0.7152E 03
TO3	PO3	U	DRMS	EPS	CSF	PRDLE	CPT35
0.7065E 03	0.5814E 04	0.1147E 04	0.3366E 00	0.1937E 01	0.8891E 00	0.2666E 01	0.6634E 00
RC35	ET35	DP35	DPQ	PSTH	ETS	NS	RCS
0.2542E 01	0.7717E 00	0.4663E-01	-0.3183E 00	0.1748E 01	0.7105E 00	0.6963E 02	0.2380E 01
MEXIT	MDLE	DQX	TRF	EFFI	DPOP	PSLE	DIBF
0.8437E 00	0.6833E 00	0.7944E-01	0.9371E 00	0.8475E 00	0.3072E-01	0.1951E 01	0.6859E 00
EFFIM	MG	MDEX	DPTD	ALPHD	ALPLE	A*/A	ET15
0.8143E 00	0.8667E 00	0.8511E 00	0.3083E-02	0.1364E 02	0.1908E 02	0.1121E 01	0.7291E 00
VTH4	VR	MTHR	BTHR	RDPTH	POEXIT	RDPEX	CCPA
0.9946E 03	0.2875E 03	0.7986E 00	0.9863E 00	0.1192E-01	0.2429E 01	0.8905E-01	0.5378E 00

TABLE A-1 (CONT)

CENT COMP INLET CALC RC-2.7 60

DATA

TRIG	DELSF	CC	C3	C1	C5	C6	TRIGR
0.1000E 01	0.0	0.2000E 01	0.1200E 01	0.5000E-02	0.2500E 01	0.5850E 02	0.1500E 01
D1	D1/D2	N	W	D3	ALPHA	IGV	BH
0.2000E 00	0.4630E 00	0.3359E 05	0.1358E 01	0.6520E 00	0.2200E 02	0.2200E 02	0.3100E-01
BFI	BLH	BLM	BLTH	RR	VRATD	CPA	C2
0.0	0.8500E 00	0.9400E 00	0.7300E 00	0.1221E 01	0.6000E 00	0.1000E-01	0.0
NO OF BLADES	AD	BH2	UD	PHIPD	WD	ALPS	C7
0.3200E 02	0.1410E-01	0.2600E-01	0.1918E 04	0.6250E 00	0.9950E 00	0.1640E 02	0.1046E 01
C8	C9	C10	C11	C12	C13	RNMCR	CMT
0.1050E 01	0.1500E 00	0.1900E 01	0.6500E-01	0.4500E-01	0.5000E-01	0.8700E 00	0.5440E 00

RESULTS

POP	PRTTE	HE	W/A	MT	GG	RHOS	MAX
0.2107E 04	0.2759E 01	0.5252E 02	0.1197E 02	0.1541E 00	0.1005E 01	0.7524E-01	0.1429E 00
PHI	AI	VT	CTHT	BETAG	PHIP		
0.1388E 00	0.1114E 04	0.1716E 03	0.6430E 02	0.7711E 02	0.2899E 00		

STANDARD FIXUP TAKEN , EXECUTION CONTINUING

0.9779 0.9849 0.9497 0.8174 3.7584 0.4134 0.8402
0.9743 0.9862 0.9497 0.8174 3.7584 0.4134 0.8402

URMS	PF	PSI	EFFH	DQ	RNMIT	TO4	TO3D
0.5920E 03	0.2895E-01	0.7942E 00	0.9205E 00	0.6861E-01	0.6406E 00	0.7271E 03	0.7174E 03
TO3	PO3	U	DRMS	EPS	CSF	PRDLF	CPT35
0.7075E 03	0.5811E 04	0.1147E 04	0.3366E 00	0.1937E 01	0.8918E 00	0.2660E 01	0.5582E 00
RC35	ET35	DP35	DPQ	PSTH	ETS	NS	RCS
0.2541E 01	0.7592E 00	0.4452E-01	0.1654E-01	0.1959E 01	0.7073E 00	0.6635E 02	0.2402E 01
MEXIT	MDLE	DQX	TRF	EFFI	DPOP	PSLE	DIBF
0.8460E 00	0.6819E 00	0.9011E-01	0.9530E 00	0.8334E 00	0.3265E-01	0.1948E 01	0.6418E 00
EFFIM	MG	MDEX	DPTO	ALPHD	ALPLE	A*/A	ET15
0.7991E 00	0.3643E 00	0.8480E 00	0.3105E-02	0.1274E 02	0.1896E 02	0.3510E 00	0.7229E 00
VTH4	VR	MTHR	BTHR	RDPTH	POEXIT	RDPEX	CCPA
0.9957E 03	0.2737E 03	0.6642E 00	0.9840E 00	0.9858E-02	0.2443E 01	0.8137E-01	0.5434E 00

TABLE A-1 (CONT)

CENT COMP INLET CALC RC-2.7 60

DATA

TRIG	DELSF	CC	C3	C1	C5	C6	TRIGR
0.1000E 01	0.0	0.2000E 01	0.1200E 01	0.5000E-02	0.2500E 01	0.5850E 02	0.1500E 01
D1	D1/D2	N	W	D3	ALPHA	IGV	BH
0.2000E 00	0.4630E 00	0.3358E 05	0.1277E 01	0.6520E 00	0.2200E 02	0.2200E 02	0.3100E-01
BFI	BLH	BLM	BLTH	RR	VRATD	CPA	C2
0.0	0.8500E 00	0.9400E 00	0.7300E 00	0.1221E 01	0.6000E 00	0.1000E-01	0.0
NO OF BLADES	AD	BH2	UD	PHIPD	WD	ALPS	C7
0.3200E 02	0.1410E-01	0.2600E-01	0.1918E 04	0.6250E 00	0.9950E 00	0.1640E 02	0.1046E 01
C8	C9	C10	C11	C12	C13	RNMCR	CMT
0.1050E 01	0.1500 00	0.1900E 01	0.6500E-01	0.4500E-01	0.5000E-01	0.8700E 00	0.5440E 00

RESULTS

POP	PRTTF	HE	W/A	MT	GG	RHOS	MAX
0.2107E 04	0.2757E 01	0.5249E 02	0.1126E 02	0.1447E 00	0.1004E 01	0.7535E-01	0.1341E 00
PHI	AI	VT	CTHT	BETAG	PHIP		
0.1304E 00	0.1114E 04	0.1612E 03	0.6038E 02	0.7793E 02	0.2723E 00		

STANDARD FIXUP TAKEN , EXECUTION CONTINUING

0.9778	0.9840	0.9475	0.7996	4.3661	0.3989	0.8895
0.9741	0.9851	0.9475	0.7996	4.3661	0.3989	0.8895

URMS	PF	PSI	EFFH	DQ	RNMIT	T04	T03D
0.5918E 03	0.2719E-01	0.7942E 00	0.9161E 00	0.7274E-01	0.6417E 00	0.7300E 03	0.7192E 03
T03	P03	U	DRMS	EPS	CSF	PRDLE	CPT35
0.7083E 03	0.5808E 04	0.1146E 04	0.3366E 00	0.1937E 01	0.8942E 00	0.2654E 01	0.4766E 00
PC35	ET35	DP35	DPO	PSTH	ETS	NS	PCS
0.2539E 01	0.7482E 00	0.4311E-01	0.1867E 00	0.2063E 01	0.7005E 00	0.6413E 02	0.2409E 01
MEXIT	MDLE	DQX	TRF	EFFI	DPOP	PSLE	DIRF
0.8480E 00	0.6811E 00	0.5974E-01	0.5667E 00	0.8216E 00	0.3431E-01	0.1945E 01	0.6062E 00
EFFIM	MG	MDEX	DPTD	ALPHD	ALPLE	A*/A	ET1S
0.7862E 00	0.9630E 00	0.9459E 00	0.3158E-02	0.1208E 02	0.1896E 02	0.8693E 00	0.7154E 00
VTH4	VR	MTHR	RTHP	RDPTH	RDEXIT	RDPEX	CCPA
0.9966E 03	0.2643E 03	0.5595E 00	0.5826E 00	0.8734E-02	0.2449E 01	0.7704E-01	0.5475E 00

LIST OF SYMBOLS

A	Area
B	Blockage
b	Diffuser axial width
C	Coefficient
C_D	One-dimensional blockage factor = 1-B
C_p	Specific heat at constant pressure; static pressure recovery
C_θ	Tangential velocity
F_m	$\prod_{i=1}^{r} f_i$
f_i	Modifier factor
g	Acceleration of gravity
H	Enthalpy
IGV	Inlet guide vane
i	Incidence
J	Mechanical equivalent of heat
M	Mach number
N	Rotor speed, rpm
N_s	Specific speed = $(\sqrt{Q}\ N)/\left[JC_p\ T_0\ (R_{c_{OA}}{}^{(\gamma-1)/\gamma-1})\right]^{3/4}$, rpm $ft^{3/4}/sec^{1/2}$
$N/\sqrt{\theta}$	Impeller rpm corrected to standard conditions
P	Pressure (total)
PF	Prewhirl factor
P_{LE}	Diffuser leading-edge total pressure
P_{TH}	Diffuser throat total pressure
p	Pressure (static)
Q	Inlet volume rate of flow
q	Energy head, nondimensional by U_2^2/Jg
R	Radius
R_c	Compressor pressure ratio
$R_{c_{OA}}$	Overall pressure ratio
SF	Slip factor = $1 - (C_{\theta_2} + V_{m_2} \tan \beta_{b2})/U_2$
T	Temperature
T_T	Total temperature
U	Rotor speed
V_m	Meridional velocity
V_a	Axial velocity
Wa_c	Rate of airflow corrected to standard conditions
Z	Axial dimension

α	Flow angle a. Inducer inlet flow angle measured from the axial direction b. Diffuser inlet flow angle measured from the tangential direction
β	Relative air angle or blade angle
β_b	Impeller blade mean surface angle
γ	Ratio of specific heats
Δ	Differential
ϵ	Surface roughness
η	Efficiency
ϕ	Inlet flow coefficient = V_a/U_{rms}
ψ	Pressure coefficient

Subscripts

C	Compressor
cr	Critical
ext	External
f	Friction
a	Axial
IT	Impeller tip
LE	Diffuser leading edge
OA	Overall
ri	Rotor internal
rms	Root mean square
T	Total or stagnation
Tan	Tangency
Th	Throat
th	Theoretical
0	Inlet total
1	Inlet guide vane inlet station
2	Impeller inlet station
3	Impeller exit station
4	Diffuser inlet station
5	Diffuser leading-edge station
6	Diffuser exit station
θ	Tangential or wake